



THE UNIVERSITY
OF QUEENSLAND
AUSTRALIA

Disposable, Low-Cost, Cellulose-Substrate UAV Platform

by
MIKE REED
42197142

**School of Electrical Engineering and Information Technology,
University of Queensland
March 2013**

**Submitted for the degree of
Bachelor of Engineering (Honours)**
School of Information Technology and Electrical Engineering
NOVEMBER 2013

University of Queensland, Australia

Michael A Reed
19 Kaboora Cres.
Westlake
QLD 4074

2/11/2013

Professor Paul Strooper
Head
School of Information Technology and Electrical Engineering
The University of Queensland
Queensland 4072

Dear Sir,

I hereby submit my Thesis titled “Disposable, Low-Cost, Cellulose-Substrate UAV Platform” for consideration as partial fulfilment of the Bachelor of Engineering degree.

All the work contained within this Thesis is my original work except where otherwise acknowledged.

Yours sincerely

Michael A Reed
Student ID: 42197142

ACKNOWLEDGEMENTS

I would first and foremost like to thank my supervisor Professor Paul Pounds for his help and guidance on the project. Especially whenever things were looking dim or stagnant, he would brandish the whip of persistence and spur me to continue. Many insights into failed experiments were provided from his tutelage and the project would have surely lost the bearing it maintained without him.

My sincere thanks are also sent out to the team at Cartesian Co. with whom I often operated in tandem trading ideas, equipment and materials. If it weren't for the borrowed epoxies, shot presses, clamps, soldering guns and electronics components, I may well have drained my bank account on express shipping charges. Thank you to Ariel Briner, John Scott and Isabella Stephens.

I would also like to thank the HoneyWell representatives present at the October, 2013 Innovations Expo for providing me an olive branch in the dark times approaching the end of the project. The Automation and Control award single-handedly reinstated all faith I had in my project and gave me the drive to complete this paper. One day I will thank them properly without having been awake for more than 48 hours.

ABSTRACT

This thesis presents research in the field of developing extremely low cost platforms for Unmanned Aerial Vehicles (UAV) that can be produced so cheaply and easily as to make it entirely disposable after a single mission. Many currently existing systems typically engaged in the tasks of automated long range data collection have been limited from being adopted in widespread use. This is purely because these systems represent such high primary expense. The associated risk of damaging or losing the device prevents their use in exactly the situations in which they could be employed most effectively. Dangerous or remote situations including natural disaster monitoring, agricultural data mining and long range weather observation could benefit deeply from a more readily accessible source of collecting information. This project builds upon a previous iteration of research and prototyping by Professor Paul Pounds on the topic of being able to create a disposable platform that can fill this previously unexplored niche.

Significant challenges are presented in exploring this new territory as research and experimentation is scarce in many aspects of the project. A major challenge is providing a control electronics platform that is capable of being disposable in a monetary sense as well as in the way it degrades in the environment. Brief and limited exploration has previously been performed into the application of creating circuits onto substrates that naturally break down in the environment. This thesis outlines a manufacturing process successfully proven to be capable of producing circuits onto a paper substrate using cheap and readily available materials and equipment. Following this process, a number of functioning prototypes are presented capable of carrying high frequency digital signals and of being reflow soldered.

Alternate immediately accessible methods are also presented that take the form of (soon to be) commercially available automated machines that can produce similar results with the significant drawback of requiring chemicals that would detrimentally pollute the environment. This method comes in the form of a modified inkjet printing machine that is being developed for the hobby market in Brisbane, Australia by a group named Cartesian Co.

Processes that are likely to be capable of generating superior outcomes to the given problem are summarized and proven to be currently incapable of providing adequate support to further the current state of the project. Most notably this includes using high vacuum equipment to generate evaporation deposited metals that are capable of reproducing a conductance comparable to that of the bulk material.

In the process of generating these outcomes, a number of insightful analyses into why some processes function differently to others is presented relating to the microstructure of the patterned conductors.

Next, the topic of significantly increasing the lift and stability characteristics of a micro delta wing glider is explored – with the purpose to be used as the mechanical platform. Extensive research is outlined on the stabilization of leading edge vortices with the intention of preventing large scale layer separation even under very high angles of attack. Various methods employed in full scale aircraft in subsonic conditions are explored with their applicability to the project justified.

Additionally a unique recent advancement in the optimization of low Reynold's number airfoils is presented with analogies drawn to the vortical lifting capabilities of a delta wing. This technology relies upon the generation of transverse localized vortices in corrugations present on the airfoils surface. This principle is justified with a prototype test platform and an example design is given in the form of flat artwork designed to be cut and folded into a 3-dimensional form.

TABLE OF CONTENTS

Acknowledgements.....	iii
Abstract.....	iv
Table of Contents.....	vi
1 List of Figures	viii
2 List of Tables	x
Glossary of Terms and Acronyms	1
3 Introduction	2
3.1 Why Does the World Need Disposable UAVs?	2
3.2 Design Challenges	2
4 Prior Art and Literature Review	4
4.1 Flexible and Biodegradable Circuit Manufacture	4
4.1.1 Flexible Circuitry in Previous Work on Project.....	4
4.1.2 Stencilled Spray, Sputter and Evaporation Deposition.....	5
4.1.3 Selectively Applied Graphene Nano-Plates.....	7
4.1.4 Inkjet Printed Graphene Flakes.....	8
4.1.5 Inkjet Printing Precious Metals	8
4.1.6 Current Availability of Technology.....	10
4.2 MAV Mechanical Systems Design	12
4.2.1 Cellulose Matrix Formed Gliders.....	12
4.2.2 Low Reynold's Number Airfoil Selection.....	15
4.2.3 Increasing Lift and Control of Leading Edge Vortices	18
4.3 Control	22
4.3.1 High Altitude Path Finding	23
4.3.2 Dynamic Electronic Control.....	25
5 Theory	27
5.1 Resistance Produced by Available Production Techniques	27
5.2 Nano-Particle Low Temperature Sintering	29
5.3 Dynamic Control Power Consumption.....	30
5.4 Aerodynamics	31
5.4.1 Mass Distribution Stabilization	32
5.4.2 Dihedral Angle.....	33
5.4.3 Directional Stability.....	34

5.5	Mechanical Properties of Paper.....	35
5.6	Path Planning POMDP Search.....	36
6	Implementation and Discussion.....	40
6.1	Conductor Application Method	40
6.1.1	Evaporation Deposition	40
6.1.2	Selective Inkjet Deposition.....	41
6.1.3	Spray Deposition	42
6.2	Conductor Material Testing	43
6.3	Electrical and Mechanical Component Mounting	45
6.3.1	Conductive Epoxy.....	46
6.3.2	Solders.....	47
6.3.3	Substrate Mounting Apertures	49
6.3.4	Low Cost Conductive Pad Thickenening	50
6.4	Circuitry Environmental Concerns Remaining	51
6.5	Current and Future Prospects of Automation	52
6.6	Glider Design	53
7	Results.....	56
7.1	Electronics.....	56
7.2	Glider/Mechanical.....	58
8	Conclusion.....	61
8.1	Achievements.....	61
8.2	Future Work.....	61
9	Appendices.....	64
10	Bibliography	76

1 LIST OF FIGURES

FIGURE 4-1 PAUL POUNDS TEST PLATFORM CONSTRUCTED FROM POLYIMIDE [6]	5
FIGURE 4-2 SIEGEL'S METHOD FOR GENERATING PAPER SUBSTRATE PCBs	6
FIGURE 4-3 CONDUCTIVE EPOXY USED TO BIND SOIC COMPONENT [12]	7
FIGURE 4-4 PATTERNED GRAPHENE CIRCUIT GENERATION [10]	7
FIGURE 4-5 FUNCTIONING MICRO CAPACITOR ENHANCED WITH GRAPHENE INKJET PRINTING [15]	8
FIGURE 4-6 ROTARY ELECTROSTATIC DRIVE MOTORS PRODUCED WITH COLLOIDAL METAL PRINTING [16]	9
FIGURE 4-7 GRAPHENE ENHANCED COPPER USED FOR INKJET PRINTING [17]	10
FIGURE 4-8 INKJET PRINTED FUNCTIONAL SOIC CIRCUIT	11
FIGURE 4-9 SHINJI SUZUKI'S PAPER PLANE UNDERGOING HIGH SPEED TEMPERATURE TESTING [22]	13
FIGURE 4-10 PROJECT SPACE PLANES LANDING SITES	13
FIGURE 4-11 POWERED AND RC PAPER PLANE BY POWERUP [24]	14
FIGURE 4-12 PLANTRACO CARBON BUTTERFLY, HINGEACT CIRCLED IN RED [25]	14
FIGURE 4-13 LAMINAR SEPARATION OVER CURVED AIRFOIL [27]	16
FIGURE 4-14 FLOW ADHESION OVER FLAT PLATE AIRFOIL [27]	16
FIGURE 4-15 LEADING EDGE VORTICES ON DELTA WING, TAKEN FROM [26]	16
FIGURE 4-16 DRAGONFLY WING PROFILES [30]	17
FIGURE 4-17 CONTROLLED PERPENDICULAR VORTICES FORMED IN PROFILE CORRUGATIONS [30]	17
FIGURE 4-18 LAMINAR SEPARATION OVER CURVED AIRFOIL 2 [27]	18
FIGURE 4-19 LAMINAR SEPARATION OVER FLAT PLATE AIRFOIL [27]	18
FIGURE 4-20 FLOW ADHESION OVER CORRUGATED AIRFOIL [27]	18
FIGURE 4-21 RHS LEADING EDGE FLAP	19
FIGURE 4-22 UPSTREAM VORTEX BREAKDOWN ON RHS DUE TO DOWNSTREAM OBSTACLE [26]	20
FIGURE 4-23 APEX FLAP EXAMPLE [33]	21
FIGURE 4-24 APEX FENCE GEOMETRY EXAMPLE [35]	22
FIGURE 4-25 DOUBLE DELTA DIAMOND FILLET CROSS SECTION [36]	22
FIGURE 4-26 DOUBLE DELTA VORTEX INTERACTIONS SIMULATION [37]	22
FIGURE 4-27 HIGH ALTITUDE FOAM GLIDER [8]	23
FIGURE 4-28 3-SPACE TRAJECTORY	24
FIGURE 4-29 WIND FIELD DISTRIBUTION [41]	25
FIGURE 4-30 LATERAL AND LONGITUDINAL FLIGHT CONTROL [42]	25
FIGURE 4-31 MPU6050 ON POLYIMIDE CIRCUIT	26
FIGURE 5-1 PROPORTIONAL CHANGE IN CONDUCTANCE AGAINST FOLD ANGLE	28
FIGURE 5-2 SURFACE ROUGHNESS AGAINST SURFACE RESISTIVITY [12]	29
FIGURE 5-3 PROPORTIONAL CHANGE IN CONDUCTANCE AGAINST FOLD ITERATION	29
FIGURE 5-4 SILVER NANO PARTICLE WITH CARBOLIC ACIDS AS CAPPING AGENT	30
FIGURE 5-5 PITCH FORCE ANALYSIS	33
FIGURE 5-6 COM RESTORING ROLL TORQUE	33
FIGURE 5-7 DIHEDRAL ANGLE DEFINITION	34
FIGURE 5-8 DIHEDRAL STABILITY	34
FIGURE 5-9 DIAGRAM OF VORTEX ALTERATION FROM WINGLET SHAPE [49]	35
FIGURE 5-10 EXAMPLE VERTICAL STABILIZERS	35
FIGURE 5-11 TORQUES GENERATED BY YAW PERTURBATION	35
FIGURE 5-12 GAUSSIAN DISTRIBUTION OF WIND VECTOR [41]	38
FIGURE 5-13 SAMPLING WITHIN THE BELIEF SPACE TO REDUCE COMPUTATION [51]	38
FIGURE 6-1 INKJET PRODUCED CIRCUIT FROM CARTESIAN CO	41
FIGURE 6-2 THE EX1 CIRCUIT PRINTER BY CARTESIAN CO	42

FIGURE 6-3 AIRBRUSH SPRAY DEPOSITION	42
FIGURE 6-4 COPPER PAINT COAGULATION	44
FIGURE 6-5 COPPER SPRAY DEPOSITION	44
FIGURE 6-6 TEST SPRAY OF COPPER PAINT USING HVLP SPRAY GUN	44
FIGURE 6-7 SMALL TEST TRACK CUT FROM	44
FIGURE 6-8 LCC AND QFN BREAKOUT BOARDS IN SPRAY DEPOSITED SILVER	45
FIGURE 6-9 PRESSURE TREATMENT	45
FIGURE 6-10 CIRCUITWRITER 'PEN'	46
FIGURE 6-11 SILVER EPOXY PIN SHORTING	47
FIGURE 6-12 IMPROVED APPLICATION METHOD	47
FIGURE 6-13 SOLDER PASTE PLACED FOR SURFACE TENSION CORRECTION	48
FIGURE 6-14 INSULATING 'HALOS' GENERATED AROUND SOLDER POINTS	48
FIGURE 6-15 SOIC AND 1206 COMPONENTS SOLDERED TO INKJET PRINTED CIRCUIT BY CARTESIAN CO.	49
FIGURE 6-16 APERTURE MOUNTING METHOD - NO SOLDER	49
FIGURE 6-17 TOP AND BOTTOM VIEW OF RESISTORS SOLDERED WITH APERTURE BASED METHOD	50
FIGURE 6-18 USING NICKEL TO PROMOTE SOLDER FLOW	50
FIGURE 6-19 COPPER PASTE COATED SOLDER PADS TO PROMOTE SOLDER FLOW	51
FIGURE 6-20 SOLDER CONNECTIONS MADE USING COPPER AS A FLOW PROMOTION MECHANISM	51
FIGURE 6-21 AUTOMATIC SOLDER STENCIL PRESS	52
FIGURE 6-22 STANDARD PAPER DART INITIAL FOLDS	53
FIGURE 6-23 ALTERNATE PAPER PLANE DESIGN	54
FIGURE 6-24 APPLIED POSITIVE DIHEDRAL	54
FIGURE 6-25 GENERATING A CORRUGATED AIRFOIL DELTA GLIDER	55
FIGURE 7-1 FUNCTIONAL PAPER PCB	56
FIGURE 7-2 MOSTLY FUNCTIONAL PROTOTYPE MINUTES BEFORE CATASTROPHIC FAILURE	56
FIGURE 7-3 I2C COMMUNICATION OF PAPER CIRCUIT	57
FIGURE 7-4 I2C COMMUNICATION FROM BREADBOARD ATMEGA328P FOR COMPARISON	57
FIGURE 7-5 CARDINAL GLIDER CONTROL CIRCUITRY	57
FIGURE 7-6 CORRUGATED AIRFOIL DELTA WINGS	58
FIGURE 9-1 5030 LASER ENGRAVER BY CNCOLETECH	64
FIGURE 9-2 THE EX1 CIRCUIT PRINTER BY CARTESIAN CO. - PRESENTED HERE WITH PERMISSION	65
FIGURE 9-3 A4 LAMINATOR PROCESSING A STENCILED ARRAY OF CIRCUITS	65
FIGURE 9-4 LASER-CUT SOLDER STENCIL	65
FIGURE 9-5 HANDHELD REFLOW SOLDERING STATION	66
FIGURE 9-6 MEASURING LASER BEAM WIDTH	66
FIGURE 9-7 BEFORE AND AFTER BEAM WIDTH COMPENSATION	67
FIGURE 9-8 LASER-CUT SPUTTER DEPOSITION STENCIL	67
FIGURE 9-9 L100 AIR-SPUTTER DEPOSITED CIRCUIT BOARDS	69
FIGURE 9-10 COPPER COATED SOLDER PADS	70
FIGURE 9-11 COMPONENTS REFLOW SOLDERED TO PAPER SUBSTRATE	71
FIGURE 9-12 VISUAL REPRESENTATION OF GEOMETRIC MEAN CHORD (APPROX. MAC VISUALIZATION)	72
FIGURE 9-13 SILVER CONDUCTOR WICKED INTO MATRIX OF PAPER	73
FIGURE 9-14 HIGH RESOLUTION BUT THICK, BRITTLE AND WASTEFUL TRACKS	73
FIGURE 9-15 NICKEL BASED CIRCUITS PRODUCED WITH AN AEROSOL SPRAY	74
FIGURE 9-16 COMPONENTS MOUNTED WITH CARBON BASED CONDUCTIVE ADHESIVE	74
FIGURE 9-17 BOTTLE OF WIREGLUE	74
FIGURE 9-18 EXAMPLE OF RESOLUTION OF NICKEL ACRYLIC SPRAY ON A SET OF SOIC COMPONENT PADS	75
FIGURE 9-19 EXAMPLE ANALOGUE CIRCUIT PRODUCED WITH STENCILED NICKEL ACRYLIC	75

2 LIST OF TABLES

TABLE 5-1 RESISTIVITY	27
TABLE 5-2 PRESSURE CALC. PARAMETERS	32
TABLE 6-1 EVAPORATION DEPOSITION	41
TABLE 6-2 INKJET DEPOSITION	42
TABLE 6-3 SPRAY DEPOSITION	43

GLOSSARY OF TERMS AND ACRONYMS

UAV	Unmanned Aerial Vehicle
MAV	Micro Unmanned Aerial Vehicle
MCU	Microprocessor Unit
IMU	Inertial Measurement Unit
Delta-wing	Style of aircraft that consists only of two wings, possibly a small fuselage and no tail
Tropopause	The boundary in the Earth's atmosphere between the Troposphere and the Stratosphere occurring at approximately 10km in altitude.
GPS	Global Positioning System
Jet Stream	Channels of high speed air that are caused by pressure differentials that form around the Tropopause.
PID loop	Proportional Integral Derivative loop is a common style of feedback control
GFS	Global Forecast System, used to predict weather patterns up to 16 days in advance
Elevon	Hybrid of Elevator and aileron as it fulfills the function of both, often employed on delta wing aircraft.
Atomization	Spheroidization of a liquid to prevent flowing such as capillary action.UAV
Reynold's Number	Ratio of fluid flow inertia to viscosity
Root	Side of wing closest to fuselage
Tip	Side of wing farthest from fuselage
Chord length	Streamwise length of wing shape
Delta wing	Wing consisting of a pair of highly swept leading edges
Laser cutter	XY automated cutting system using a CO2 laser typically
Vinyl cutter	XY automated cutting system using an actuated blade
Air-sputter deposition	Placement of a material onto a substrate through being forced through an aperture under pressure
Vacuum evaporation deposition	Placement of a material onto a substrate through being evaporated under a high vacuum
Selective inkjet Deposition	Selective placement of a material onto a substrate through being ejected from an inkjet cartridge
CFD	Computational Fluid Dynamics
COG	Centre of Gravity
COL	Centre of Lift
Lipo	Shorthand for Lithium Polymer or Lithium Polymer battery
CFRP	Carbon Fibre Reinforced Plastic
MDP	Markov Decision Process
POMDP	Partially Observable Markov Decision Process
SOIC	Small Outline Integrated Circuit
QFN	Quad Flat No-leads
MEMS	Micro Electro-Mechanical Systems
I2C	Inter-IC Bus or Two wire Communication
FIFO	First in, first out
LGA	Land Grid Array

3 INTRODUCTION

3.1 WHY DOES THE WORLD NEED DISPOSABLE UAVS?

UAV robotics platforms are suited most significantly for surveillance and the dispersion of other light weight systems: most notably sensor networks [1]. The freedom lent by traversing the medium of air allows a drone to move about large and small scale environments with relatively few obstacles and obstructions. Recent developments in MEMs sensor technology has been a large contributor to UAV technology being brought to mainstream industry applications such as public beach safety surveillance [2] and even the toys industry [3]. Despite these advancements, all of these systems generally require large initial investments and then continued delicate maintenance.

The nature of a UAV leads to weight and hence power becoming a scarce commodity. This severely stunts the applications as longer flight times require greater battery life, leading to increased weight and then necessitating greater lift [4]. Additionally, any system currently on the market capable of performing a long-range flight is also limited with the premise that it must return fully functional to its launch position due to the extreme investment it represents. This can be circumvented with significant infrastructure in the area but this is counter-intuitive to the benefit of having a drone able to travel where other systems cannot [5]. A low-cost, high altitude, long range, disposable UAV would open up possibilities for sending surveillance into environments or situations that are known to be dangerous or remote as a return trip is not required.

An example of a practical implementation of a fleet of long-range disposable UAVs is in scientific data collection missions [6]. Present methods of sensor placement generally require the immediate or nearby presence of a human operator necessitating grossly expensive and potentially environmentally disruptive and/or dangerous expeditions [7]. Alternatively, if the technology comes to fruition, a fleet of glider mounted sensors could be launched from a research centre anywhere in the world to take vital data in isolated locations such as the Amazon, Antarctica or dangerous situations including an active volcano or radioactive sites. This would reduce price, danger and environmental impact (depending on hardware onboard) significantly.

As farfetched as it may sound, a well-engineered miniature paper glider coupled with a micro-electronic control system could fit these criteria seamlessly. The reduced scale of an MAV device allows for structural material that could never be considered at commonly sized systems. Due to the greatly reduced weight, such gliders could also be easily launched from high-altitude weather balloons at heights of 30km at very low cost [8]. If the gliders are made capable of autonomously navigating jet streams around the Tropopause, then inter-continental travel could theoretically be achieved for under \$100.

3.2 DESIGN CHALLENGES

The problem of generating a low-cost, high altitude, long range, disposable UAV system encompasses a number of design challenges including:

Cost: - The system must consist of components that can be sourced in bulk for low cost but more importantly the production techniques must be as simple and autonomous as possible – involving little to no human manufacture.

Biodegradability: - To enable discarding of the platform in the environment, it is important that no harmful chemicals be leached into the ecosystem. This is amplified further by the fact that many areas suited to sensor networks have a delicate ecology. An example is the monitoring of rainforest regeneration in Springbrook through a large sensor network by CSIRO [9].

Control Simplicity: - To reduce weight, power consumption and component/manufacturing costs, it is imperative that a platform consist of a bare minimum of control surfaces and feedback sensors. To gain spatial feedback, an IMU at the least is necessary but for accurate positioning, it is expected a GPS and possibly magnetometer module will also need to be incorporated.

Power Conservation: - As the ultimate goal of the project is to have a long range flight, any available battery power must be strictly conserved. Devices that sink large amounts of energy such as actuators and GPS modules must be powered for as little time as possible and as infrequently as possible without compromising adequate control. Recent advancements in lightweight solar panels may also provide an energy source during long flights and/or to sensor systems after deployment for collection and transmission. Though this is only predicted well into the future.

Passive Stability: - In order for the control system to only require occasional use of the control surfaces (see power consumption above), the aerodynamic frame of the UAV must be passively stable under the expected conditions. This imposes particular requirements upon the materials choice as well as shape design.

Robustness: - While the system is not necessarily required to remain functional after it has touched down in its final destination, it still must be capable of withstanding the rigours of high altitude weather conditions. These may include rapidly changing wind conditions that cause body flexure, high humidity and temperature extremes.

Flight-path Calculation: - In the higher atmosphere conditions that the UAV will be subjected to, there exist jet streams of very high speed winds and pockets of significantly varying pressure. In order to maximize the flight range and to prevent unwanted course alteration, path finding must include these phenomena from recent updates with very limited computational power.

The following paper is the description of research, work and analysis performed as an extension to the paper written by Paul Pounds titled “Paper Plane: Towards Disposable Low-Cost Folded Cellulose-Substrate UAVs”. In the paper, Pounds proposes a unique solution to the problem at hand by justifying a paper substrate as both the mechanical form for the MAV as well as the support structure for the control circuitry. The work outlined in this document seeks to further the research and experimentation provided by Pounds to move closer to a fully functioning prototype in the hopes that we can one day achieve the impossible and send a paper plane around the globe.

4 PRIOR ART AND LITERATURE REVIEW

4.1 FLEXIBLE AND BIODEGRADABLE CIRCUIT MANUFACTURE

The control circuitry of the Micro Unmanned Air Vehicle (MAV) system has some very unique and restricting design constraints imposed by the design principles of the device as a whole. To reiterate briefly in the context of the circuit support and production method:

- Economical – Manufacturing methods cost as well as materials cost must both be kept on par with the goal of making a system that is disposable even after a single mission. There already exists technologies to produce flexible circuit boards in industry but they are potentially far beyond the reach of disposability.
- Ultra-lightweight – The weight of electronic components will make a significant impact in the case of an MAV of this size – this imposes the use of components in the smallest possible packages. Additionally, any power losses induced through resistance in the tracks will directly impact the amount of power storage or generation necessary.
- Biodegradable – There currently exists no standard industry substrate that is fully bio-degradable. An alternative substrate must be developed to the point of usability for the goals of this project to be achieved.
- Robustness – During high-altitude flight in the open environment, strong wind forces, high humidity, wide temperature ranges and even precipitation could be encountered. Ideally the system will be highly resistant or impervious to these conditions.
- Flexibility – With the ultimate aim of generating the mechanical form and control circuitry from the same material, it becomes necessary to have a substrate that is flexible and formable. Ideally the circuit would also be capable of withstanding these forming processes to allow for circuit manufacture on a flat surface.

An ideal substrate that is able to fulfil nearly all of these design principles superbly is paper. As of the point of writing this paper (November 2013), there exists no commercially available solution for generating circuits on a paper substrate. However, research has been ongoing for paper to be implemented as a basis for flexible Printed Circuit Boards (PCB) as this will minimise many of the issues noted above which could have a large impact on many industries. Some applications include flexible solar cells, thin film transistors, cheap lightweight displays and energy-storage devices [10]. This presents a unique set of challenges as paper is comprised of a delicate and porous matrix which prevents the use of many chemical and mechanical etching processes that are common in industry [11] – collectively referred to as subtractive patterning. Instead researchers are looking towards additive methods that build up the conductive layer in the shape of the required pattern, removing the need to actively pull material away from the paper [12].

As a side note, biodegradable plastic substrates do exist however are all unsuitable due to their low glass transition temperature or chemical instability at low temperature. If soldering and/or nano particle sintering is to be performed, these substances are unsuitable.

4.1.1 FLEXIBLE CIRCUITRY IN PREVIOUS WORK ON PROJECT

Flexible circuits already exist in industry as a standard but expensive method of providing a flexible substrate for connecting elements as well as component mounting in rare cases. This is most often

implemented onto a polyimide substrate base and many PCB fabrication warehouses exist that can offer this substrate to within a 10 working day delivery frame [13]. Polyimide is used primarily because it can withstand the chemical processes required to etch artwork into the copper as well as the heat required for soldering processes. This allows for polyimide substrates to be integrated easily into many existing technologies for PCB manufacture including solder paste stencilling, automatic component placement and oven reflow soldering [13].

Polyimide based substrate PCBs have been implemented in a previous iteration of this project with success, at least in the sense of electrical connections [6]. The design was able to reliably support packages down to the Quad Flat No-leads (QFN) component specification which in turn allows the integration of useful sensor modules, in this case the popular Inertial Measurement Unit (IMU), the MPU9150.

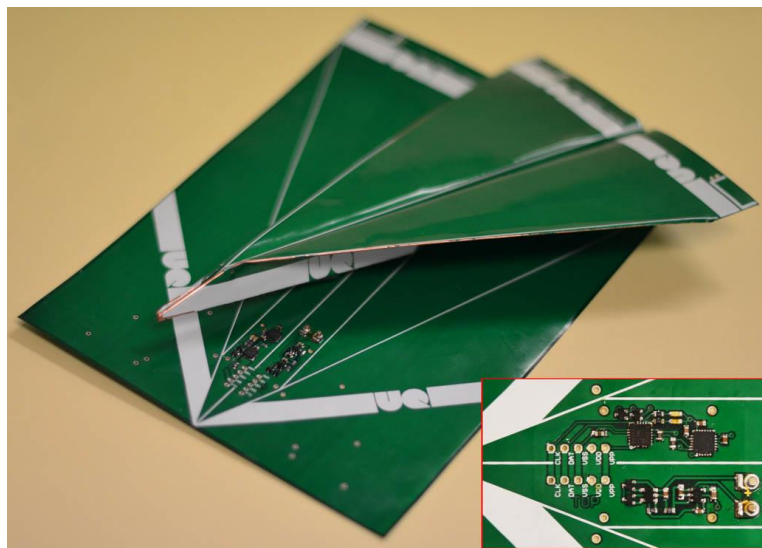


Figure 4-1 Paul Pounds Test Platform Constructed from Polyimide [6]

This system was produced only as a proof of concept however and the main points in which this approach falls down are:

- The cost of polyimide based PCBs is extremely high when not produced en masse, notably reducing the feasibility of prototyping. For example a 100x100mm prototype typically costs \$50–200/piece (single sided) and \$100–250/piece (double-sided) in addition to up to a \$1,000 tooling fee when purchased in small quantities (~10 pieces) [12].
- The minimum folding radius (typically $600\mu m$ [12]) and thickness of polyimide (typically $140\mu m$ [12]) is not ideal. Thus preventing tight, sharp folds as well as reducing the achievable ‘sharpness’ of the planform leading edge.
- The system is entirely non-biodegradable
- Weight of the system is considerably more than a paper based counterpart.

4.1.2 STENCILLED SPRAY, SPUTTER AND EVAPORATION DEPOSITION

In 2010 researchers at Harvard University released a paper describing a methodology to generate conductive artwork onto standard 80GSM paper that was demonstrated to successfully support a set of analogue circuits. This paper is in the public domain and is titled “Foldable Printed Circuit

Boards on Paper Substrates” [12] provided by the Advanced Functional Materials journal. The process used in this instance is best described by a graphic provided in the paper, please see Figure 4-2.

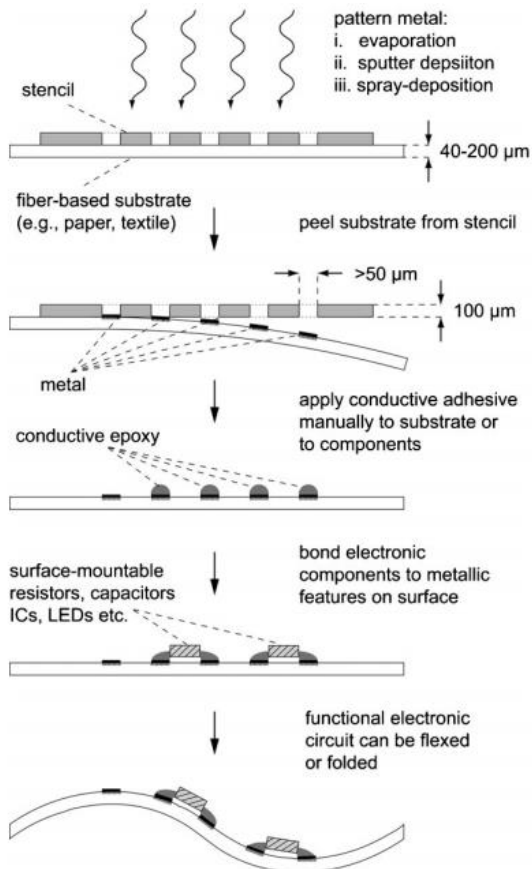


Figure 4-2 Siegel's Method for Generating Paper Substrate PCBs

Despite the incredible properties that were achieved in the example specimens presented by Siegel there is still a number of significant challenges that arise from implementing these techniques alone:

- Evaporation deposition necessitates expensive equipment and a significant vacuum ($> 20\mu\text{Torr}$).
- Evaporation deposition will result in a less porous structure of the conducting metal which increases conductance but reduces fold repeatability. In the particular application of a disposable MAV, fold repeatability is unnecessary and so this is in fact an advantage.
- Material deposition in all cases bar spray deposition is very slow and expensive in terms of power and machine time. This still allows for adequate conductance in feasible time frames but increased thickness is costly. This leads to next point.
- The produced specimen is unable to be soldered. As will be discussed later in this section, this is largely due to the thickness of conductor deposited. This prevents assembly from being an automated process, requires a skilled operator to prevent shorts in application of epoxy and limits the minimum component pin spacing that can be used. Refer to Figure 4-3 for an example of how the Small Outline Integrated Circuit (SOIC) package is pushing the limits of the epoxy's and the technician's capabilities.

- The alternative electrical and mechanical binding of components (conductive silver epoxy) is brittle once cured [14]. This results in micro cracks forming through the electrical connections during flexure of the material and either generating an intermittent or entirely open connection.

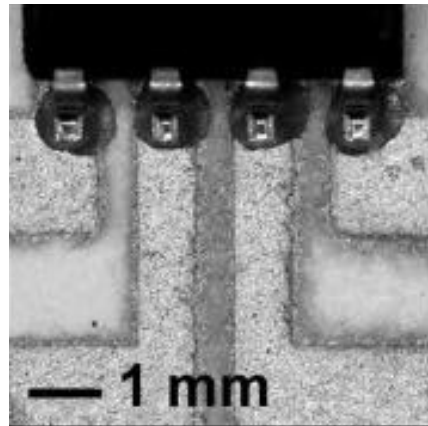


Figure 4-3 Conductive Epoxy Used to Bind SOIC Component [12]

4.1.3 SELECTIVELY APPLIED GRAPHENE NANO-PLATES

In an attempt to build directly upon the work performed by Siegel and his associates, researchers at the Korea Advanced Institute of Science and Technology have been performing experiments into selectively applying graphene nanoplates onto paper substrates [10]. In the paper released in a 2013 publication of Advanced Materials titled ‘Foldable Graphene Electronic Circuits Based on Paper Substrates’ Hyun and his associates generated rudimentary analogue specimens that attempted to overcome the problem of losing conductance through repeated folding. The specimens were generated by pressing the graphene particles through a membrane filter selectively with an operator controlled pen as shown in Figure 4-4.

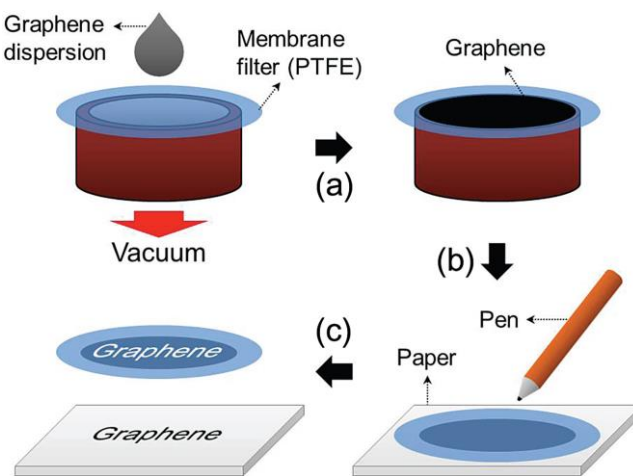


Figure 4-4 Patterned Graphene Circuit Generation [10]

The resulting conducting tracks were capable of sustaining 80% of their original conductance even through over 1000 folding cycles [10]. Despite this, the base resistances weren't even stated, the achieved electronics were only very simple LED circuits and the application method is currently far from capable of achieving fine resolution artwork.

4.1.4 INKJET PRINTED GRAPHENE FLAKES

There does however exist different methods for applying graphene onto flexible substrates in a manner that could eventually generate similar properties to those explored by similar techniques to Siegel. These involve mixing mechanically exfoliated graphene flakes into an ink and filling standard inkjet cartridges to pattern the material down. In previous research, this basic principle has shown to be viable in producing simple electronics with most tests centred around printing onto synthetic materials such as polyimide. However a large barrier to integration of the technology into industry is the great difficulty and hence cost surrounding the production of the graphene flakes [15].

Researchers from the KTH Royal Institute of Technology also released a paper in Advanced Materials during 2013 that describes a process of generating high quality graphene flakes using solution phase exfoliation with ethanol and ethyl cellulose. In the paper they are able to generate functioning printed resistors and a rudimentary proof of concept of a micro super capacitor by first applying a layer of conducting silver as show in Figure 4-5 [15].

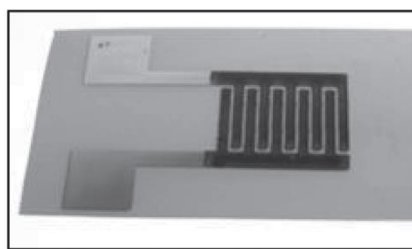


Figure 4-5 Functioning Micro Capacitor Enhanced with Graphene Inkjet Printing [15]

This technology has not yet matured to a state of usability in general circuit manufacture due to it's lacking of conductance as well as many practical issues that arise during manufacture. These include controlling the viscosity to ensure accurate printing, preventing aggregation of flakes inside cartridges and reducing the number of layers that must be applied (caused by the necessity of a low graphene content to allow for flow through inkjet nozzles). In the long term, graphene may be a much more suitable conductor due to the abundance of its constituent elements and its ability to flex repeatedly however, for now, it remains too expensive to produce and the penalty of non-repeating fold lines is acceptable at least in the context of disposable MAVs.

4.1.5 INKJET PRINTING PRECIOUS METALS

The final technology to be explored is a process that has been explored extensively in industry but has not breached any wide scale production or adoption due to the current barriers in cost and assembly processes. That is the inkjet printing process of metal micro particles in either a colloidal like substance or in suspension with a viscosity enhancing agent and cellulose Van Der Waals barrier.

Inkjet printing methods using precious metals (particularly in colloidal liquids, typically with around 10%wt metals) has existed in viable methods for years. These processes have been shown to be capable of producing functional Micro Electro-Mechanical Systems (MEMS) sensors as far back as 2002 using precious metal conductors such as gold or silver [16]. Refer to Figure 4-6 for an example of a specimen generated with this process. These precious metals can only be used due to: their ability to easily generate nano-particles and colloidal structures, high conductivity, low sintering temperature for nano-particles and their resistance to oxidation.

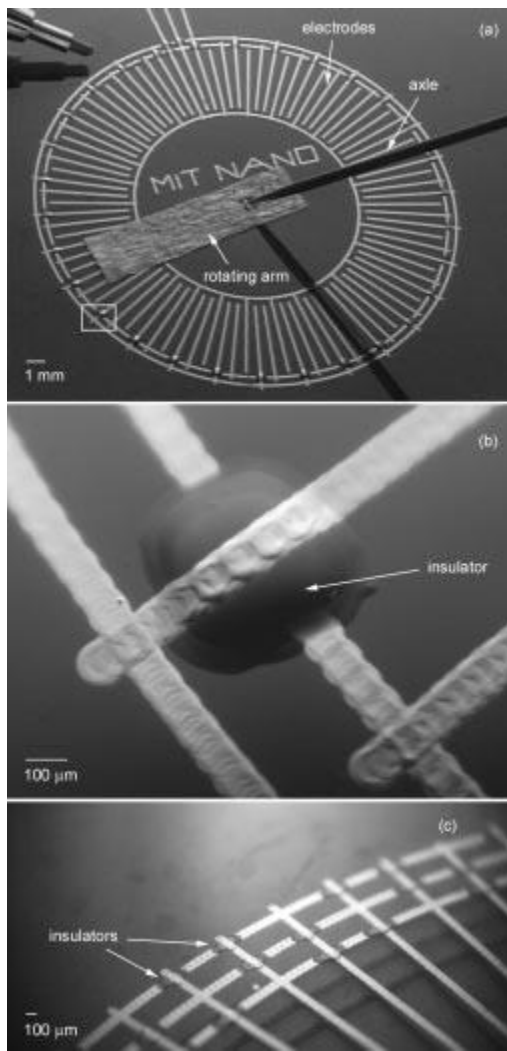


Figure 4-6 Rotary Electrostatic Drive Motors Produced with Colloidal Metal Printing [16]

The cost associated with creating these precious metal inks as well as maintaining the hardware to pattern them has kept this technology from being developed beyond laboratory experiments.

Additionally the scale on which the machinery is being produced is generally only usable for micro-scale projects – this prevents the creation of PCBs that connect already manufactured components and focuses more upon generating new components from scratch [17].

Graphene printing can be considered largely an expansion upon this technology and other researchers have attempted to meet mid-way on these processes to generate something reasonably cost-effective and viable as the rest of the technology catches up. An example of this is the paper produced by Luechinger and Stark at the Institute for Chemical and Bioengineering in Zurich, Switzerland. In this example, it is attempted to implement a cheaper but less conductive and more corrosion prone metal, that is copper. A nano-colloid is generated with copper through the use of graphene as a protective shell to enhance the ability to generate nano particles [17]. This was a very promising breakthrough as lower cost metals were previously unable to be implemented into a nano-colloidal structure for the purposes of inkjet printing. None the less, the mixture was still not sufficiently conductive, resulting in even thick tracks exhibiting resistances in the kΩ range (Luechinger notes that densification sintering wasn't applied to the specimen) [17]. Please refer to

Figure 4-7 for a summary of resistance achieved with this method and an image of an analogue example specimen.

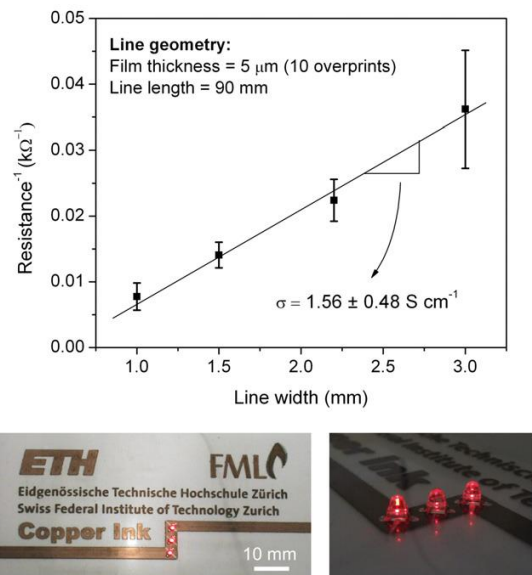


Figure 4-7 Graphene Enhanced Copper Used for Inkjet Printing [17]

4.1.6 CURRENT AVAILABILITY OF TECHNOLOGY

Regardless of future potential prospects, the most important parameter for the scope of this paper is the immediate applicability. The cost of inkjet printing of Silver can be partially mitigated by reducing the amount of processing required to generate the ink as well as to modify the inks to be printable in generic inkjet cartridges. Both of these have been successfully achieved by a start-up company in Brisbane name Cartesian Co. [18] by taking advantage of a chemical reaction between two readily available substances. The chemical reaction between Silver Nitrate and Ascorbic Acid has been previously explored even in the field of inkjet printing technology [19]. Many of these solutions used the Ascorbic acid reaction as a basis with viscosity modifiers and conductance enhancers added into the inks. Additionally, the focus of these papers has been predominantly on a basis of increasing conductivity and resolution without touching base on any of the practical limitations of introducing the technology into industry – most notably exploring the ability of attaching components. The author has been partially working in tandem with the Cartesian Co. team and have been able to adequately address many of these concerns. The final objective of this work is to have a fully operational machine capable of producing conducting tracks (capable of passing digital communications as well as accepting reflow soldering) on a vast range of substrates including paper. Cartesian CO. is undertaking a crowd sourcing campaign to further develop and manufacture a line of machines expected to be despatched for delivery in mid 2014 [18]. Of even greater importance, the machine is marketed at a hobby level price range with a current projection of ~\$1100. For an example of an early prototype refer to Figure 4-8 which later supported digital communications in the SPI protocol.

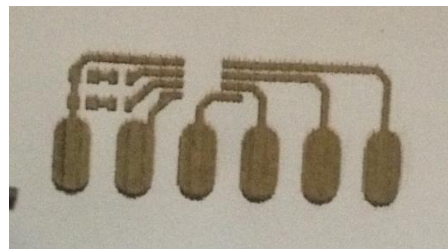


Figure 4-8 Inkjet Printed Functional SOIC Circuit

Some drawbacks of the machines being released by Cartesian Co. are the number of successive passes required to generate sufficiently conductive tracks, the achievable resolution (which is predicted to be improved but currently is capable of supporting SOIC standards as a minimum feature size) and its capabilities in nano-particle sintering (this is explored further in Section 5.2).

4.2 MAV MECHANICAL SYSTEMS DESIGN

The final mechanical form of the disposable MAV must also conform to the set of generic design principles that dictate the system as a whole. To reiterate briefly in the context of the mechanical form:

- Economical – The system must be disposable in both the sense that it is designed for a single mission but also ideally accounting for the possibility that a proportion of launched systems won't even make it to their intended destinations. This means that some typical materials generally reserved for aviation due to their high strength to weight ratios are off-limits (typical examples are carbon-fibre, titanium etc.).
- Ultra-lightweight – The final system will be unpowered and will make a controlled gliding descent but it is also intended to piggy back the control circuitry, a sensory payload and ultimately communications systems and solar power generation device/s. At the scales considered, this implies an extremely stringent weight specification of the mechanical base form.
- Biodegradable – With the intention of likely discarding the system in the environment at the point of touchdown, many light-weight plastics as well as chemical binders must be disregarded due to the impact that would be made to the local biosphere.
- Minimal Power Consumption – Weight restrictions limit the power able to be supplied on-board as well as the amount of energy that could eventually be trickle fed through solar modules in future iterations. This imposes that the mechanical form would be intrinsically stable under all conditions encountered.
- Robustness – The system must be capable of enduring the high-altitude weather patterns encountered over a long-range mission without compromising the aerodynamic qualities of the form or failing to provide mechanical support necessary for the in-built control circuitry.

While these design criteria appear almost entirely incompatible in the context of full scale aviation, promising research and even successful experimentation has been performed on subsets of these principles. Conglomerating some of the most applicable work performed ultimately leads to the conclusion that a cellulose based fibre matrix (ie. paper, cardboard etc.) material formed into a micro-scale delta wing is capable of upholding the design principles listed above.

The following section outlines the pertinent information taken from various reputable sources in order to form the basis on which the final design was developed.

4.2.1 CELLULOSE MATRIX FORMED GLIDERS

Paper aircraft generally have a history of being related purely to recreational purposes, this makes it hard to believe that such a design could mark a significant step in UAV technology. However, with the scaled size of MAV devices, the conventional exotic materials often employed in aeronautics (eg. Titanium, expensive composites) become less and less practical [4]. When you consider that the design goal is also to make the device disposable, these choices are rendered entirely useless. Even the most light-weight and economical materials conventionally used in MAV's such as balsa and polystyrene foam require significant processing and manufacturing steps that would not lend themselves to mass machine production [20].

Paper, however, provides a biodegradable, readily available, extremely low cost material. A lift producing paper aircraft form can be constructed from a standard sheet of A4 printer paper or stiff card through simple and autonomous machining processes such as stamping, pressing and forging [21]. It has also been proven that standard printer paper can operate as a viable substrate for constructing conductive circuit. Having a paper cellulose structure as the sole material of an MAV is in fact a notion that has been commercially investigated in major industries for at least 5 years.

In 2008, the Japanese Space Agency (JAXA) announced funding of \$285,700 to Shinji Suzuki to research generating paper aircraft for atmospheric re-entry from the International Space Station [22]. The only modification planned to be made to the material was a heat resistant coating to prevent combustion while entering the atmosphere.



Figure 4-9 Shinji Suzuki's Paper Plane Undergoing High Speed Temperature Testing [22]¹

Paper aircraft have even recently been engineered specifically for long-distance flight. A German group called 'Project Space Planes' [23] affixed SD memory cards to 200 stiff paper planes and launched them from a weather balloon at more than 36km above the ground in early 2011. These planes had no electro-mechanical control and stabilized passively through the shape of the plane design.



Figure 4-10 Project Space Planes Landing Sites

Luckily some planes were able to exploit high-altitude jet streams, leading to landing destinations as far as the West coast of North America and even Sydney, Australia (see Figure 4-10 Project Space Planes , the black circle indicates the launch position in Germany).

This demonstrates that a cellulose substrate, formed and folded paper plane is capable of passively stabilizing itself sufficiently for intercontinental, high altitude flight (albeit uncontrolled).

¹ <http://techcrunch.com/2008/01/21/spaceships-to-be-made-out-of-paper-if-japan-folded-paper-plane-society-hasanything-to-say-about-it/>

In terms of controllable paper MAV craft flight, the field seems to be generally unexplored with one or two commercial exceptions. A company named PowerUp has recently appeared in technology media reports (around Feb. 2013) for releasing a small super-capacitor powered paper plane as a novelty toy, see Figure 4-11. The device consists of a standard folded paper plane with a module mounted to it containing a Bluetooth 2-way communication module, small super-capacitor, drive motor, drive shaft and propeller and presumably a pressure sensor module. At its present state, the manufacturers have not yet discovered a cost-effective and reliable method of providing actuated control surfaces and so the device is currently little more than a novelty [24].



Figure 4-11 Powered and RC Paper Plane by PowerUp [24]

This specific issue was partially addressed in a previous iteration of this project under Dr. Paul Pounds. In the original paper upon this subject, Dr. Pounds implements a small electromagnetic elevon device produced by Plantraco [6] dubbed the HingeAct. The device exhibited the ability to manoeuvre its control surface sufficiently for the application and the device has been integrated into many other successful MAV applications. An example is the Carbon Butterfly also produced by Plantraco and shown in Figure 4-12. The carbon butterfly employs a HingeAct as the rudder control surface and is capable of a tight enough turning circle to easily achieve indoor flight.



Figure 4-12 Plantraco Carbon Butterfly, HingeAct Circled in Red [25]

With a total flying weight of 3g (the HingeAct being 0.2g itself), the Carbon Butterfly has roughly the order of weight attempting to be replicated in this project [25]. However there are still a set of design principles in the HingeAct and associated projects (such as the Carbon Butterfly) that severely divert from that of a long range glider:

- High power draw – it is designed to be operated on the range of 0-5V with a total series resistance of 150Ω . This results in a power draw range of 0 – 165mW for a single actuator. For a long range MAV with severe energy restrictions from weight, this is unacceptable unless a method of operating it very sparingly is found [25].
- High Cost – the HingeAct is marketed toward a niche hobby market in which it has a large monopoly, this in tandem with the fact that it must be hand produced painstakingly by a technician has yielded a current cost per unit of ~\$17.95AUD [25].
- Delicacy – the HingeAct unfortunately sacrifices robustness for its reduced weight. While it is useable, hand assembly by an experienced technician, the rigors of mass production and high altitude weather may be far beyond what the system can handle and retain operation.

The HingeAct is, for now, the only reasonably viable option at MAV's of this scale and so research must continue in improving its robustness and reducing manufacture cost. The issue of power draw however may inevitably be unavoidable and can only be circumvented by providing as much system stability as possible through passive means and eventually providing ongoing power through a solar cell.

<http://www.microflight.com/Online-Catalog/>

4.2.2 LOW REYNOLD'S NUMBER AIRFOIL SELECTION

In the case of the flow conditions of MAV flight, the Reynold's number is very often significantly lower than values used in the dominance of aeronautical research. This is because the Reynold's number (a numerical representation of the ratio of fluid flow inertia to viscosity) is directly proportional to the effective chord length of the specimen as well as the relative fluid velocity. Both of these parameters are orders of magnitude lower than values experienced in manned flight or even most explored UAV applications.

A viscosity dominated flow (extremely low Reynolds number) over an airfoil is largely characterized by the generation of a laminar-separation bubble somewhere on the top surface. Laminar separation is the cause of turbulent vorticity that in most cases will induce stall [26]. The growth of this separation bubble is highly promoted by large adverse pressure gradients – such as those generated by a rounded, blunt leading edge of a generic curved airfoil. In Figure 4-13 Laminar Separation over Curved Airfoil , you can see this bubble bursting into full separation of the flow from the top edge of the airfoil, leading to a stall condition of low lift and high drag. Conversely, the sharp tip of a thin plate airfoil causes pressure to change much less drastically and hence impedes the formation of laminar separation – forestalling the stall condition. This is demonstrated in Figure 4-14 Flow Adhesion over Flat Plate Airfoil where the flat plate is clearly providing a much greater connection to the top flow – leading to a much higher lift to drag ratio.

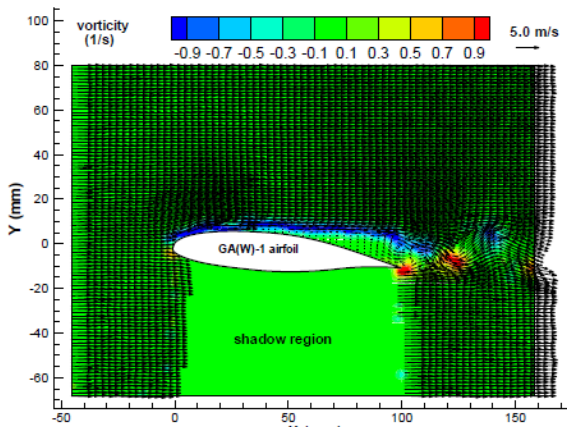


Figure 4-13 Laminar Separation over Curved Airfoil [27]

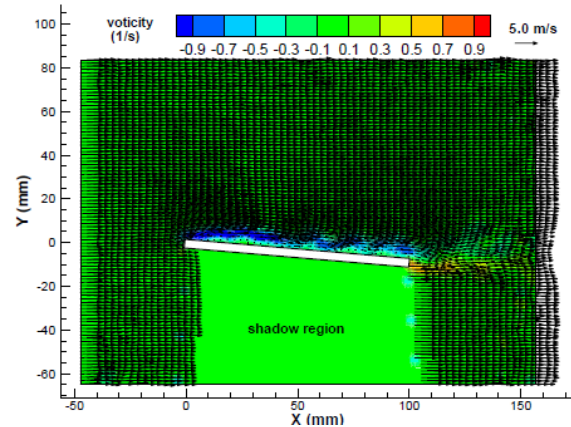


Figure 4-14 Flow Adhesion over Flat Plate Airfoil [27]

Unfortunately that isn't the whole solution. While flat plates are more effective at preventing stall than rounded airfoils – they're still limited in the lift and range of angles of attack they can achieve, this is generally considered a limitation of low Reynolds number flow. So the question is whether there exists a method to prevent turbulent laminar separation while still inducing higher lift.

The only general solution to this challenge thus far is the intended generation and control of turbulent flow in the form of localized vortices. In particular, great research has been performed into the lift characteristics of leading edge vortices created by highly angled delta wings with a sharp leading edge. This is because similar effects become useful at supersonic speeds and during landing conditions for full scale aircraft [28]. In the case of highly angled delta wings, the flow velocity gradient over the leading edge is repeated linearly along the slope of the wing. This effect induces a local pressure field that favours vortical air flow parallel to the leading edges of the wing Figure 4-15.

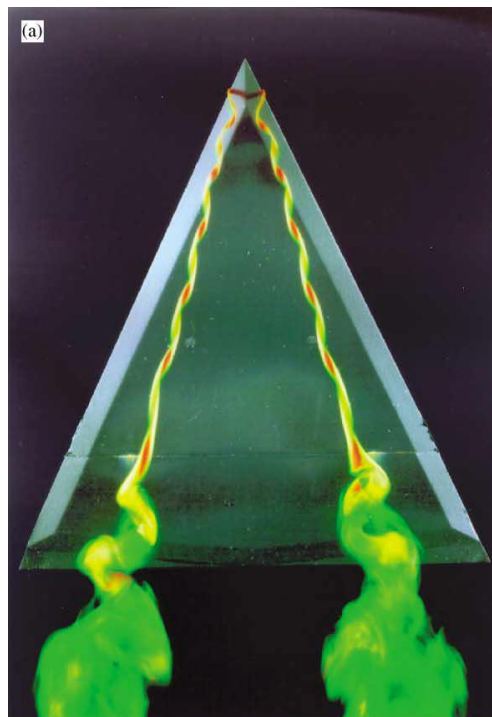


Figure 4-15 Leading Edge Vortices on Delta Wing, Taken from [26]

The geometry of these vortices will generally follow a conical shape with increasing radii as they approach the trailing edge but the axial path that the cone shape follows as well as the rate of change in radii is dependent upon flow conditions and to a greater extent: geometry of the craft [29]. Importantly, the pressure gradient that induces the circular flow also acts to keep these vortices against the top surface of the wing (as the pressure reduction will generally follow the change induced by the leading edge). In turn, the pressure reduction at the boundaries of the vortex acts to direct flow over the leading edge, along the surface of the conical shape and past the trailing edge – this will act to reduce the uncontrolled laminar separation that leads to a stall condition [26].

As the radius of the cone increases it will eventually reach a critical point at which the general structure of the flow disintegrates into unorganized turbulent conditions in which the axial and swirl velocities experience a rapid deceleration – this is incapable of consistently redirecting flow. For stable lift and predictable control of a delta wing shape, this breakdown must occur downstream of the trailing edge of the wing. As angle of attack is increased, the inertia of the flow will prevent the central axis of the vortex from being pulled down so closely to the surface. This in turn increases the distance between the central axis and gradients formed at the leading edge, resulting in an overall increase of the cone radius rate of growth. As this effect is increased, the vortex breakdown point migrates upstream along the flow axis. As it passes over the trailing edge, lift begins to drop significantly as well as introducing instability conditions as unstable flow berates the rear control surfaces [26].

The exact conditions that lead to this vortex breakdown point have not yet been fully identified but large amounts of research have indicated the general factors that contribute to the process. Notably, the Reynold's Number does not experimentally affect the breakdown state and the most highly contributing factor is the apex geometry and to a lesser extent the overall sweep angle.

A secondary, far less developed method of stabilizing the large-scale flow over the airfoil is to induce a series of controlled vortices perpendicular to the direction of airflow which will act in a similar way to the leading edge vortices described above (see Figure 4-17). The inspiration of this design actually stems from the wings of a dragonfly which research has shown have developed a corrugated cross-sectional profile for exactly this purpose as shown in Figure 4-16 [30].

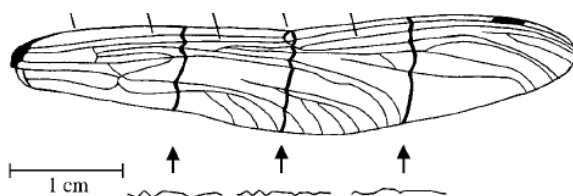


Figure 4-16 Dragonfly Wing Profiles [30]

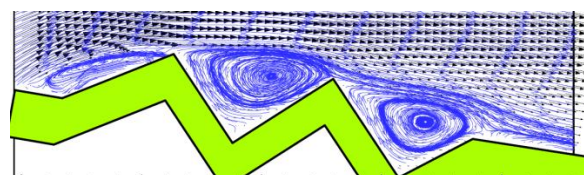


Figure 4-17 Controlled Perpendicular Vortices Formed in Profile Corrugations [30]

This phenomenon has been experimentally demonstrated by Tamai under wind tunnel test conditions at a Reynold's number of ~34,000 [27]. The direct benefit of preventing stall condition at higher angles of attack is readily displayed in Figure 4-20 where the overall flow field of the airfoil is seen to be laminar. The flow field of a corresponding rounded airfoil and flat plate both demonstrating large-scale separation leading to stall is demonstrated in Figure 4-18 and Figure 4-19 respectively.

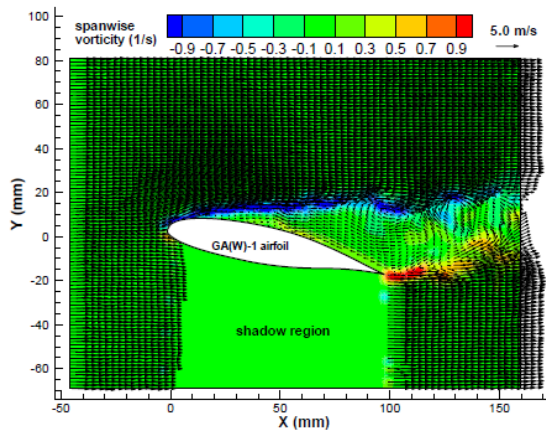


Figure 4-18 Laminar Separation over Curved Airfoil 2 [27]

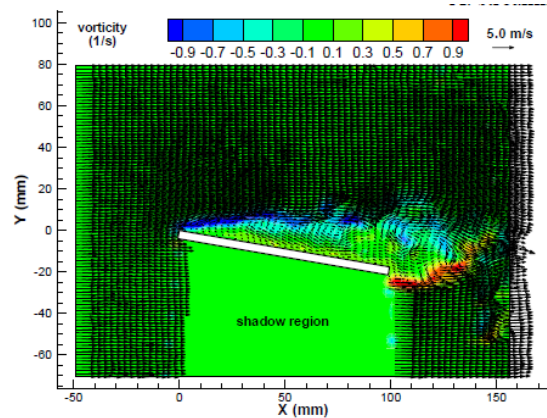


Figure 4-19 Laminar Separation over Flat Plate Airfoil [27]

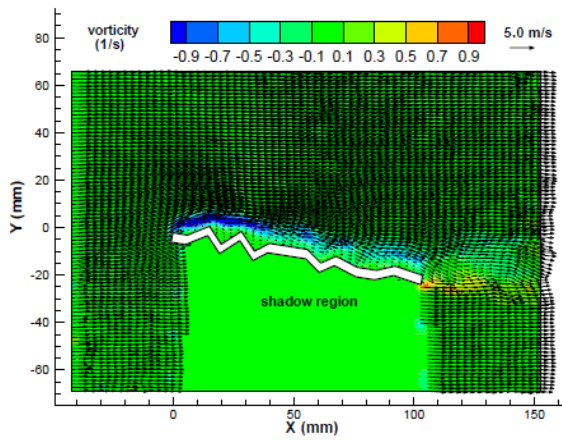


Figure 4-20 Flow Adhesion over Corrugated Airfoil [27]

This second form of flow stabilisation is beneficial in that the vortices are much better contained within the valleys of the corrugations, making the localized flow separation less likely to expand to full scale turbulence. However, this is in equal parts detrimental due to the fact that this also limits the effective range of influence that the vortices can provide.

Being that the latter form of controlled separation is so new to research and is far less explored (as its usefulness lies predominantly in the field of MAV technology), practical optimization methods are yet to be explored including combining the design with other techniques. Additionally, an analytical approximation to the changes in the lift coefficient remains unexplored.

4.2.3 INCREASING LIFT AND CONTROL OF LEADING EDGE VORTICES

The following section outlines some of the optimization methods that have been explored in the field of stabilizing leading edge vortices along a delta wing shape. Many of the solutions outlined have been explored in the context of supersonic delta flyers. The research is applicable due to the invariance of vortex breakdown conditions to Reynold's number and in many cases, results were based upon wind/water tunnel tests with specimen of comparable size to the proposed MAV [26].

Due to the unknown nature of the vortex breakdown state, it is very difficult to produce definitive solutions to the problem of sustaining the flow structure over a wide range of conditions in a predictable fashion. This is important to allow for controllability over a larger range of angles of attack, roll angles as well as being robust to dynamic disturbance forces (particularly important for

MAVs moving through tropopause jet streams). In the particular application of a low-cost, disposable MAV, these changes must be in the form of passive/intrinsic and unpowered control methods such as static control surfaces. The dominant general topics that are covered in previous research involve dynamic air jet injection, controlled leading edge surfaces and some limited research on static leading edge extended surfaces. A brief summary of some notable experimental outcomes of these static solutions and how they may be applicable are presented here.

Leading Edge Control Surfaces

Beginning in the 1970's a researcher named Rao began performing experiments on the effect of adding substantial control surfaces to the leading edge of highly swept trapezoidal wings. Rao discovered that the employment of these leading flaps were most effective when applied to the 75% of the leading edge starting from the wing tip. This provided increased lift of greater than 18.4% and had minimal effect on drag [26]. Later Marchman and Grantz improved upon Rao's work in generating tests that showed a tapered leading edge flap with a downward deflection improved performance further (see Figure 4-21). This forced vortex generation to occur over the flap and produced a lift force vector perpendicular to its surface leading to an induced thrust force instead of drag [31]. Unfortunately this research centred around the active control of the flaps, though it's not explicitly stated if this is purely to reduce drag during supersonic flight or whether this is also required for subsonic, high angle of attack flight. This effect also has the potential gain of redirecting vorticity away from the trailing edge control surfaces as explained below.

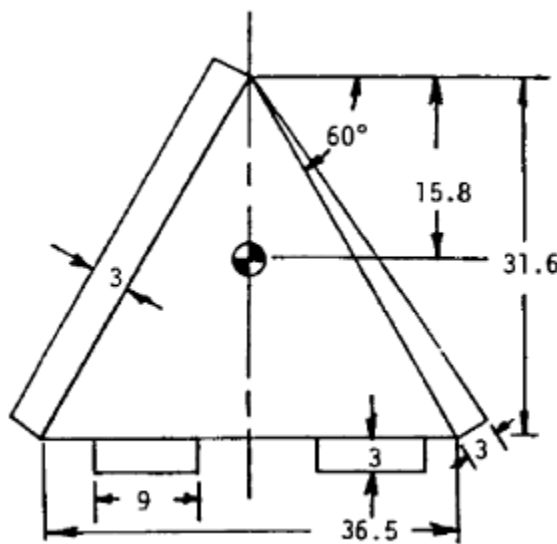


Figure 4-21 RHS Leading Edge Flap

Trailing Edge Control Surfaces (Elevons)

The term elevon is a portmanteau of the terms elevator and aileron as the surfaces are designed to be employed on a delta wing shape to provide both pitch and roll control. The corresponding control signals are traditionally summated mechanically or electrically to provide the overall angle required in each control surface (ie. roll requires an increased differential, pitch requires tandem change in one direction). Elevon control is particularly beneficial in the case of an MAV as it minimizes the number of actuated control surfaces for control. One of the pioneering researchers into leading edge vortex control was Werle at Onera, who discovered an important parameter in the

placement of these rear control surfaces. Notably in his work on visualizing flows over a 60° delta wing at 20° angle of attack, it was found that placing an obstacle in the path of the vortical axis downstream of the trailing edge caused a rapid expansion of the core radius upstream along the lifting surface [26]. This in turn can lead to heavily asymmetric lifting forces on the wings as one vortex is sustained and the other breaks down upstream of the trailing edge as shown in Figure 4-22. Combined with this, it has been shown that leading edge vortices can exhibit momentum as a given unit, causing transient oscillation to sudden changes such as a quick change in roll angle or rapid change in a rear control surface. With these two properties together, it can be hypothesized that placing a control surface directly along the axis of a leading edge vortex can lead to lift differentials opposing the intended change. For example a rapid change to a strong positive angle in the starboard elevon could cause the vortex path to momentarily jump from the wing providing a momentary loss in lift, causing an opposing roll angle. In the same way, if the elevon provides enough disturbance, it is possible that it pushes the vortex breakdown point upstream to the point of causing complete quasi-static stall of that wing.

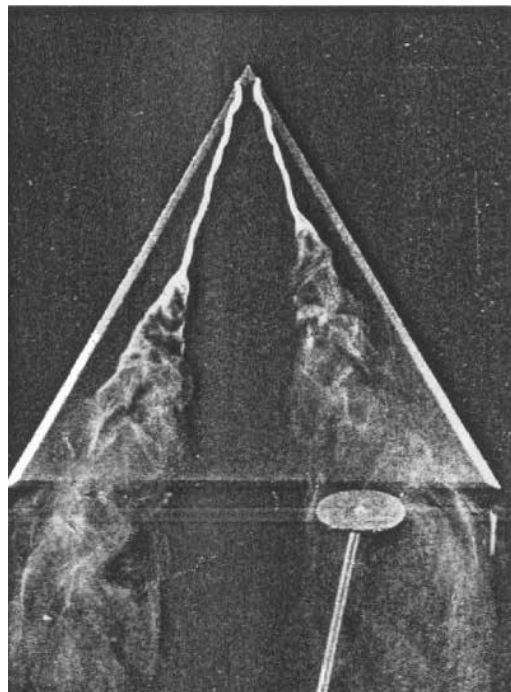


Figure 4-22 Upstream Vortex Breakdown on RHS due to Downstream Obstacle [26]

In supersonic aircraft, the elevons are designed to provide maximum controllability and so often exploit this position to generate the fastest and strongest effect. In the application of a long range MAV that is instead designed for stability and must only submit to minor trajectory alterations, it may be more suitable to divert the vortex path away from the elevons with leading edge control surfaces or simply by selecting the position of the elevon appropriately (with the downside of reducing the achievable torques in pitch and roll).

Strakes

Strakes are a control surface generally more suited to fuselage based aircraft and are less applicable to the proposed MAV. This small section is included purely as a further justification for not considering strake surfaces during development. Marchman performed further analysis on leading

edge control surfaces and their integration and comparison to strake surfaces. It was noted that strakes can act to reduce the breakdown angle at which stall occurs but at the cost of generally reducing the overall lift to drag ratios. Marchman then goes on to specifically state that while the two technologies can be integrated without cross interference, the choice of what to include should be based around the requirements on lift to drag ratios and other practical issues [32]. Despite this, the research also found that with careful tuning strakes and leading edge surfaces when combined could achieve slightly higher lift to drag ratios than leading edge surfaces alone. For this reason (and the fact that a strake has its research based in a static design), if further gliding ability is deemed necessary, it may be worthwhile to revisit the subject.

Apex Flap

The apex flap is a control surface proposed and tested by Rao and Buter and then extended by Klute et. al to the ‘drooping apex flap’. The principle of operation is to modify the effective angle of attack of the delta to increase vortex generation intensity at the apex without requiring an increase in pitch of the total craft, which increases overall flow separation and drag [33]. Klute’s research demonstrated significant delays in the vortex breakdown location with a maximum being achieved at an angle of -15° of the apex [34]. These surfaces were originally designed to be actuated, though this is with the expressed intention of making the delta shape flat again for supersonic flight [33]. Therefore a static/passive solution may be suitable for the MAV glider. The apex hinge line was tested at the quarter chord position as demonstrated in Figure 4-23.

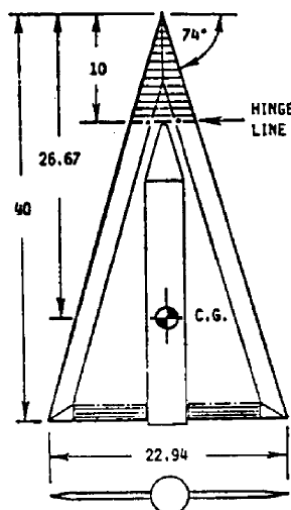


Figure 4-23 Apex Flap Example [33]

Apex Fence

Another control surface, again designed to be static for subsonic flight and stowed for supersonic flight, had a similar design goal to the apex flap. The Apex fence, investigated by Wahls et al, sought to increase upper surface suction levels to control the vortex breakdown position. It was found that position and geometry of the fences affected the generation of the leading edge vortices as well as their breakdown locations, refer to Figure 4-24 for an example. Wahls experiments yielded a maximum increase of 10% of upper surface suction levels [35]. The passive nature of this surface again makes it a candidate for further testing in the context of the disposable MAV.

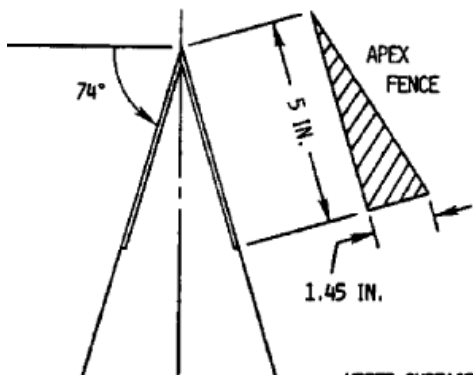


Figure 4-24 Apex Fence Geometry Example [35]

Canards

Canards can be employed in a manner that can be considered analogous to the apex flap in that the canard (being a small wing placed fore of the main wing) generates a strong vortex flow that aids in preventing separation over the rear wing. This method has been put in place to great effect in famous aircraft such as the Saab Viggen which has amazing lift capabilities at high angle of attack subsonic flight. This allows for the vehicle to land at much lower speeds as well as increasing subsonic control ranges [28]. A major drawback in the application of this method to a paper based MAV is that the canard must supply proportionately large lifting pressures in most ‘lifting configurations’ which will likely be more than a paper cantilever can support. A more subtle but similar approach to this is a double delta configuration as demonstrated in Figure 4-25. One limitation that will occur with some double delta configurations is unfavourable intertwining of the vortices generated at each ‘level’ as shown in Figure 4-26. A method of mitigating this drawback was investigated by Hebbar et. al by providing different geometries to the strake/wing junction. The most effective of these is also displayed in Figure 4-25 with the vortices being successfully separated over a wider range of angles of attack as well as delaying vortex breakdown

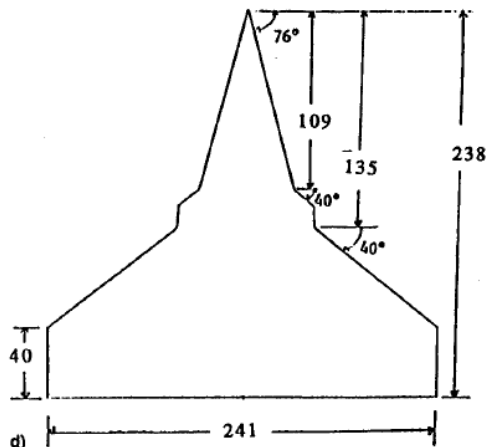


Figure 4-25 Double Delta Diamond Fillet Cross Section [36]

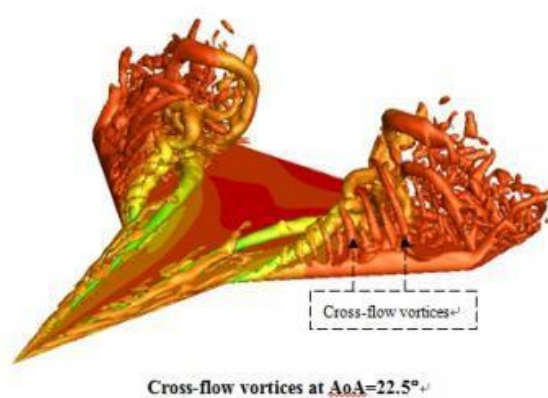


Figure 4-26 Double Delta Vortex Interactions Simulation [37]

[http://www.sciencecodex.com/detachededdy simulations and analyses on new vortical flows over a 7640 double delta wing-114877](http://www.sciencecodex.com/detachededdy_simulations_and_analyses_on_new_vortical_flows_over_a_7640_double_delta_wing-114877)

4.3 CONTROL

4.3.1 HIGH ALTITUDE PATH FINDING

A near-space UAV project named “FPV To Space and Back” was recently performed by David Windestål. A slightly larger and heavier foam glider (pictured in Figure 4-27) was launched from around 30km above Sweden through the use of an 800g high-altitude balloon with the goal of having a constant video link to a human controlled foam glider [8].



Figure 4-27 High Altitude Foam Glider [8]

This is a demonstration of electro-mechanical control of a UAV system over a long-range flight (flight time was 108 minutes including reasonable proportion of freefall with distance from launch site to landing site of 101km). Some important notes to take from this project (all information can be found at his project website²) are:

- A relatively low cost weather balloon can be sourced to launch a payload that would be roughly equal to an array of paper planes and a rudimentary launching structure.
- A weather balloon can be filled with Hydrogen in place of Helium at a reduced cost but significantly increased risk.
- Radio communications to a high atmosphere UAV are possible but would benefit from a mobile mounted and automated 2 axis antenna controller.
- Operating actuators and any moving parts subjected to the ~-60°C at and above the Tropopause and lower Stratosphere requires careful temperature testing.

Unfortunately Windestål did not provide comment on the control of the craft through the jet streams and lucked out in failing to record this section of the flight. However, he does briefly touch on the importance of predicting their trajectories as well as that of consecutive ‘layers’ of air in predicting the initial flight path of the carrier balloon. Windestål in fact makes use of an automated trajectory generator which uses the Global Forecast System (GFS) meteorological predictions to create a probable flight path and final burst position [38]. The algorithms behind the path generator are not available and very little information is given in general but Windestål describes the prediction of burst position as ‘spooky accurate’.

Ideally a similar system could be created that takes into account the rate of descent of the MAV glider but implements a search algorithm to determine the ideal entry point into the jet streams to reach the intended destination. The data mining challenge of this is made very easy by the automated download systems set in place by the GFS which allows for predictions of all major meteorological phenomena up to 8 days in advance (or 16 days with reduced accuracy). Due to the

² <http://rcexplorer.se/projects/2013/03/fpv-to-space-and-back/>

necessity of high (and low) altitude weather prediction for many other applications including commercial aviation, data packets containing only the requested information for the latest updates can be easily automatically pulled from FTP servers. These data packets come packaged in uniquely compressed file types named GERBER2. These can be most easily exported to preferred data structure types by using a package named GrADS (or the open source version openGrADS) including a supported extension dubbed pyGraDS that allows for direct automatic piping to python applications [39].

The greatest difficulty is in generating a search method that can parse through the massive data structures in a time frame that can allow for the GFS predictions to remain relevant. It must also be taken into consideration that download times for the data as well as path upload times to the MAVs and the actual flight duration may be very significant in relation to the 8 (or 16 day) timeframe. The one saving grace of the system being that the problem does not need to be solved ‘online’ due to the GFS predictions.

Some small amount of research has been conducted into the optimization of UAV path-planning through discretized \mathbb{R}^2 wind patterns as well as specifically gliders in the context of thermals in \mathbb{R}^3 . A paper released in May 2013 by the University of Seville (Spain) Robotics, Vision and Control Group describes a method of using a Bounded Recursive Heuristic Search based upon Depth-first search to optimize glider trajectories through pre-determined points of interest. The system was designed to be run ‘online’ very efficiently and was experimentally demonstrated in an airfield using simulated thermals as selectively applied thrust generators to the gliders [40]. Results were very positive as is demonstrated in the example of a trajectory shown in Figure 4-28 however the model (containing only locations of thermals and points of interest) is not sufficient for the application in question.

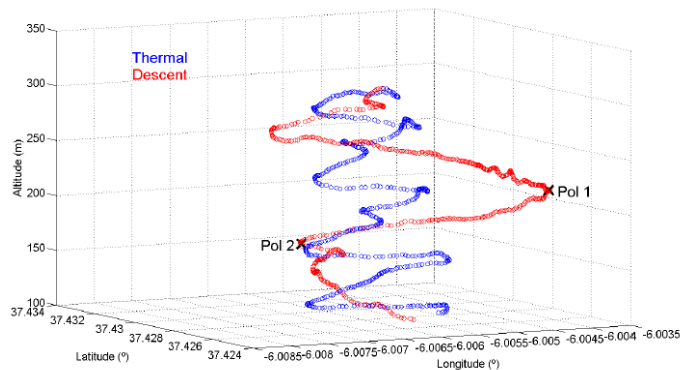


**Figure 4-28 3-Space Trajectory
Optimized Point of Interest Trajectory Incorporating Thermal Simulation [40]**

Another paper released from the Queensland University of Technology during 2012 outlines a process of implementing a Markov Decision Process for optimizing trajectories of general unmanned vehicles through a 2D flow field [41]. Experimental results are limited to very low resolution simulation (as shown in Figure 4-29) and so little can be drawn about the efficiency or feasibility of performing the policy following process on an embedded MCU. However the principle is shown to

be sound and the paper projected physical experiments of the process to be carried out by mid 2013 – information on this is yet unavailable.

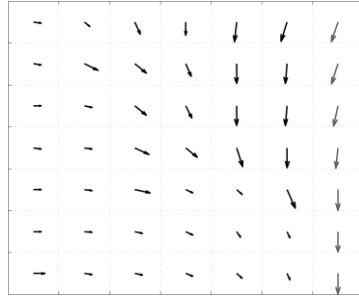


Figure 4-29 Wind Field Distribution [41]

4.3.2 DYNAMIC ELECTRONIC CONTROL

Take stuff from preliminary report, very briefly touch on how this is power intensive and is ideally minimized with intrinsic aerodynamic stability in the planes form.

The control necessary for stabilizing flight in the disposable UAV will ideally be simpler than that implemented in most modern quad-copters and advanced fixed-wing crafts. Computational ability is limited in the case of the disposable MAV and so the complexity and power constraints on algorithms must be kept to a minimum. It is common practice in fixed wing aircraft to de-couple lateral and longitudinal control such as in the control system for a fixed wing aircraft presented by researchers from Brigham Young University in their 2005 paper “Autonomous Vehicle Technologies for Small Fixed-Wing UAVs” [42].

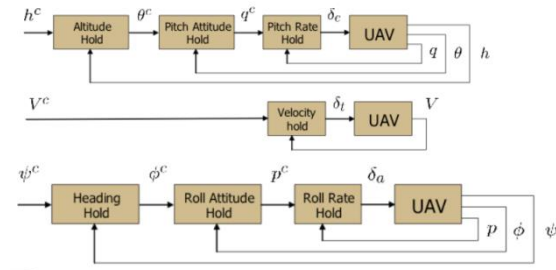


Figure 4-30 Lateral and Longitudinal Flight Control [42]

The paper outlines a simple, automatic stabilization and path-finding system for on-board autopilot. The controller takes as input: a 3-axis rate gyro, a 3-axis accelerometer, absolute pressure altimeter and a standard GPS receiver. Because the sensors used at the time of writing the paper were not advanced enough to have system in system Digital Motion Processors (DMP), a set of Kalman filters were implemented to generate state variables for the 3 control chains. Each stage of the control chains were controlled with a simple PID filter that was hand tuned according to some simple aerodynamics and then fine-tuned by trial and error.

This approach is particularly well suited to the proposed original electronic design proposed by Prof. Pounds. Pounds’ prototype system included the MPU6050 IMU sensor that contains the same inputs necessary to replicate the simple control plan put in place by Beard [6]. A newer revision of the chipset, the MPU9150 has sought to add an additional sensor containing a 3-axis magnetometer as well as allowing access to an internal temperature sensor. The form factor of the newer chip is

identical to allow for drop-in replacement of the previous revision with only minor additions to the protocol [43]. Additionally the chip contains the capability of programmable low-pass filters to each output of each sensor as well as the option of providing on board sensor fusion for the 9-axes of sensor data. This entirely removes the need for processor based Kalman filters and brings the complexity of the control algorithms to a trivial point. The power requirements of implementing this sensor fusion are yet to be sufficiently investigated but the chip does provide a large 1024 byte First in First Out (FIFO) buffer that can allow for the controller to periodically be placed into a low-power sleep mode while further data is collected. At least it will allow for less frequent I2C communications between the controller and sensor chip as well as freeing up computation time and memory space for other tasks in the controller.

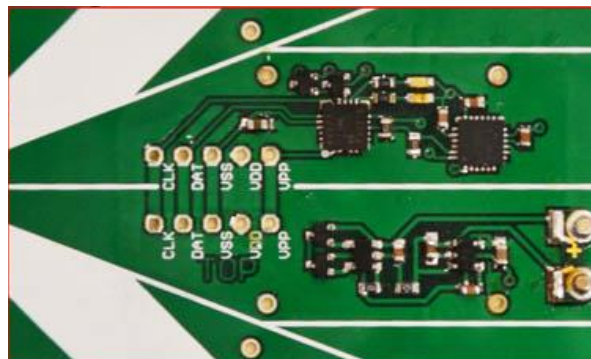


Figure 4-31 MPU6050 on Polyimide Circuit Installed Into Original Disposable MAV Prototype [6]

The MPU-9150 is currently only available in a Land Grid Array (LGA) standard package which is ideal in terms of weight and size (the total package dimensions being 4x4x1mm) but is also a curse in terms of what is currently economical and possible with paper based circuits. As of November 2013, the smallest package that can be found to have been successfully bound to a paper substrate with functional communications is an LCC 24-pin package measuring 6.5x6.5x1.5mm (this was performed by the author and is outlined in Section 7.1).

5 THEORY

The following chapter outlines any analytical processes undertaken by the author in the process of developing the prototypes discussed in chapter 6. Additionally, further analyses were compiled that are directly applicable to further work to be performed upon the project – these were not put into practice and/or experimentally dis/proved simply due to time restrictions imposed on the project. Before any further experimental work is to be done on the project, the author strongly suggests studying this chapter of the paper to use as a basis for fundamental design or improvements.

5.1 RESISTANCE PRODUCED BY AVAILABLE PRODUCTION TECHNIQUES

Resistance calculations upon the various different methods of generating conducting tracks are difficult to gauge analytically. This is because the resistance is highly dependent upon the microstructure generated which can vary unpredictably with minor changes in applied layering and post-production modification. The most accurate relationship that can often be presented is an experimentally generated relationship between the bulk resistance of a material and common parameters of production (such as number of inkjet printed layers).

It should be noted that densification sintering as described in Section 5.2 can potentially reduce most methods resistance to very close to bulk resistance.

The bulk resistance of a material can be calculated using EQNS (5-1) and Table 5-1 assuming a reasonably constant temperature. It becomes clearly obvious from Table 5-1 why silver, copper and gold are so often used to generate the conductor material and also why Aluminium would be an ideal substitute if it can be layered down adequately (with an increase in resistance of only 67.9% meaning for equivalent resistance, track thickness must be increased proportionately). Another point to be taken from this is that the bulk resistance of silver and copper is very similar, however copper often leads to a much lower patterned resistance due to its behaviour at nano-scales as described further in Section 5.2.

$$R = \rho l / wh \quad (5-1)$$

R = resistance, ρ = Material Resistivity
 l, w, h = Conductor length, width, height respectively

Table 5-1 Resistivity

Material	Bulk Resistivity (Ωm) at 20°C	ρ/ρ_{copper}
Silver	1.59×10^{-8}	0.946
Copper	1.68×10^{-8}	1.000
Annealed copper	1.72×10^{-8}	1.024
Gold	2.44×10^{-8}	1.452
Aluminum	2.82×10^{-8}	1.679
Calcium	3.36×10^{-8}	2.000
Tungsten	5.60×10^{-8}	3.333
Zinc	5.90×10^{-8}	3.512
Nickel	6.99×10^{-8}	4.161
Iron	1.0×10^{-7}	5.952
Platinum	1.06×10^{-7}	6.310
Tin	1.09×10^{-7}	6.488
Lead	2.2×10^{-7}	13.095
Carbon (graphite) //basal plane	2.5×10^{-6} to 5.0×10^{-6}	148.810 to 297.619

NOTE: the Carbon entry may be inaccurate to current manufacturing methods

<http://chemistry.about.com/od/moleculescompounds/a/Table-Of-Electrical-Resistivity-And-Conductivity.htm>

The next important effect on resistance to estimate is the reduction in resistance between the angle of a fold line over a conductor. The most relevant source on this topic is from Siegel in a paper that investigates circuitry generated onto a paper substrate using spray, sputter and evaporation deposition – three of the four most viable patterning methods. Figure 5-1 taken directly from the paper quantifies a number of experiments performed on an evaporation deposited tin conductor onto Xerox 32 lb glossy photo paper over various bend angles. Markedly the reduction in conductance from a positive bend is comparable to that of a negative bend. In both cases, conductance drops most significantly in the first and last 20° with a small plateau around 70-110°. As a simplified linear analysis (as shown in EQN (5-2)) was assumed using three known points stated in the paper [12].

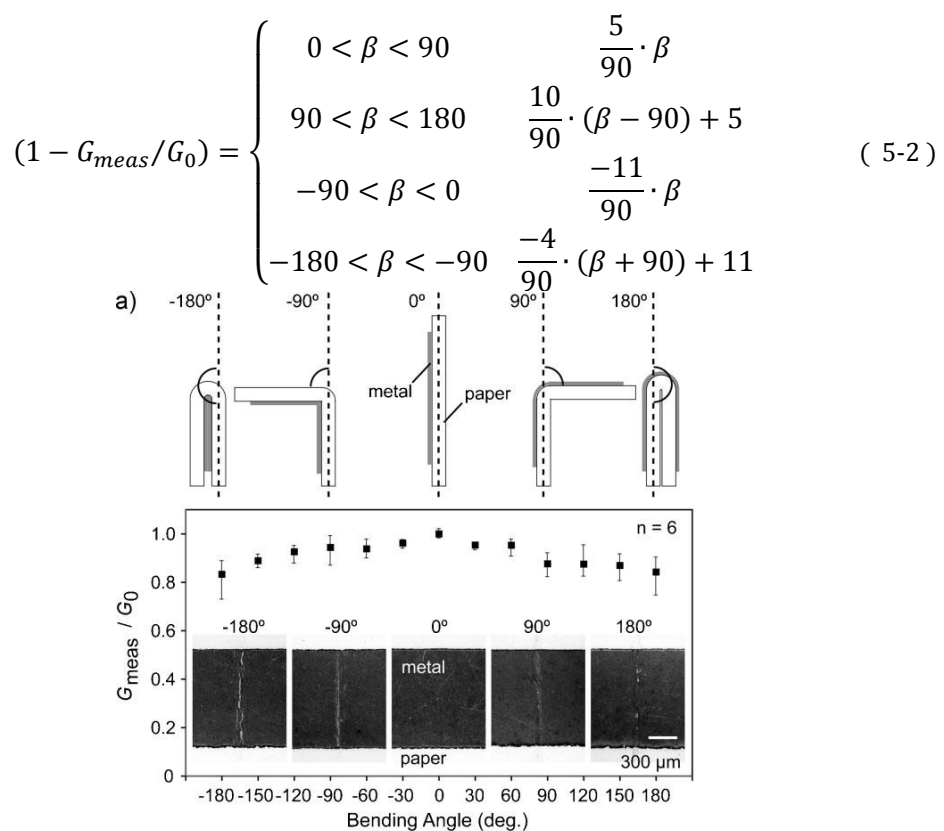


Figure 5-1 Proportional Change in Conductance Against Fold Angle

The final parameter in determining the resistance of a track is the surface roughness of the substrate material. Again this was investigated in Siegel's paper – with a brief plot provided displaying information for some common cellulose substrates (see Figure 5-2). With the intention being that ultimately the most common/cheapest material be implemented as a substrate, the most obvious candidates are newspaper and common printer paper. Interestingly the surface resistivity appears to remain roughly constant between a glossy brochure substrate and standard printer paper. This suggests that the mathematically fit relationship provided by Siegel (see EQN (5-3)) should be relied upon only as an initial gauge and further experimentation is necessary to determine an optimum

material. The benefit of using printed paper (or preferably a less processed version thereof) is that it will contain far less contaminants and artificially introduced property enhancers as well as being cheap and always readily available.

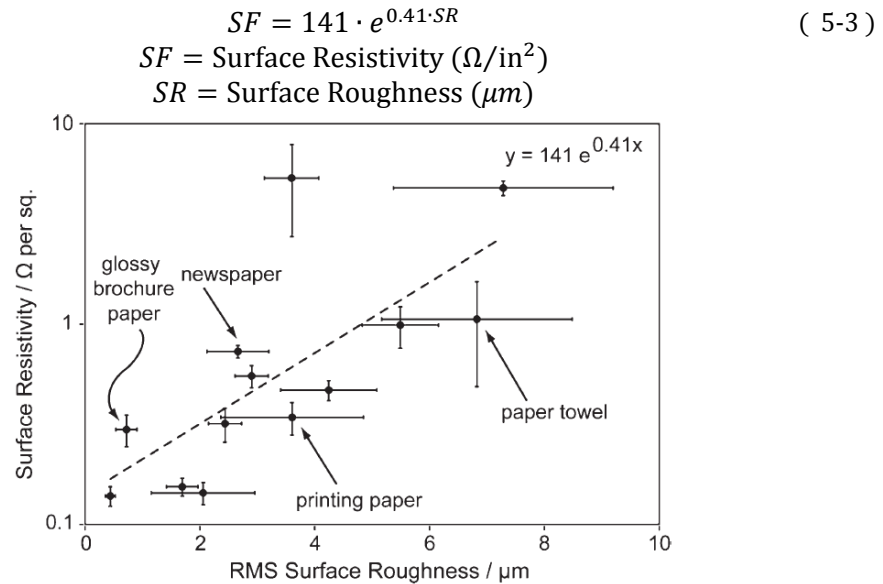


Figure 5-2 Surface Roughness Against Surface Resistivity [12]

Siegel also provided experimental data on the reduction of conductance with repeated folding – the data is shown in Figure 5-3. This was not developed into a theoretical model as the intention of design in the case of the disposable MAV is not to have folds repeated. This is of course relevant to many other applications however and is provided here for reference [12].

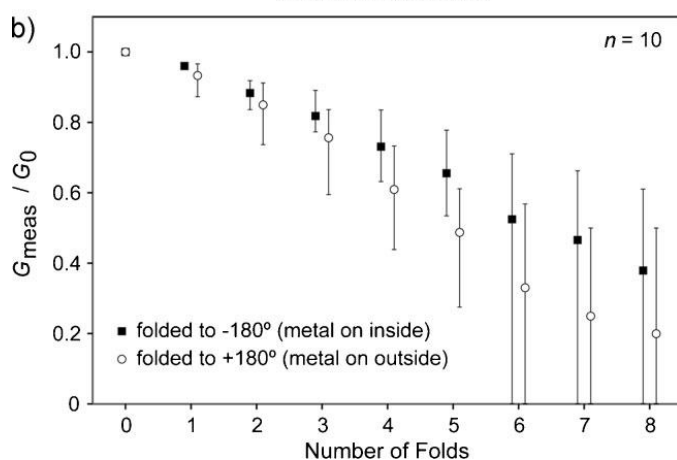


Figure 5-3 Proportional Change in Conductance Against Fold Iteration

5.2 NANO-PARTICLE LOW TEMPERATURE SINTERING

Relate it to soldering temperatures, discuss possibility of evaporation deposition circumventing this but how that's not necessarily amazing as paper can be made to withstand the higher temperatures and high temperatures are needed for soldering anyway

The inherent flexibility, ability to be passed through small apertures, reduced conductance from bulk and difficulty with soldering concerning commercially available silver particle solutions can be

explained by the way in which the nano particles are formed. In a 2010 paper published by German researchers Perelaer and Schubert, the process by which electrical connections are made in a nano-particle based silver suspension is explained thoroughly (including methods of allowing for low temperature sintering) [44]. A very informative diagram from the paper is provided in Figure 5-4. In short, the paper outlines how the silver particles are highly capable of being encapsulated into a chemically generated ‘shell’ which allows for extremely small particles to be formed that would otherwise coalesce due to the massive reduction in melting temperature at these scales.

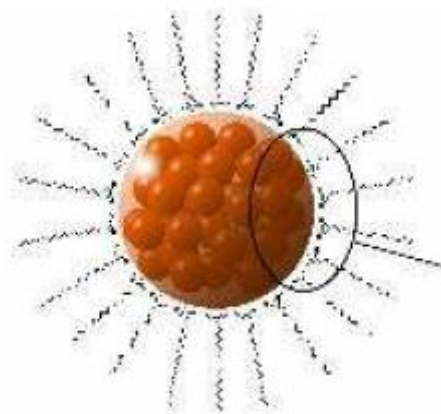


Figure 5-4 Silver Nano Particle with Carbolic Acids as Capping Agent

These individualized particles form the silver precipitate present in the varnish suspension. Copper and other metals are less capable of achieving this chemical state and so paints and varnishes are much more prone to coagulation and ‘glugginess’. However the downside of having these isolated particles is that bonds to the conducting path as a whole are far less strong and the particles are easily capable of achieving melting temperature once this capping agent is broken down. It is for this reason that when presented to a molten solder globule, the silver particles will tend to coalesce into the solder and pull themselves from the relatively weak bonds holding it into the cellulose matrix [44].

However, as soon as the bonds of this capping agent are broken, the Silver particles can readily form into one another. This allows a densification of the conductors at a temperature well below that of the bulk melting temperature – allowing for conductance comparable to that of the bulk material. This process has not been explored in this project but should be considered in larger scale manufacturing as it can possibly reduce the requirements on the Silver suspension immensely.

5.3 DYNAMIC CONTROL POWER CONSUMPTION

Note that the following analysis does not take into account the use of a GPS module which will greatly affect the outcomes once implemented.

A point of potentially very high significance is that dynamic control may be entirely out of scope for the majority of long range flights of the disposable MAV due to power restrictions. As outlined in Section 4.2.1, the proposed actuation method of rear control surfaces is a magnetic coil device having a series resistance of 150Ω . Assuming the system is powered from a single cell regulated to 3.3V and conservatively taking the average control force percentage to be 5% of the maximum,

EQNs (5-4) and (5-5) give an estimation of average power consumed. This power draw is still very significant when compared to the allowable energy from micro lipo single cells.

$$P_{\max} = V^2/R = 3.3^2/150 = 72.6\text{mW} \quad (5-4)$$

$$P_{ave-elevon} = P_{\max} \cdot 0.05 = 3.63\text{mW} \quad (5-5)$$

The MPU9150 does not provide operating currents for implementing the DMP motion fusion but does provide average current consumption for the case of Gyro + Accelerometer (Magnetometer and DMP disabled) and Magnetometer only at 8Hz sampling (DMP, Gyro, and Accelerometer disabled). The total current consumption of the MPU9150 is conservatively assumed to be the summation of these two values in the calculations shown in EQN (5-6).

$$\begin{aligned} P_{ave-MPU} &= IV = V(I_{mag} + I_{accel+gyro}) \\ &= V(3.9 \cdot 10^{-3} + 3.5 \cdot 10^{-4}) = 14.025\text{mW} \end{aligned} \quad (5-6)$$

The microcontroller itself is partially variable to the final choice in processor but for now calculations will be performed on the chipset included into Prof. Pounds original control circuitry, the PIC16F87X [6]. A more significant factor on power consumption from the Micro Processing Unit (MCU) is the clock speed at which the system will operate. EQNs (5-7) and (5-8) give estimations on current consumption based upon clock speeds of 4MHz and 32kHz as average values are provided in the datasheet at these speeds.

$$P_{ave-MCU32\text{kHz}} = IV = 6 \cdot 10^{-4} \cdot 3.3 = 1.98\text{mW} \quad (5-7)$$

$$P_{ave-MCU4\text{MHz}} = IV = 2 \cdot 10^{-5} \cdot 3.3 = 0.066\text{mW} \quad (5-8)$$

For comparison, the original prototype designed by Prof Pounds [6] was designed to be powered from a 25mAh single cell lipo weighing in at ~1g. EQN (5-9) demonstrates that under the suggested conservative assumptions on power draw shown in EQN (5-8), the MAV could only last 3.86 hours assuming 32kHz MCU clock and no power draw from the DMP or 3.55 hours assuming 4MHz MCU clock and no power draw from the DMP.

$$\begin{aligned} T &= \frac{E}{P_{ave}} = \frac{3.6 \cdot CR \cdot V}{(2 \cdot P_{ave-elevon} + P_{ave-MPU} + P_{ave-MCU32\text{kHz}})} \\ &= 1.4 \cdot 10^4 \text{s} = 3.86\text{h} \end{aligned} \quad (5-9)$$

$$\begin{aligned} T &= \frac{E}{P_{ave}} = \frac{3.6 \cdot CR \cdot V}{(2 \cdot P_{ave-elevon} + P_{ave-MPU} + P_{ave-MCU4\text{MHz}})} \\ &= 1.3 \cdot 10^4 \text{s} = 3.55\text{h} \end{aligned} \quad (5-10)$$

T = Operating Time, E = Batt. Energy

CR = Current Capacity Rating of Battery

5.4 AERODYNAMICS

Analyses into the effect that delta wing leading edge vortices have upon the aerodynamics of the craft have been thoroughly investigated. Some research has even been performed on the applicability of this work to the standard ‘paper dart’ and how its aerodynamic properties could be

predicted or improved [45]. The standard planar airfoil lift theory calculates the lift and drag forces on a wing as in EQNS (5-11) and (5-12).

$$\text{Lift} = c_l(\alpha) \frac{1}{2} \rho c l v^2 \quad (5-11)$$

$$\text{Drag} = c_d(\alpha) \frac{1}{2} \rho c l v^2 \quad (5-12)$$

c_l = dimensionless lift coefficient, c_d = dimensionless drag coefficient, ρ = air density,

c = chord length, l = wing length, v = relative air speed, α = angle of attack

Polhamus provides an estimation to the vortical lift effect on a delta wing by supplementing the planar airfoil lift theory [46]. In this he splits the lift coefficient into the summation of individual planar and vortical coefficients c_{lp} and c_{lv} respectively.

$$c_l = c_{lv} + c_{lp} \quad (5-13)$$

$$c_{lp} = k_p \sin(\alpha) \cos^2(\alpha) \quad (5-14)$$

$$k_p = 4 \tan^{0.8} \left(\frac{\pi}{2} - \Lambda \right) \quad (5-15)$$

$$c_{lv} = k_v \sin^2(\alpha) \cos(\alpha) \quad (5-16)$$

$$k_v = (k_p - k_p^2 k_i) \cdot \frac{1}{\cos(\Lambda)} \quad (5-17)$$

$$k_i = \frac{\partial c_d(\alpha)}{\partial c_l(\alpha)^2} \quad (5-18)$$

Λ = leading edge sweep angle

Where k_i is the induced drag parameter [46].

NOTE: air density cannot be substituted as a constant due to the huge range of altitudes to which the glider will be subjected. Instead, pressure values can be estimated from a conversion between altitude and pressure as given in EQN (5-19) which was taken from a paper released by the Portland State Aerospace Society [47].

$$P = 100 \cdot \left(\frac{44331.514 - z}{11880.516} \right)^{1/0.1902632} \quad (5-19)$$

P = Pressure (Pa), z = Altitude (m)

Table 5-2 Pressure Calc. Parameters

Symbol	Value	Unit	Desc.
P_0	101325	Pa	Pressure at zero altitude (base pressure)
T_0	288.15	K	Temperature at zero altitude
g	9.80665	m/s^2	Acceleration due to gravity
L	$-6.5 \cdot 10^{-3}$	K/m	Lapse rate
R	287.053	$J/(kgK)$	Gas constant for air
Rh	0%	Dimless.	Relative humidity

5.4.1 MASS DISTRIBUTION STABILIZATION

The mass distribution of the gliders supporting materials and control avionics together have a strong affect on the longitudinal (pitch) and spiral (roll) stabilities.

The longitudinal stability is a property determined by the centre of lift (COL), centre of gravity (COG) and trimmed rear control surfaces. In general, if the COL is located aft of the COG, the system can be made stable by trimming the rear surfaces to a set angle [48], as is the general convention with paper planes. This can be achieved purely because the system contains a summation of pitch moments equal to zero. The conventional ideal for distance between the COG and COL in a delta wing is 10% of the MAC (see Section Appendix C) which can be achieved simply by altering the position of control avionics. With this parameter set, the trim angle and size of the static rear surface for a particular desired speed and pitch angle can be calculated with moment analysis [48] as shown in Figure 5-5 (note that no pitching moment is applied for symmetric airfoils however depending on the final choice of airfoil, may be present). However, this requires accurate estimation of the lift force on the delta wing as well as the drag on the rear surface which are difficult to determine analytically with the vortex modifiers intended to be employed. Alternatives include trial and error or extensive Computational Fluid Dynamics (CFD) analysis.

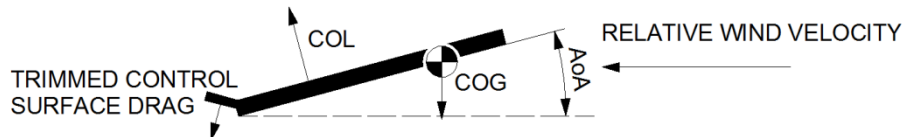


Figure 5-5 Pitch Force Analysis

The position of the COM in the yaw axis can increase or decrease spiral (roll) stability by providing a pendulum effect in the case of sideslip. This is once again a simple force balance principle in that when an aerodynamic roll disturbance is applied to the craft, it will roll about the COL. If the COG is located below this point, the perturbed sideslip configuration will generate a restoring torque as demonstrated in Figure 5-6. This implies that placing the control avionics below the lifting surface is very important as having the COG higher than the COL has an opposing effect of instability tending to flip the craft. The dynamics of this motion is further affected by the dihedral angle as described in Section 5.4.2 below.

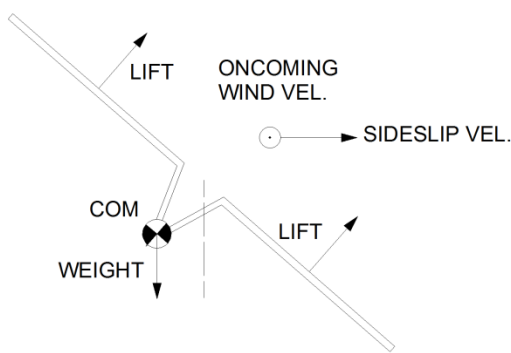


Figure 5-6 COM Restoring Roll Torque

5.4.2 DIHEDRAL ANGLE

Control of the dihedral angle as demonstrated in Figure 5-7 is very useful in increasing the passive spiral (roll) stability of a fixed-wing craft. This is a potential weak point in the low aspect ratio delta design due to the geometry of its stubby, long wings. Similar to the effect provided by a lowered COM as shown in Section 5.4.1, when a disturbance is provided to the roll of the craft, the angled lift

vectors provide a side slip condition. However in the case of a wing pair with positive dihedral, the horizontal and vertical components are no longer equal as shown in Figure 5-8. The result is an aerodynamic restoring torque that increases trigonometrically as roll angle increases (again very similar to the COM pendulum effect). The downfall of increasing the dihedral is that a proportion of lift is no longer exerting a vertical force (it is angled in to the fuselage) and is reacted by the opposing wing generating static internal forces in the frame. Therefore as dihedral angle increases roll stability will also increase but the lift-to-drag ratio and glide angle will decline. The extent to which the property should be set must be gauged through eventual accurate analysis of the lifting properties of the wing or alternatively through successive trial and error.

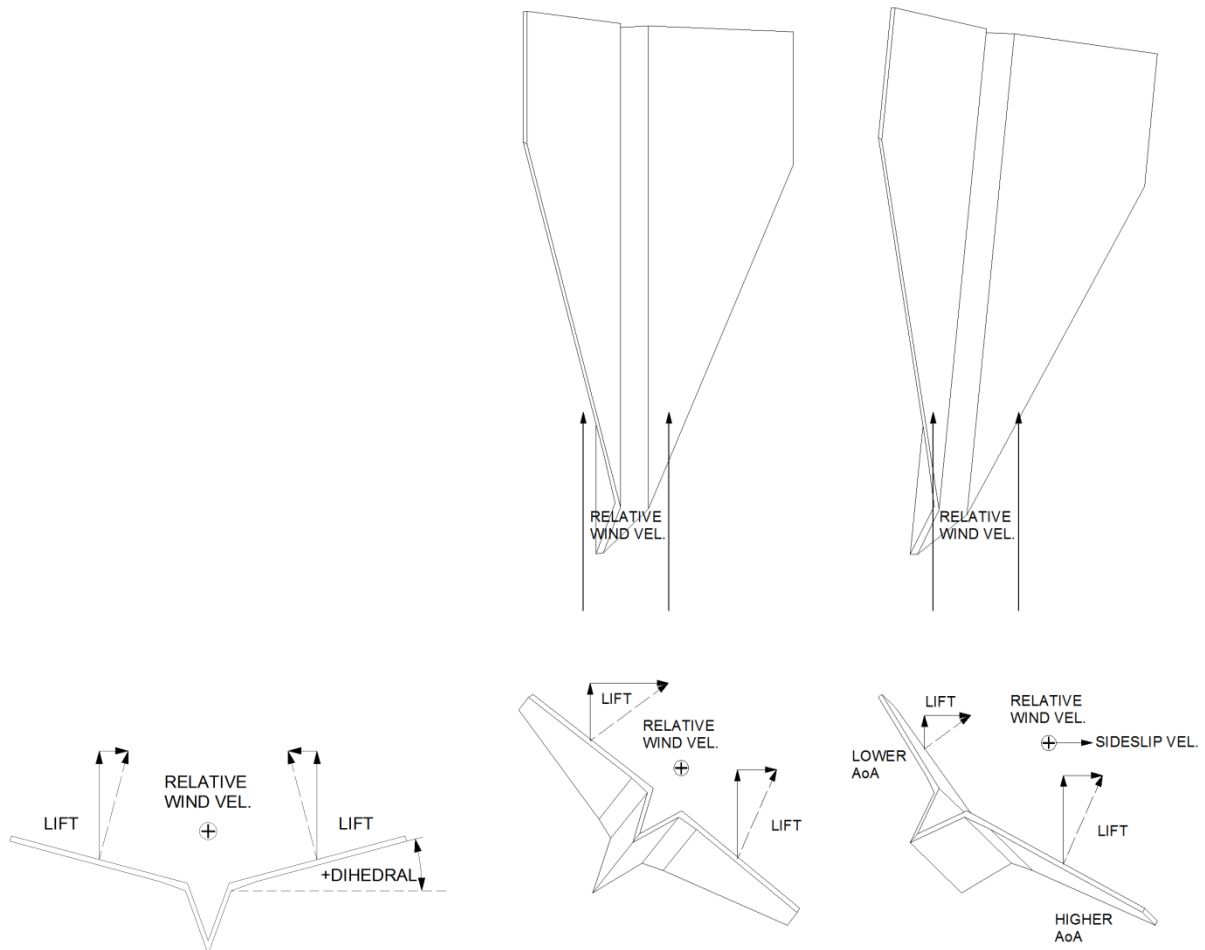


Figure 5-7 Dihedral Angle Definition

Figure 5-8 Dihedral Stability
How Roll Causes Side-Slip and Restoring Torque with Positive Dihedral

5.4.3 DIRECTIONAL STABILITY

Directional or Yaw Stability can be drawn from any vertical surface on the craft as it presents surface area and hence a drag restoring torque during a turn. In the case of the paper glider, these will take the form of rear dorsal fins and if the final design includes it, the standard paper dart 'spine' that is used to hand launch the device. Another potential vertical stabilization surface is the winglet. Winglets have also been shown to assist in stabilizing leading edge vortical flow aft of the trailing edge (see Figure 5-9, this does little to help prevent large scale separation over the wing but can reduce the vortex drag a small amount [49]. Note that the torques generated can be calculated from the general drag equation and the moment arm distances from the COG as in EQN (5-20).

$$\text{Drag} = c_d \frac{1}{2} \rho v^2 A \quad (5-20)$$

$c_d = 0.8$ for angled flat surface, A = Presented SA

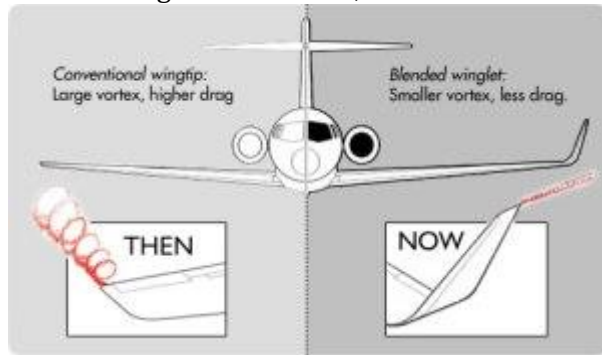


Figure 5-9 Diagram of Vortex Alteration from Winglet Shape [49]

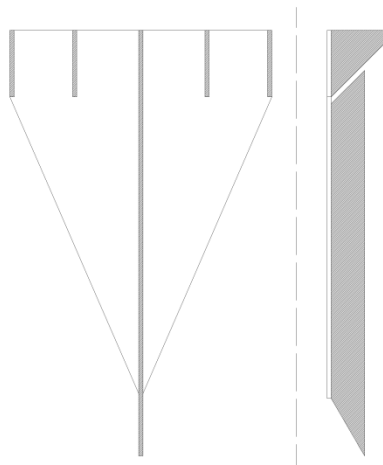


Figure 5-10 Example Vertical Stabilizers
Bottom and Side View of Delta Wing

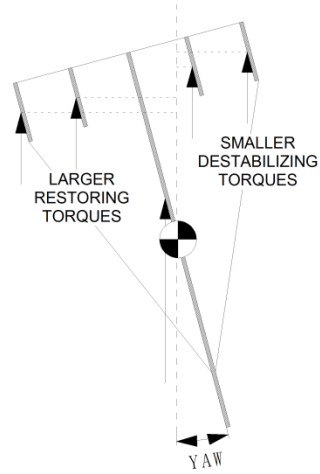


Figure 5-11 Torques Generated by Yaw Perturbation

5.5 MECHANICAL PROPERTIES OF PAPER

Take stuff and cite from Paul's paper, don't really need more than what he has I think.

The following section is a paraphrasing and in some cases direct extracts from a paper released by Prof. Pounds that best covers this topic in the context of the application [6].

Paper is generated as a disorganized cellulose fibre array that allows it to maintain relatively high tensile strength isotropically. This can be up to as much as 30GPa (comparable to some low-end carbon fibre) but is typically similar to that of oak or medium density fibreboard (MDF), being ~2.5GPa [50]. Densities of paper specifications are designated in industry as “grams per square-meter” or GSM with standard office paper generally considered to be 90 GSM with a thickness of 0.11mm. “The specific strength of paper (tensile strength per unit mass) is 30 kNmkg⁻¹, superior to that of some aluminium. The density-cubic specific modulus of paper which dictates bending performance is approximately 3.4 m⁸kg⁻²s⁻², very close to the 3.5 m⁸kg⁻²s⁻² of aluminium [50]” [6]. Ideally bending stress applications such as cantilever fuselage construction would be performed by carbon fibre reinforced plastic (CFRP) due to its significantly superior bending performance. However, extremely high labour requirements (and associated costs) involved in its construction push it out of scope for a disposable craft. A potential alternative is to include a single extremely

thin carbon fibre rod (~1mm OD) along the trailing (and potentially leading) edge of the craft with the drawback of violating the design principle of biodegradability.

“In comparison with these other popular UAV materials, paper weighs less, has comparable tensile strength and specific strength, and is competitive in bending strength. Paper clearly outperforms polystyrene, a common light-weight UAV and radio-controlled aircraft material. The major weakness of paper is in its low stiffness” [6]. The reduction in stiffness can however be shown to be a non issue with great reduction in scale. The bending stress of a wing in stable flight can be given by EQN (5-21).

$$\sigma = \frac{L \cdot l}{2J} z \quad (5-21)$$

z = vertical deflection at wingtip, L = lift force
 $l/2$ = bending moment arm, J = second moment of area

If the cross-sectional profile of the wing is approximated to a rectangle, the second moment of area can be approximated as in EQN (5-22).

$$J_{xx} = \frac{c \cdot h^3}{12} \quad (5-22)$$

c = chord length, h = airfoil thickness

The lift L on a single wing at a cruising state will be equal to half the mass of the craft, therefore the value scales with the cube-law to a linear dimension. If the craft is then considered to be scaled down proportionately by a linear factor of x , the corresponding linear values z, c, h and l are all scaled by x . This leads to the relation shown in EQN (5-23).

$$\sigma \propto \frac{x^3 \cdot x}{x \cdot x^3} x \rightarrow \sigma \propto x \quad (5-23)$$

This demonstrates that the bending stress experienced by a scaled MAV will reduce proportionally to its linear size, reducing dependence upon bending strength. “Consequently, vehicles at a diminishing scale (such as paper craft and insects) can exploit materials that would be insufficient for larger scales - any material could be used, provided the vehicle designed is sufficiently small. In practice, paper and card stock have proven to be excellent substances for small fabrications [12]. Furthermore, the fixed thickness of paper stock means that in practice decreasing the scale a paper aircraft wing is not accompanied by decreasing thickness; thus, the effective rigidity of a paper aircraft will greatly exceed that anticipated by cubic variational analysis.” [6].

5.6 PATH PLANNING POMDP SEARCH

Talk about policy iteration as where the main focus should be, maybe also touch on value iteration. Discuss how reward functions can be estimated according to the summation over all parameter reward values. Discuss interpolation between data points as well as reducing memory requirements by performing sampling in the data space as well as the belief space.

As discussed in Section 4.3.1, a Markov Decision process has been proved to be capable of searching through a discretized parameter space (such as wind vectors) in order to optimize a trajectory. In practice with the disposable MAV, it is not possible to have a constant feed on its exact position as

calls to the GPS and to a lesser extent other sensors are extremely power consuming. Instead coordinates must be verified at only key increments throughout the flight with positional data being dead-reckoned from these points using known assumptions on wind speed and/or data from the IMU. This forces a partial observability (hence Partially Observable Markov Decision Process or POMDP) over the problem which increases computational complexity but also allows for potentially vastly superior power efficiency. This also requires the algorithm operate in a space of probability functions of ‘belief’ over each potential state or a belief space.

First a set of reward functions must be generated for the purposes of quantifying the cost of every action taken as well as the reward from achieving goals. To enable the algorithm to incorporate costs of performing actions (regardless of their outcome) the reward must be a function of both the belief state space and the action taken. For the purposes of the disposable MAV the only positive reward is gained from touching ground within a particular radius of the intended destination, the costs can be derived from a variety of sources including:

- Relative humidity or probability of precipitation in regions would incur a severe penalty due to potential craft and electronics damage.*
- High vorticity winds could incur a minor penalty as their direction is far less able to be predicted.*
- High speed winds could also incur a minor penalty due to loss of control conditions in and potential damage to the craft.*
- Cloud cover could in future be used to induce penalty in order to ensure solar generation panels have sufficient incident radiation.*
- Making a turn maneuver would incur a reasonable penalty due to the power cost in operating the control flaps. †
- Similarly a call to GPS requires vast amounts of energy and should have a heavy penalty associated. However this action will also have the effect of collapsing the belief space to a tight distribution over the actual position of the craft. †
- Polling of the IMU will also have an associated minor penalty but can be modeled to restrict the expansion of the belief space in the corresponding time step. †

* These reward functions are invariant to the action taken.

† These rewards are invairant to the current belief space.

These individual parameters must each be generated by their own functions with the total simply being the summation as demonstrated in EQN (5-24). It should also be noted that

$$R(b, a) = \sum_i R_{param-i}(b, a) \quad (5-24)$$

b = belief space, a = action
 $R_{param-i} = R_{GPS}, R_{IMU}, R_{cloud\ cover}, \dots$

Next the probability distributions for the outcome of each action as well as the probability distributions for parameters such as wind direction must be quantified. Unfortunately these must

often be experimentally determined, particularly the distribution of outputs for a given action³. One example for predicting the distribution of wind given it is measured (or predicted) to follow a particular direction is provided in a paper described in Section 4.3.1 by Wesam et. al. In their paper, the wind is simply assumed to be distributed over a scaled normal distribution from the provided direction as shown in Figure 5-12. Further research into the distributions for different actions and data points provided by the GFS is certainly required before this section of the project can be expanded further.

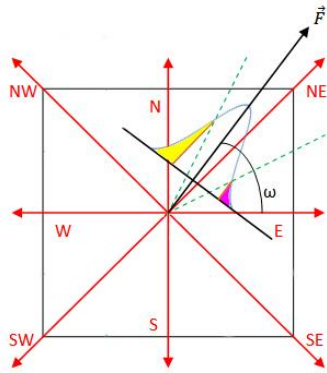


Figure 5-12 Gaussian Distribution of Wind Vector [41]

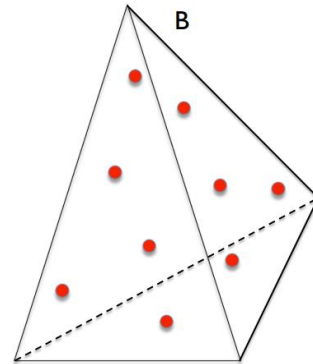


Figure 5-13 Sampling within the Belief Space to Reduce Computation [51]

There are two potentially viable solutions to generating an optimal trajectory given the above information: expected value iteration and policy iteration over the belief space. Due to the extremely vast quantities of data being used, it is recommended that a method is implemented of effectively reducing the resolution of data and using this in a value iteration algorithm. This can be achieved using EQN (5-25) along with restricted sampling of the belief space as visualized in Figure 5-13.

NOTE: Pseudo-code for POMDP value iteration

```

For all b {
    Initialize  $V^0(b) = \min_a(R(b, a))$ 
    Loop {
        For all b {
             $V^{t+1} = \max_a(R(b, a) + \gamma \sum_{b'} T(b, a, b') V^t(b'))$ 
        }
    } Until  $|V^{t+1}(b) - V^t(b)| < \epsilon$  for all b
     $V^i(b)$  = Expected reward value at belief space  $b$ 
     $T(b, a, b')$  = prob. of  $b'$  given action  $a$  is taken at  $b$ 
     $\gamma$  = finite Horizon reduction factor
  
```

[51]

Once a sufficiently reduced space can be used to generate an optimal policy, a method of cutting down the policy further must be created in order to allow for the computational space of an embedded chip to handle it. It may be that a small external memory chip can be added to the system if absolutely necessary.

³ For example if the plane attempts to turn left to exactly 15° it may actually finish the manoeuvre somewhere between 10° and 20° centred at 15°.

There remains a large amount of work to be performed on this topic and it may be a sufficiently challenging project in its own right. Future iterations may be forced to recruit more researchers to this specific topic or drastically simplify the approach.

6 IMPLEMENTATION AND DISCUSSION

The author sought to perform as much work as possible in order to develop a set of manufacturing processes and design principles to generate test platforms with as much functionality as possible. Ultimately the first goal of generating a functional printed circuit board onto a paper substrate proved vastly more difficult and involved than originally anticipated. This led to a dominance of the experimentation and processes explored to focus heavily around paper PCB manufacturing.

In addition to this, extensive research was performed into aerodynamic design principles that could be incorporated into the mechanical form of the glider (as outlined in Section 4.2). Due to time restrictions of the project and priority in circuit manufacture, these were not fully explored, with only the transverse vortical generation of the dragonfly airfoil being developed to a functioning prototype (along with other minor prototypes).

The following section outlines the experimental processes undertaken to arrive at the final prototypes as well as providing a summary of what is recommended to be done next in continuation of the project.

6.1 CONDUCTOR APPLICATION METHOD

Following from the conclusions drawn from research on the direct applicability of various application methods presented in Section 4.1, it was determined that the only technologies that are currently in a state to be immediately extended to functioning prototypes were:

- Stenciled spray deposition using aerosols and atomizing pressure sprays
- Stenciled evaporation deposition under high vacuum
- Inkjet deposition of precious metals

However inkjet deposition at its state in early 2013 was beyond the cost requirements of larger PCBs let alone disposable applications. Evaporation deposition required very costly machinery as well as being too slow to be able to generate large quantities.

A brief description of some other methods that failed entirely is provided in Section

6.1.1 EVAPORATION DEPOSITION

In an ideal situation the author would have preferred to have further developed evaporation deposition strategies as they have provided extremely promising results in producing resistances approaching that of bulk metal material. If the process could be developed to a point of being able to produce large quantities in adequate thicknesses, evaporation deposition could be the ideal conductor application method most specifically in disposable applications. However, the requirements of a very high vacuum generator as well as other special equipment and associated hazards, this process was simply out of scope for this project. The author fully intends to further research on this topic and there also exists ‘enthusiast researchers’ that are providing valuable insights into the process with their own experiments [52].

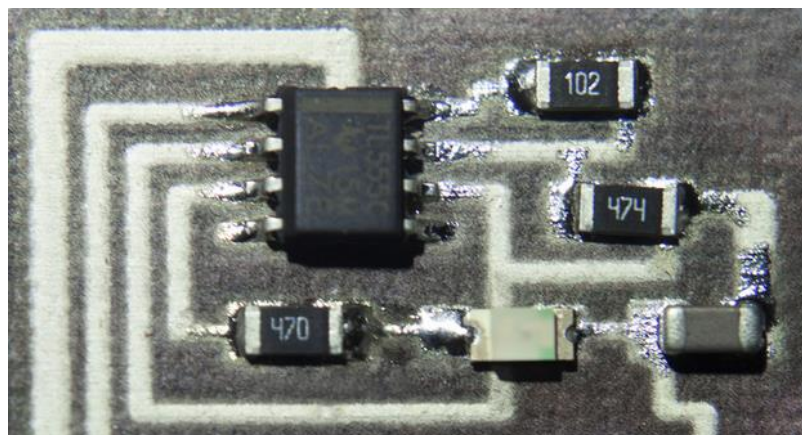
The major benefits and drawbacks of the inkjet deposition method are summarized in Table 6-1 Evaporation Deposition.

Table 6-1 Evaporation Deposition

POSITIVE	NEGATIVE
Very high conductance achievable allowing for non-precious metals to be used as conducting material.	Very high initial investment required for machinery.
It is hypothesized that given the densified microstructure of patterned conductors, soldering could be applied very effectively provided solder pads can be thickened appropriately.	Machinery (including but not limited to vacuum chamber) presents high safety danger.
High resolution achievable for any material that can be evaporated. Resolution limited only by stencil.	Material can only be deposited in a very slow fashion and production size is limited to the size of the vacuum chamber.

6.1.2 SELECTIVE INKJET DEPOSITION

Inkjet deposition has also had a mild breakthrough towards direct marketability in recent months through the Brisbane based startup company Cartesian Co. During the start of this project, development on functional prototypes had only just begun but during October 2013 the development team with minor assistance from the author has been able to easily (with little to no human labour) produce circuits onto thick poster card that is capable of supporting SOIC components and with a sufficient conductance to allow digital communications. Of even greater importance is that as long as correct practices are maintained, the circuits can be readily reflow soldered with a comparable success rate due to the unique microstructure produced from the machine. The author intends to continue work with the Cartesian Co. team to further develop the process and increase resolution. This method is currently fully capable of producing good quality circuits onto a paper substrate provided the design does not require finer pitch components than SOIC. An example is provided in Figure 6-1 in which a simple analog 555 timer circuit has been reflow soldered to thick card with a handheld soldering gun.



**Figure 6-1 Inkjet Produced Circuit from Cartesian Co
Presented Here With Permission**

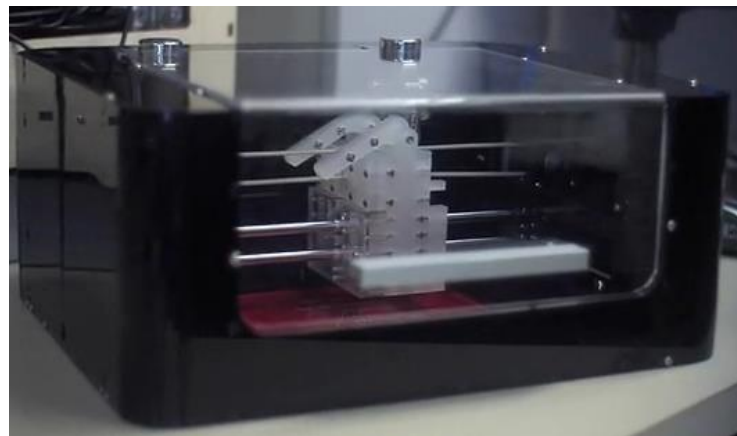


Figure 6-2 The EX1 Circuit Printer by Cartesian Co.
Presented Here With Permission

The major benefits and drawbacks of the inkjet deposition method are summarized in Table 6-2 Inkjet Deposition.

Table 6-2 Inkjet Deposition	
POSITIVE	NEGATIVE
Process is almost entirely automated, does not require skilled technician to operate.	Process can only be currently used with a single conducting material – Silver generated from Ascorbic reaction with Silver Nitrate.
Silver Nitrate powder and Ascorbic acid can be used to generate inks much less expensively than metallic colloidal inks.	Process is slow to build up adequate conducting paths – though this can be largely mitigated through having the production automated.
Machinery will be available for private purchase at less than \$1,200 AUD in the coming months.	Limitation to achievable resolution at current stage – this is however projected to improve during 2014.

6.1.3 SPRAY DEPOSITION

The actual prototypes demonstrated throughout the paper were produced using an atomizing pressure spray method that in the author's case took the form of a simple hobby airbrush and compressor. This method requires virtually no high cost equipment nor serious operational danger and can generate very high resolution artwork that is limited purely by the stencil resolution in conjunction with the conductor microstructure. Lending to this, the author was able to personally produce prototypes of one sort or another in excess of 50 individual circuits, refer to Figure 6-3 for an example. Without this availability or ease of production many subsequent tests would not have been possible.

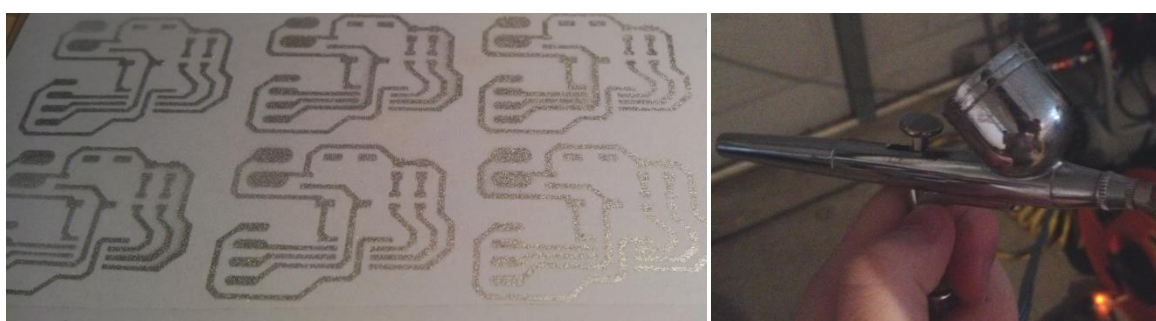


Figure 6-3 Airbrush Spray Deposition

LEFT: Patterned Circuit Produced with Airbrush Spraying, RIGHT: Airbrush Used for Spraying

The major benefits and drawbacks of the spray deposition method are summarized in Table 6-3 Spray Deposition. For a detailed explanation of the final prototyping method using spray deposition, refer to Section Appendix A.

Table 6-3 Spray Deposition	
POSITIVE	NEGATIVE
Does not require expensive, dangerous or difficult to acquire machinery. Full process can be undertaken in a matter of minutes.	Limitations on the type of conductor that can be patterned. The material must be capable of evenly flowing through a tiny aperture (ideally 0.2-0.3mm) without clogging the needle release system. The only readily available material capable of this was expensive micro-particle silver suspension varnish.
Conducting tracks exhibit flexibility well above that expected from bulk material.	The microstructure from materials that can be readily sprayed does not natively support soldering as is explained in Section 6.3.2.
Thickness of tracks can be increased very easily and quickly to improve conductance. Other simple post-processing methods can increase conductance by up to a factor of 8.	Conductance produced is well below that of bulk material without potentially substrate damaging sintering processes.

6.2 CONDUCTOR MATERIAL TESTING

After spray deposition (and later inkjet deposition as an alternative) was chosen as the application method, there remained only two choices as a conductor material: copper and silver. Before this was finalized however, a wider range of options were explored in the context of separate application methods. These other materials and the reason for disregarding them is provided in Section Appendix E.

Copper – Despite silver having been proven to be ideal for deposition through restricted nozzles due to it being simple to produce micro particle suspensions (discussed in Section 5.2), copper was a very tempting material for sputter deposition. Commercially available copper conductive paint can be purchased from suppliers such as Caswell for roughly a third the price of the Silver based counterparts with an approximate price density of $\$0.025/cm^2$. The author purchased a 4oz bottle of Copper Conductive paint for $\sim \$60$ AUD and it becomes very clear when the bottle is first opened why Silver is so superior. Even with vigorous agitation and water dilution up to a ratio of 5:1, the copper paint still forms small coagulations even while sealed in the bottle, see Figure 6-4. The viscosity of the paint is simply not consistent or smooth due to the size of the copper particles. This provides a significant issue for the purposes of spray deposition with an airbrush as the material must pass through an aperture between 0.2 – 0.3mm thick as well as effectively reducing the resolution achievable. It was found that attempting to spray the paint was impossible with the given nozzle diameter even after extreme dilution, fully open trigger action and even after straining through a micro-weave. Figure 6-5 is an example of the outcome of all the experiments.

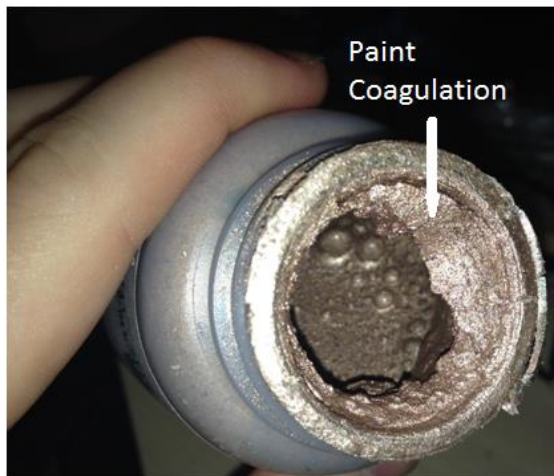


Figure 6-4 Copper Paint Coagulation

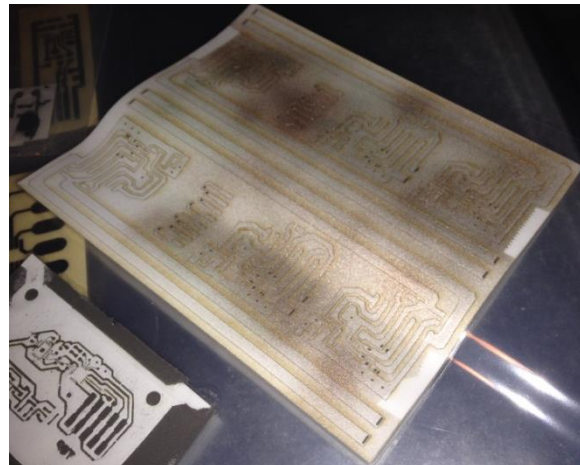


Figure 6-5 Copper Spray Deposition

NOTE: Uneven, Thin Spraying of Copper Paint Before Large Blockage Prevents Further Spray Until Vigorous Cleaning of Airbrush

The next step was to attempt to employ a High Volume Low Pressure (HVLP) paint gun to spray the copper in an attempt to see the effect of a thicker effective nozzle diameter. The HVLP operates in a very similar fashion to the airbrush but contains an effective nozzle diameter of ~3mm and sprays with a pressure of ~1-3 PSI (it also doesn't require a separate compressor device. This proved much more effective in allowing even flow of the copper but forced vastly greater volumetric flow. In a test spray (pictured in Figure 6-6), it can be seen that the minimum area sprayed at once was forced to be increased to a radius of around 400mm and so much material was laid down so quickly that the moisture began to warp the newspaper. If the process can be further perfected, it would appear to still remain ideal for mass production with the speed at which a HVLP spray gun can deliver a conductor. Conductance measured on this specimen was actually highly comparable to that of silver (the strip shown in Figure 6-7 has a resistance of 13.4Ω before any form of post-processing, almost identical to a silver spray of similar geometry before treatment); though it was difficult to gauge the volume of Copper paint that had been consumed.



Figure 6-6 Test Spray of Copper Paint using HVLP Spray Gun



Figure 6-7 Small Test Track Cut from

Finally it should be noted that solder was readily able to flow onto a sufficiently thick copper paint surface (as detailed in Section 6.3.4). These experiments suggest that the copper paints could well be a perfect substitute for micro particle silver based suspensions for spray deposition. However due to the finicky consistency and thicker viscosity, great care must be taken in its storage and

circuits can only be produced in large batches with a HVLP spray gun – approximately the surface area of an A4 sheet or bigger.

Silver - As briefly mentioned above, silver has been previously shown to be ideal for airbrush spray deposition [12]. Experimental tests showed this to be highly accurate with the final process for stencilling silver taking as little as 20 minutes from completed artwork to patterned conductor. As is fully detailed in Section Appendix A, a product named only L100 Conducting Silver produced by Kemo Electronic was found to have the ideal viscosity for airbrush without any aftermarket decanting or dilution. The material acts perfectly as an atomizing paint that dries instantly on contact with the paper, preventing any warping of the surface. Due to its microstructure of interconnecting but non-densified particles, the material is extremely flexible and does not affect the mechanical properties of the substrate. Silver particle size within the suspension is also small enough to have no effect on the resolution of the stencilling technique, leaving perfectly crisp, sharp lines. This property allows for the possibility of incorporating packages as small as the QFN form factor in future prototypes – refer to Figure 6-8 for an example. The extremely thin layer achievable in the material also lends itself greatly to pressure treatment through a stamping or rolling press – this effect is shown in Figure 6-9 and was able to reduce resistance by a factor of 3.

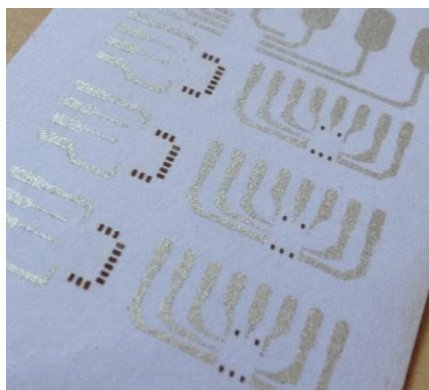


Figure 6-8 LCC and QFN Breakout Boards in Spray Deposited Silver

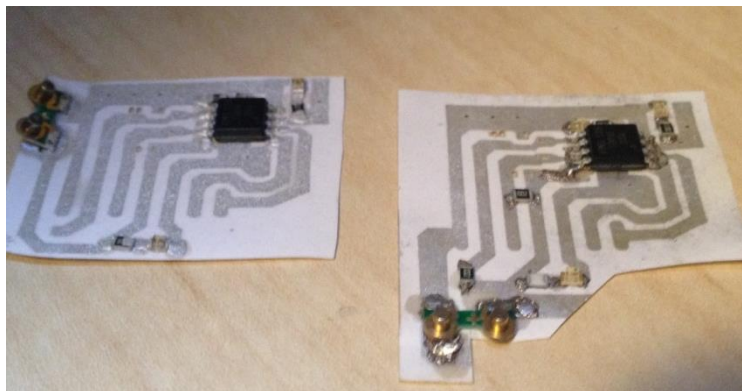


Figure 6-9 Pressure Treatment
LEFT: Non Pressure Treated, note 'sparkly' finish, RIGHT: Pressure Treated. note flat mirror like finish

The most significant limitations of the material are:

- Price – being $\sim \$0.08/cm^2$ to achieve resistances well within tolerance for digital communications.
- Agitation – Because the material used was a silver/alcohol suspension, if the mixture is left to settle, the Silver particles will gather at the base of the container. During application the suspension had to be continually agitated and deposited as quickly as possible. This prevents the material from simply being placed into an inkjet cartridge for instance. It should be noted that this problem has been solved using nano-colloids and some other chemical combinations but these require costly processing.
- Solder Flow – A significant problem that the author wrestled with for months was a way for components to be soldered to the tracks produced by spray deposited Silver. This is detailed in Section 6.3.2.

6.3 ELECTRICAL AND MECHANICAL COMPONENT MOUNTING

As touched on in Section 6.2, robust and highly conductive component mounting methods was a strong focus of the project for a wide period of time. This resulted in hundreds of small experiments taking place in an effort to allow for solder flow across spray deposited tracks. The ultimate goal was to allow for solder to flow in a similar fashion to that of copper clad fiberglass boards. This would allow for assembly methods already put in place in industry such as solder stenciling and reflow soldering to be ported directly across. Ultimately this goal was achieved in the case of both spray and inkjet deposition (solder flow across inkjet printed circuits being achieved primarily by the Cartesian Co. development team). Additionally a convincing hypothesis is proposed as to the cause of the previous failures.

6.3.1 CONDUCTIVE EPOXY

The solution that is often applied to the problem of binding components to alternative flexible substrates is simply to use a conductive epoxy [12][52]. This method is attractive because it doesn't require any heat source to cure and can provide highly conductive connections if a Silver based epoxy is used. Some research shown in Section 4.1.2 [52] indicated that this method yielded very brittle connections and was not well suited to boards that will undergo medium to high flexure around the points where components are mounted. Testing conducted by the author confirmed each of these claims through producing a set of MCU circuits with components bound only with conductive silver epoxy generated by decanting thinner from a product named CircuitWriter, see Figure 6-10.



Figure 6-10 CircuitWriter 'Pen'

The first significant point to make on the topic of using conductive epoxies to bind components is that they are extremely limiting in terms of technician skill and time required as well as the minimum achievable pitch spacing of components. In the first attempt at using the conductive epoxy, it was found that 0805, 1206 and larger components could be quite easily placed by dabbing a small pillow of epoxy onto the pad and simply pressing the component in – provided the epoxy was sufficiently viscous. However, when it came to SOIC package components, it quickly became clear that any material pushed out from beneath the pins would short all of the connections very quickly and easily (see Figure 6-11). If sufficient force wasn't applied then when the epoxy dried, the binding force to the component was minimal to non-existent.



Figure 6-11 Silver Epoxy Pin Shorting



Figure 6-12 Improved Application Method

The next natural step was to use a sharp implement to place the epoxy over the component pin and flow it down onto the track – similar to how solder flows over a pin. This was found to be possible but extremely difficult with many failed attempts produced in the process. Ultimately it was found that tweaking the consistency of the epoxy to the perfect amount was sufficient to allow for a success rate >85% but the process still took many minutes for a single component. A set of operational circuits containing an MCU and a trio of output LEDs was manufactured with this method, a microscope image of the connections is provided in Figure 6-12.

After testing these circuits for various other purposes it was found that handling them gently would eventually cause intermittences in the connections, particularly when the paper was pressed flat or flexed to a negative angle. It was found that this was caused by micro-cracks forming between the silver epoxy and the components, reapplying the epoxy would prevent the problem until it had cured sufficiently again and become brittle.

In summary, conductive epoxies are a solution to mounting components but it is severely inhibited by lacking the surface tension ‘correction’ ability that solder has as well as being far too brittle to be used in circuits intended to be flexed.

6.3.2 SOLDERERS

Make sure to discuss the difference in consistency and ability to flow between leaded and non-leaded solders but discuss the possibility of non-leaded high temperature solders potentially being feasible but approaching temperature ranges that would damage the paper. Also obviously discuss here why solders don’t work on thin tracks that aren’t completely densified

Solder is an alternative to the conductive epoxy mounting method that was as of mid-2013 not able to be used on paper based circuits (no papers, news coverage or any other examples could readily be found by the author). As mentioned in Section 6.3.1, solder allows for surface tension to draw the material to the bare conductors of components and tracks. This allows for mild realignment in components as well as not requiring paste to be placed exactly – often technicians will lay a continuous line of solder for a row of fine pitch pins (see Figure 6-13). The combination of these properties has allowed for SMD PCB assembly to become automated in all stages of production, laying paste, placing components and reflow soldering all without operator intervention.



Figure 6-13 Solder Paste Placed for Surface Tension Correction

Many papers do not explicitly state the reason that solders are not used in their prototypes and simply brushes away the subject by stating positive characteristics of epoxies. Siegel does state that rosins used in solder can wick into the paper and damage it's properties [12] – this was not found to have any detrimental effects in this case and was eventually mitigated altogether.

However applying solder to a spray deposited silver micro particle surface is not as straight-forward as that of solid copper on a fiberglass substrate. It was concluded that the micro particles of Silver precipitated to the substrate did not have adequate bonding to the papers matrix or the other particles of Silver, particularly with a thin layer. This led to the Silver particles being wicked into the molten solder rather than vice versa, leading to insulated 'halos' around solder points as displayed in Figure 6-14.



Figure 6-14 Insulating 'Halos' Generated Around Solder Points
NOTE: Also Causes Solder To Coalesce Over Component Pins

Alternately the silver particles generated from the ascorbic reaction in the inkjet deposition method are allowed to formulate in comparatively large structures. Also given that the liquid Silver Nitrate is allowed to partially wick into the papers fibrous matrix before the chemical reaction forms it into silver, it is hypothesized by the author that the bonds to the total conductive structure as well as the substrate is much stronger. This allows for soldering to be performed directly, albeit with great care – as shown in Figure 6-15. This technology was not developed to this stage until late September 2013 which is why greater focus hasn't been lent to improving resolution on these machines.

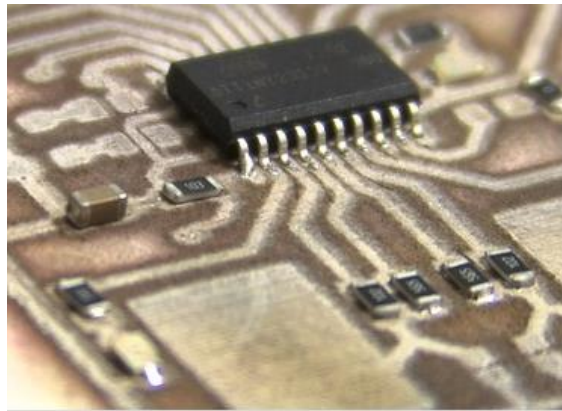


Figure 6-15 SOIC and 1206 Components Soldered to Inkjet Printed Circuit by Cartesian Co.
Presented here with Permission

As a final point, the chemical composition of the solders used should be very carefully chosen. This will control three parameters: the ability of molten solder to flow on the board, the toxicity of the solder and temperature at which reflow occurs. All experiments outlined in Section 6 used a standard Lead, Tin eutectic solder due to issues being encountered with low temperature Bismuth based solders reflowing to inkjet printed circuits. However further experiments should focus on integrating a lower temperature solder and/or a lead-free solution.

6.3.3 SUBSTRATE MOUNTING APERTURES

In an attempt to solve the originally encountered inability to solder components, the author conducted a range of experiments involving cutting various sized apertures into the substrate. This allowed for binders to be placed on the opposite face to the component and in some cases attempted to help induce solder flow along the silver tracks. The first experiment to gain some traction was cutting holes over portions of where a component's pin would sit and gluing the component the opposite side to the conducting tracks – this would allow application of conductive epoxies much more easily and sped up the assembly process mildly. An example of this process is shown in Figure 6-16 in which the silver track was actually attempted to be sprayed over the aperture as well to possibly remove any necessity of applying epoxy.

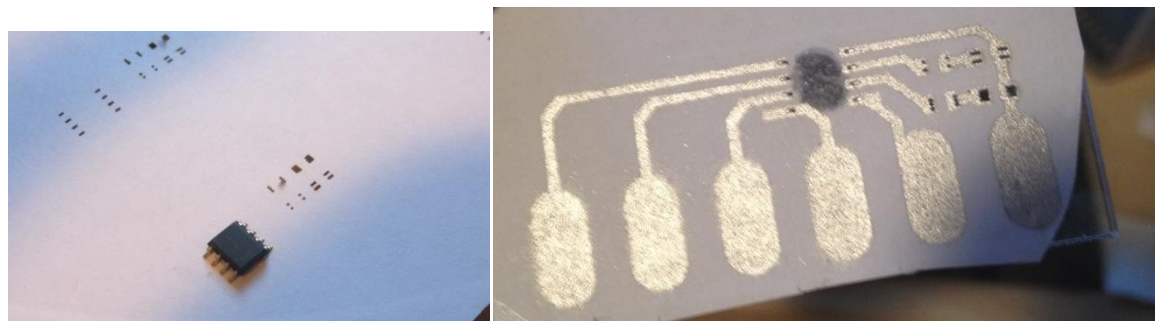


Figure 6-16 Aperture Mounting Method - No Solder
LEFT: component carefully super-glued with pins over apertures, RIGHT: airbrush spray deposited silver directly over aperture

While these methods increased the ease with which cold binding materials could be applied, it increased stress on the connections by reducing the connection surface area. This led to all connections failing very early into testing – proving that this method was not viable.

A brief mention is given to a range of experiments conducted by the author to promote solder flow over the silver tracks using apertures in the substrate. Countless configurations including solder on the same side, opposite side, both sides as well as providing an array of micro apertures, a single micro aperture, a single large aperture and every possible permutation of all these conditions were tested. One set of tests even attempted to impregnate the solder with ferritic fine steel shavings in order to draw it through the matrix with an electromagnet (it should be noted that this was unsuccessful as the shavings could not be made fine enough to even penetrate artificial micro apertures to an adequate level). An example is provided in Figure 6-17. These experiments were founded on the original belief that solder simply wasn't flowing onto the silver rather than the explanation given in Section 6.3.2. Therefore all experiments failed – they are listed here for the sake of completeness and to prevent the same process from being undertaken again needlessly.

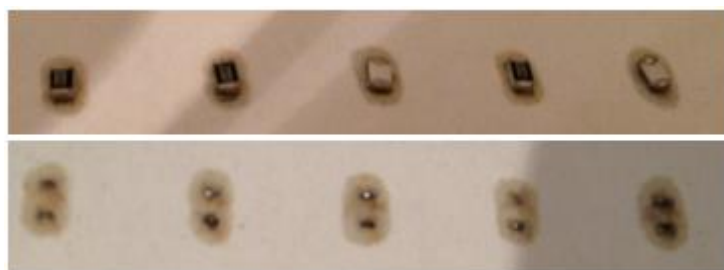


Figure 6-17 Top and Bottom View of Resistors Soldered With Aperture Based Method

6.3.4 LOW COST CONDUCTIVE PAD THICKENING

Following weeks of experimentation, a viable solution to the problem of soldering to the spray deposited paper circuits presented itself. After the parameters responsible for causing the soldering problems were identified, research began into modifying the surface of the conductors over the solder pad positions. This material coating was required to be highly conductive, curable to a solid state, have a microstructure capable of promoting solder flow and provide sufficient adhesion to the conducting surface even during flexure (implying the material be reasonably ductile).

Some brief experiments were performed into using a Nickel Acrylic mixture spray deposited using a solder stencil over the original circuit as shown in Figure 6-18. These experiments provided some mildly promising results but success in continuity from the conductor to the component pin occurred on the order of 50%.

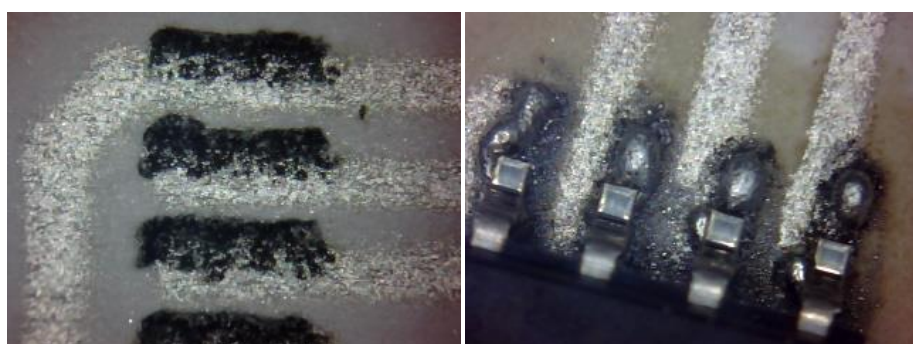


Figure 6-18 Using Nickel to Promote Solder Flow
NOTE: this stencil was applied slightly off centre

The same principle was then attempted using the Caswell Copper paint but the mixture was too thin to not short connections during the curing process. However the substance was then thickened by artificially removing some of the thinning agent using a needle after a sample was let settle for a short number of hours. This lent a paste like consistency to the material and it was able to be applied much in the same way as solder paste (of course much greater care must be taken in aligning the stencil however). As shown in Figure 6-19, this cured to a ductile, solid block as thick as the stencil material (paper in this case).

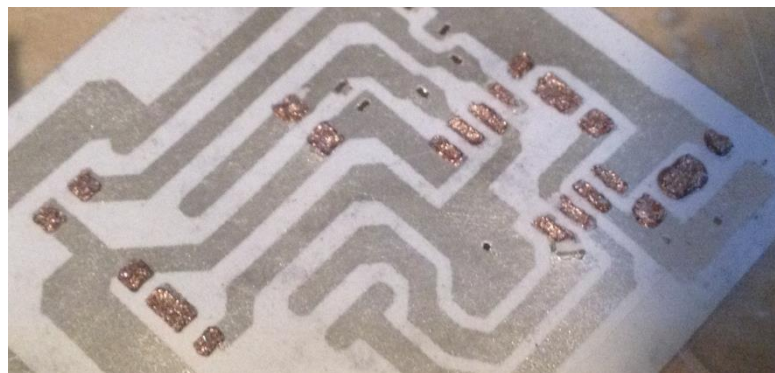


Figure 6-19 Copper Paste Coated Solder Pads to Promote Solder Flow

Owing to either the inherent particle size of the copper in the paint or the thickness with which the material was applied, solder was able to easily flow onto the surface of the copper. Figure 6-20 demonstrates a rushed prototype of this process – this prototype was reflow soldered with extreme ease and has remained fully functional even through being handled and bent/twisted by multiple individuals during a technology expo held at the University of Queensland. It is expected that the ability of the solder to flow will increase further if the copper can be laid in a slightly thinner layer and then pressure treated to provide a smooth surface.



Figure 6-20 Solder Connections made using Copper as a Flow Promotion Mechanism

6.4 CIRCUITRY ENVIRONMENTAL CONCERN REMAINING

A common factor between the two most immediately viable circuit patterning methods (inkjet and spray deposition) is that they operate most effectively using silver. Silver salts such as Silver nitrate are known to be toxic and corrosive. Environmental outcry from products that pollute the environment with silver has occurred in the recent past, most notably with a range of Samsung

household appliances that use silver nano-particles to sterilize bacteria. In reality, the most damaging silver compound is silver nitrate by a significant margin [53]. Unfortunately this does not guarantee that public outcry will not occur if a generally safe compound is produced for spray deposition.

This does however ensure that the technology being used by Cartesian Co. will probably never be suitable for disposal in the environment. The process used simply cannot avoid leaving substantial amounts of Silver Nitrate in the substrate. Some methods have been attempted to mitigate this including gently hand washing the circuit post printing but this is only applicable for non cellulose based substrates.

This information is an added incentive to develop the viability of Copper paint for spray deposition using a HVLP spray gun as well as developing the evaporation process to be more accessible. In both cases the conductor is swapped out for a less environmentally damaging element.

6.5 CURRENT AND FUTURE PROSPECTS OF AUTOMATION

The following is a brief description on the viability of automating the processes at each stage of manufacture at the current time as well as in the future.

Conductor Deposition Automation

The inkjet deposition process lends itself directly to automated and unsupervised production. The technology of the Cartesian Co. printer could simply be scaled up to print over larger volumes at a time. It is recommended by the author that other technologies be explored more thoroughly first due to the inherent environmental toxicity of Silver Nitrate.

The spray deposition method does not currently have technology directly supporting the mass manufacture of the process. It is however reasonable to relate other technologies to potentials of future technology. Most notably machines are currently operating in industry that will automatically press a solder stencil onto a PCB to automate the application of solder paste (see Figure 6-21). If a similar rigid stencil could be generated for the entire profile of the circuits conductor, a similar machine could press the mask onto a sheet of standard paper. While this occurs, an automated gantry could be fit with a spray gun of some sort to apply the conductor. A significant speed bump that would have to be overcome in this case is to have the suspension continually agitated to prevent settling or coagulation of particles.

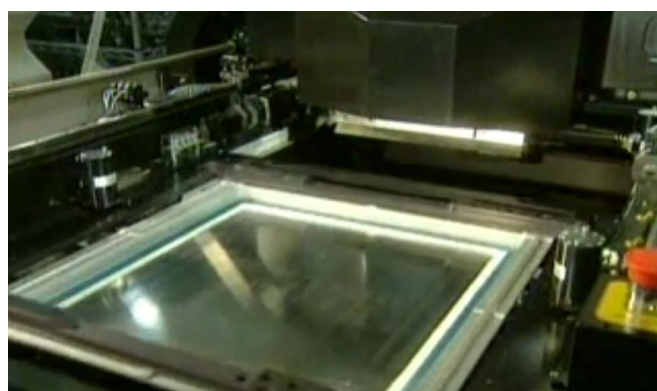


Figure 6-21 Automatic Solder Stencil Press

Evaporation deposition could undergo a similar process as spray deposition but the system would also be forced to be held under a vacuum. This severely complicates the machinery and will probably not be possible in the near future, especially without serious research funding.

Component Placement and Soldering

With the exception of the electromagnetic elevons, all other components to be included in the system will be surface mount packages. Considering Copper paste can be applied to the board in the same way as solder, the machines described above and shown in Figure 6-21 could also be applied to preparing the circuit for soldering. Following this, automatic pick and place machines could be employed to locate components and finally a conveyor reflow oven can finish the process.

Of course placement and soldering of the elevons must still be conducted by a technician (however they themselves are hand-assembled so this extra step is not so great of a gap). Any of the automation processes mentioned above could also be applied to a less extreme extent only automating small parts of the processes as is common with lower production runs.

6.6 GLIDER DESIGN

It is very clear from the reviewed literature that a generic delta shape is a practical and efficient form factor for an MAV glider. While some sources may suggest a superior option (at larger scales) would be to employ a sailplane configuration, the associated geometry is very difficult to achieve with the bending strength lent by a paper form. The leading edge vortex lift is also an effect that appears to be entirely necessary due to the inefficiency of generic planar lift at the Reynold's number values being considered.

Initial test platforms of gliders took the form of standard folded paper planes simply because they have a large and enthusiastic online community devoted to experimentally determining optimum designs. Any dart based design will almost always begin with standard 45° folds to the centre spine followed by a second pair of 67.5° angled folds, this is demonstrated in Figure 6-22. These initial folds allow the plane form to achieve a 67.5° leading edge sweep angle as well as concentrating a density of mass at the apex (note however that the COG remains at the centre of the sheet of paper).

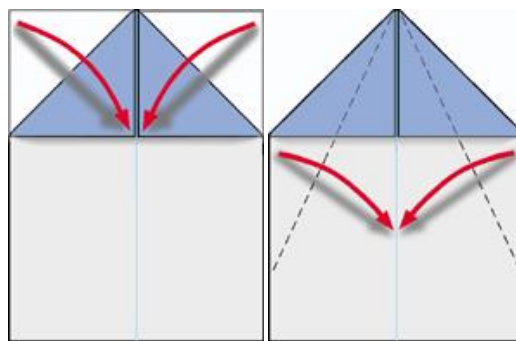


Figure 6-22 Standard Paper Dart Initial Folds

The next pair of important factors concern the roll stability of the craft. It is well known the standard paper dart contains a central spine that is generally considered to be a handle surface purely for launching the craft. Analysis presented in Section 5.4 however suggests that this surface also acts to

lower the COG and hence provide a restoring torque during roll. This was subjectively shown to be accurate by briefly testing an identical model with and without the spine handle. Incorporation of a similar design in the final glider not only to push paper mass below the lifting surfaces but also to provide a mounting surface for the circuitry lower than what would otherwise be available. This design consideration is provided in Pounds mechanical glider design in his original paper [6].

An alternate design was found online (and is purportedly very popular among casual enthusiasts) that does away with the standard central spine in place of a set of static control surfaces on the underside of the craft. This design is displayed in Figure 6-23 and a set of folding lines can be found in Section 7. The design is ‘advertised’ as being highly stable even under rough outdoor conditions, despite containing being designed with no dihedral or any forms of vortex stabilization. The results were actually surprisingly positive with the design being capable of righting itself to stable flight from any given orientation provided it has enough altitude before it hits the ground.



Figure 6-23 Alternate Paper Plane Design



Figure 6-24 Applied Positive Dihedral

Following the simple addition of a positive dihedral angle the gliders slope appeared only affected in a very minor fashion whereas the roll stability and hence ability to follow a direction was significantly improved.

The next steps taken were to attempt to graft a low Reynold’s number corrugated airfoil into this design. It should be noted that this first test example did not include a dihedral angle as it was to be used as a control experiment. The design was first generated using a vacuum former and a thermoplastic called High Impact Polystyrene (HIPS) before it was developed to be folded from flat card. An image of the CAD drawing used to generate a mould as well as the 3D printed mould in place over the vacuum former is provided in Figure 6-25.

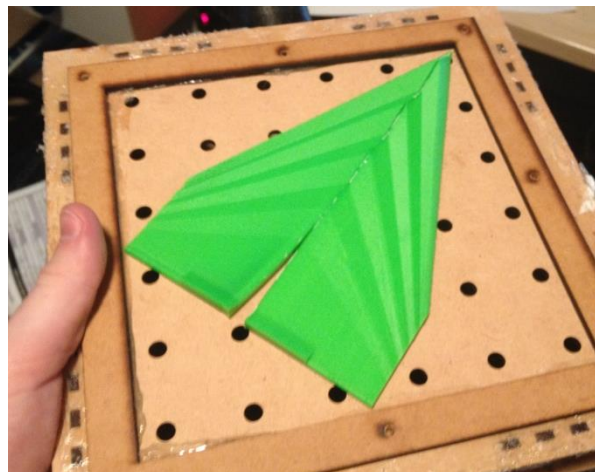
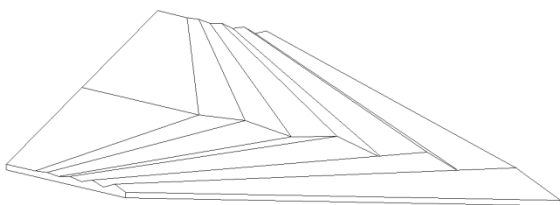


Figure 6-25 Generating a Corrugated Airfoil Delta Glider

An example of this design in HIPS as well as a card foldable version (including flat design plans) is provided in Section 7. Preliminary tests of the glider were very exciting with increased elevator trim leading to very steep angle of attack cruising configurations that could achieve very high glide ratios.

Unfortunately further development and quantifiable tests were unable to be completed as focus was pressed upon the circuit manufacture. Despite this, basic principles outlined in the Literature Review and Theory sections were experimentally shown to be accurate. Much further work can be done on improving the qualities of this design simply by employing and testing the alterations deemed applicable in the Literature Review.

7 RESULTS

The final outcomes of this project are predominantly based in the design principles and manufacturing processes optimized to the application. However a small amount of functional prototypes were generated through the course of the project and are outlined in this chapter.

7.1 ELECTRONICS

An economical and practical method of generating functional circuits in small and large quantities was produced that had the following features (example pictured in Figure 7-1):

- Repeatedly capable of supporting an LCC 24-pin package measuring 6.5x6.5x1.5mm.
- Capable of supporting reflow soldering up to and including temperatures required for standard lead, tin eutectic solder pastes. Note that thus far, only lead, tin eutectic solder pastes have been adequately explored in the final design.
- Significantly improved robustness of connections to flexure of the substrate around components when compared to conventional conductive epoxy paste methods.
- Minimum stencil feature size of $400\mu m$
- Projected cost of $\$0.08/cm^2$ when produced in batches of single prototypes without sourcing specialty chemical suppliers. This cost can also be severely reduced using the inkjet printing method with reduced resolution that is currently capable of supporting SOIC components reliably (with improvements projected for the coming months [early 2014]).

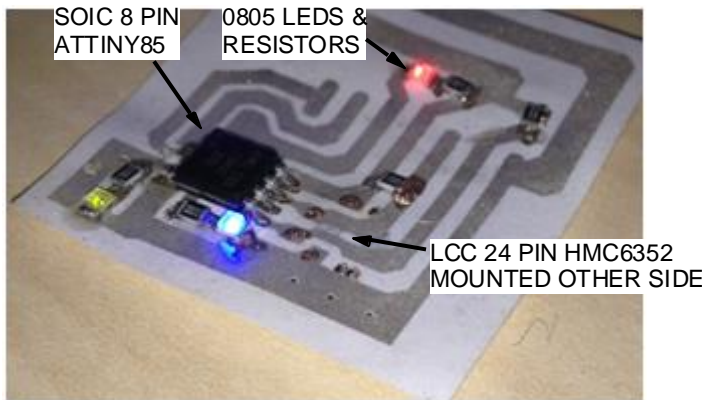


Figure 7-1 Functional Paper PCB

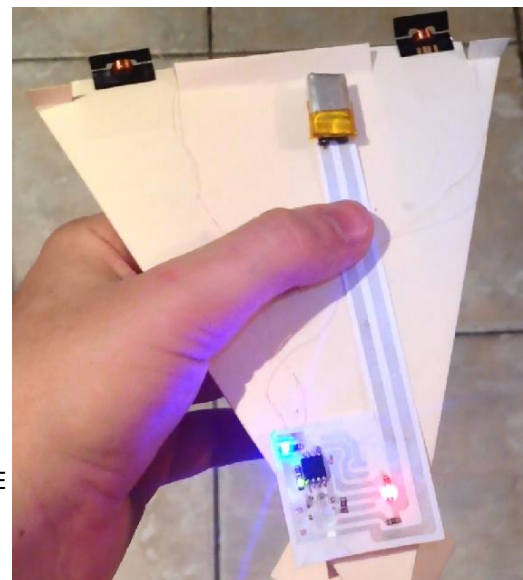


Figure 7-2 Mostly Functional Prototype Minutes Before Catastrophic Failure

The prototype shown in Figure 7-1 mounts an MCU with I2C connections to the Honeywell magnetometer module pictured (HMC6352). This prototype (as well as two others produced) was capable of communicating with the magnetometer module successfully and controlling two PWM outputs according to a PID control loop intended to align a glider prototype to a specific cardinal direction see Figure 7-2 Mostly Functional Prototype Minutes Before Catastrophic Failure. Unfortunately only a brief recording of the full system was taken before both actuators developed an unidentifiable fault causing them to cease functioning.

The I2C communications were also recorded onto an oscilloscope and are displayed in Figure 7-3. Unfortunately placing probes onto the paper circuit with a good connection proves more difficult than most generic PCBs and it is difficult to determine if the connections themselves are inducing parasitic qualities or if they are inherent to the circuit (it is also possible that the TWI interface on the attiny85 is causing discrepancies).

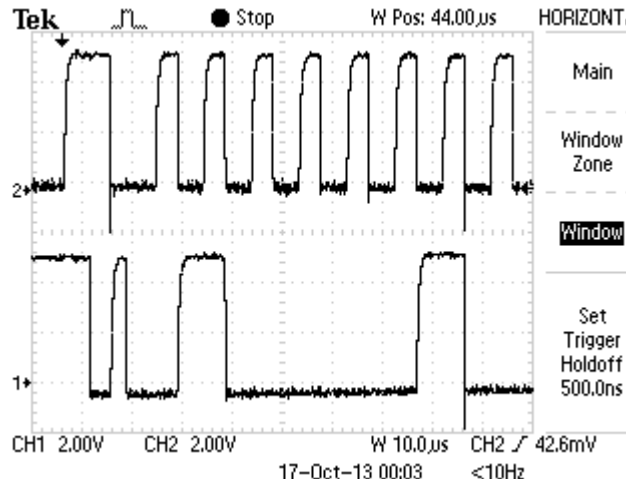


Figure 7-3 I2C Communication of Paper Circuit

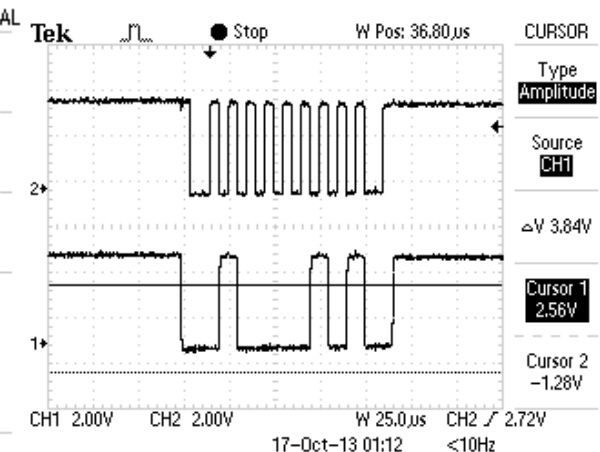


Figure 7-4 I2C Communication from Breadboard

Atmega328P for Comparison

A CAD graphic of the final design is displayed in Figure 7-5. It should be noted that the battery is designed with a significant distance from the main circuitry in the design placed onto the glider as shown in Figure 7-2 – this is due to the fact that the neodymium magnets in the battery connector as well as the elevon actuators severely distorted the readings given by the magnetometer.

NOTE: the blue squares in the graphic were originally for compression apertures to hold the components down after the circuit was laminated.

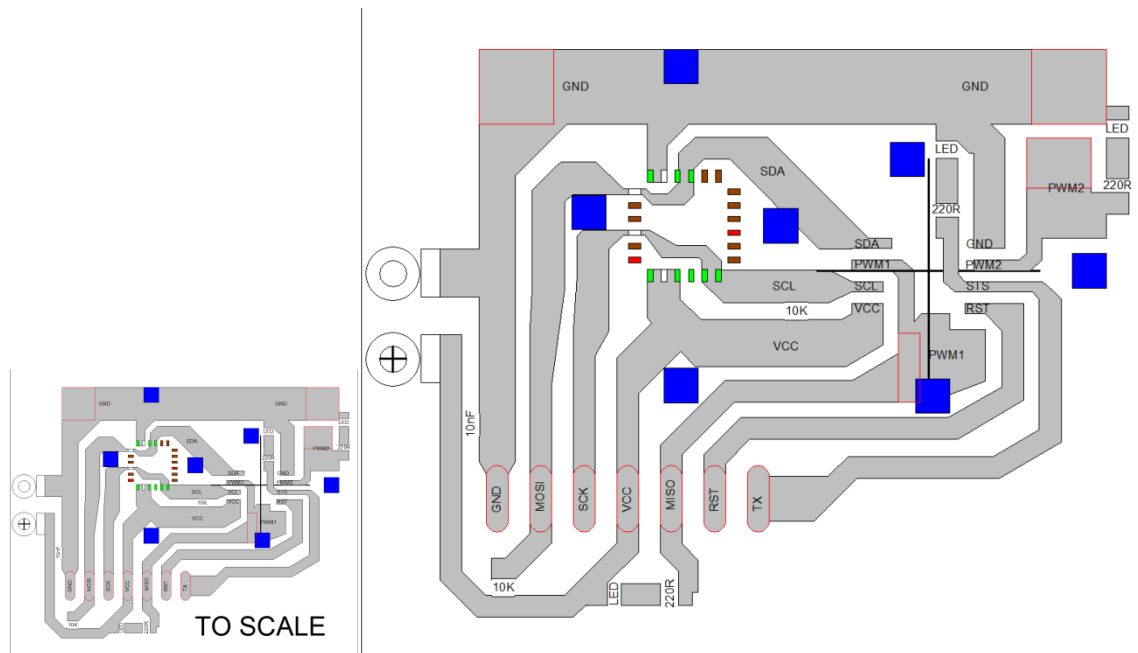


Figure 7-5 Cardinal Glider Control Circuitry

7.2 GLIDER/MECHANICAL

The final model generated in the final stages of the project is very far from a complete design. However it is capable of sustaining a noticeably harsher angle of attack than an identical form produced in flat sheet as well as a less pronounced increase in spiral stability.

There is ample amounts of further experimentation required that is largely outlined in Section 536.6. Despite this, design of the craft has comparatively much deeper wells of well developed research to draw from (as shown from the information presented in Section 4.2) and it is not expected to be as involved as developing the circuit manufacture methods, especially considering the required knowledge is all presented in this report – it simply requires someone to continue testing.



Figure 7-6 Corrugated Airfoil Delta Wings

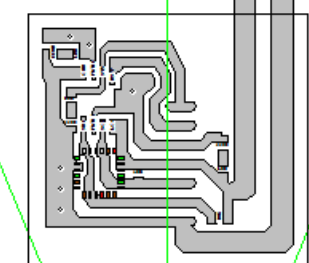
LEFT: Manilla Card Assembled Dragonfly Airfoil in Delta Configuration, RIGHT: Same Produced in Vacuum Formed HIPS

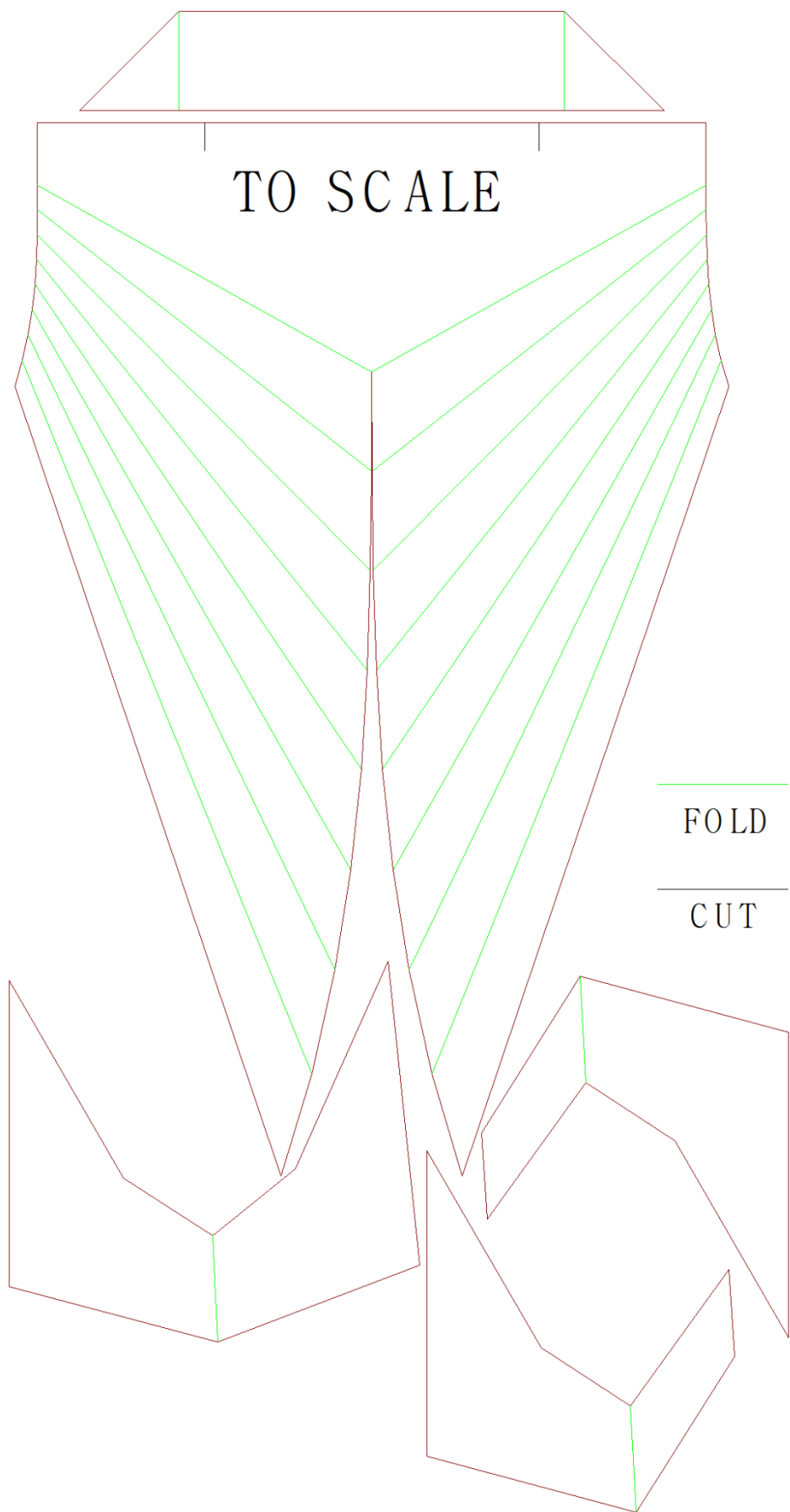
Given below are the flat sheet folding designs for the original non-corrugated delta glider (with the circuitry artwork in its intended position overlayed) along with the glider pictured in Figure 7-6 Corrugated Airfoil Delta Wings

TO SCALE

FOLD

CUT





8 CONCLUSION

This thesis has reported upon extended research, design and experimentation into the development of a low-cost, high altitude, long range, disposable UAV. Particular focus was provided to analysis and experimentation performed in manufacturing of paper substrate circuit boards appropriate to this application. Extensive research and experimental knowledge is recorded for the purposes of future development of the processes. The aerodynamic properties of how the glider operates were thoroughly investigated and widespread research on the topics of improving these qualities are concisely listed. A subset of this research was experimentally applied to a number of prototypes to evaluate their validity and a set of experiments are laid out to continue this process to further improve the system.

8.1 ACHIEVEMENTS

A final set of steps were outlined that were proved to be capable of generating fully functioning circuits capable of abilities never seen before in the academic context of paper substrate circuit manufacture.

- The final prototype circuit boards were capable of generic reflow soldering and maintaining robust connections under flexure of the substrate. The ability to reflow solder paper substrate circuits was yet to be demonstrated to the public prior to this project – it is an achievement that will hopefully spur a regaining of traction in the project.
- The ability to incorporate a 6.5x6.5x1.5mm LCC package is also a large step in the direction of ubiquitous paper based digital devices. MEMS sensors at much smaller scales had been demonstrated to be inkjet printable however research was yet to move past the SOIC package in terms of large scale component interconnection.
- The passage of digital communications through a paper based embedded device is also an ability yet to be presented in associated literature. It is a vitally important step in applying the latest technological leaps in embedded MEMS sensing and autonomous micro vehicle control to the field of disposable electronics.
- Honeywell Control and Automation Prize – UQ Innovations Expo 2013

A comprehensive set of design parameters based around the optimization of MAV delta vehicles was collected including cutting edge research being performed into ultra low Reynold's number conditions. A set of glider prototypes were built to evaluate the validity of this research.

A small number of geometric alterations were experimentally evaluated and were seen to appreciably increase the stability and overall performance of the system

8.2 FUTURE WORK

The project is far from completed and the current state suggests some natural follow on development.

Electronics

- Performing further experiments on substituting silver in the spray deposition method with copper.

- Re-evaluating and re-performing tests on generating QFN footprints implementing the latest soldering techniques described.
- Recording an analysis of more scientifically rigorous experimentation on the circuit boards now that the design process has begun to stabilize.
- Detailed environmental evaluation of the inkjet printing process to determine if it should be entirely disregarded.
- Extensive testing over a number of ultra lightweight solar panel modules.
- Incorporation of a GPS module into control circuitry.

Mechanical Form

- Performing a CAD analysis of mass distribution to determine the optimal mass to add to the nose and where to apply it to cause the COG to be as close to 10% MAC fore of the COL.
- Designing a mounting method for the control circuitry that will place it well below the lifting surfaces.
- Including a positive dihedral angle into the corrugated glider with extended experimentation into various values and their practical impacts on glide performance
- Introduction of a pair of apex fences and experimentation on changing.g their size
- Including a quarter chord apex flap at a fixed angle of 15° and evaluating its effect on glide performance.
- Designing a pair of fixed leading edge control flaps according to design principles described in Section 4.2.3.
- Altering the planform shape to a double delta configuration using diamond shaped fillets and evaluation of its effects.
- Varying the position of the rear trimmed surfaces to be in (and out) of the path of the leading edge vortex core.
- Various combinations and permutations of the above.

Luckily, if a laser cutter (and ideally a vacuum former) is made available to the design engineer, a huge number of prototypes can be generated very quickly and with little to no associated material cost.

Control/Path Planning

- Development of a simulated dynamic model of the craft as well accurate analysis of power requirements for each possible action.
- Investigation and estimation of time requirements for POMDP search.
- Development of basic environment model containing reward functions associated with belief space distributions.
- Determination of a method to compress a policy function to a simplified path plan that can be held on an embedded chip.
- Long term goal – have fully operational path planner and simulator including GUI outputs.

It is unfortunate that the project became caught up so severely in what was originally intended to be only a small section of the project. None the less very important breakthroughs were made in the design process that are imperative to completing the project. The author has no doubt that a

successful interstate or even intercontinental flight is achievable and will monitor development of the project keenly alongside future endeavours.

Deus ex Machina

9 APPENDICES

APPENDIX A. DETAILED FINAL METHOD OF PRODUCTION

The following section outlines the final set of manufacturing processes that were used to generate the best performing circuits onto a paper substrate. Prior to further development on the project carefully study of this section is recommended to gain familiarity with the processes from which the next iteration of control circuitry can be developed. Note that this section does *not* outline the full development process leading to the results presented (including justification for not including other particular processes, chemicals and materials) and as such if further development is to be performed specifically on circuit manufacture that the entirety of Appendix A be studied prior to commencing work.

Some brief points upon this production method:

- This method was developed around the concept of supporting the ability to rapidly prototype new designs and methods on a small scale to reduce the cost and time of developing the process itself. As such, minor changes to materials and methods should be considered on a higher production scale, this was however a long term goal throughout development and alternative mass production methods are highlighted in the relevant sections of the process.
- A dominant driving force behind this process is to allow the final board to be capable of reflow soldering and generally be handled as a generic FR4 PCB for assembly purposes. This is the main way in which this method is differentiated from standard practices of producing conductive traces onto a paper substrate.
- Some alternative methods and equipment are suggested, however only the specific method the author used will be outlined.
- Some select specialized equipment/machinery is required for this process, it should be determined that sufficient access to these devices is achievable before committing to an extended project implementing this process. The equipment requirements are outlined below.

Equipment Requirements (small scale production and prototyping):

- Air-pressure sputter deposition and vacuum evaporation deposition both require a method of generating a stencil for application of the conductor. This action can be performed by a hobby-grade laser cutter or a hobby vinyl cutter (with reduced precision but greater ease of transferring stencil).



Figure 9-1 5030 Laser Engraver by CNColetech

- An alternate to sputter or evaporation deposition is selective inkjet deposition – this requires a device that can print using a set of chemicals to produce silver traces. By 2014, such devices should be available commercially at a realistic price range from a Brisbane based company - Cartesian Co. (CartesianCo.com). The achievable resolution from such machines is currently (as of November 2013) comparable to that of the hobby vinyl stencil method but also acts to remove a large majority of potential practical issues as well as reducing the cost and time of individual prototypes. The resolution is also projected to increase with future iterations (possibly with simply further development on the current iteration) but is not yet available.

- Post processing of all track generation methods benefit from mild heat, flash and/or pressure treatment. None of these are strictly required but will assist in increasing the conductance of tracks and in turn requiring less conductor material – reducing costs and some weight. The most accessible and cheapest device that yields the greatest benefit is a standard A4 laminator. Further flash treatment can be provided by a high powered camera flash device and pressure treatment is ideally provided by a shot press or metal pressure roller (such as a modified pasta sheet roller).

- Next a method of generating an accurate solder stencil is highly beneficial for pad copper application as well as the solder itself (but again not completely necessary if the technician has patience and a steady hand). This is again achievable with a laser cutter or vinyl cutter but an alternative is to outsource production to a commercial solder stencil supplier.

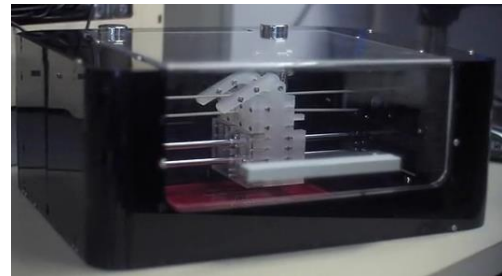


Figure 9-2 The EX1 Circuit Printer by Cartesian Co. - Presented Here With Permission

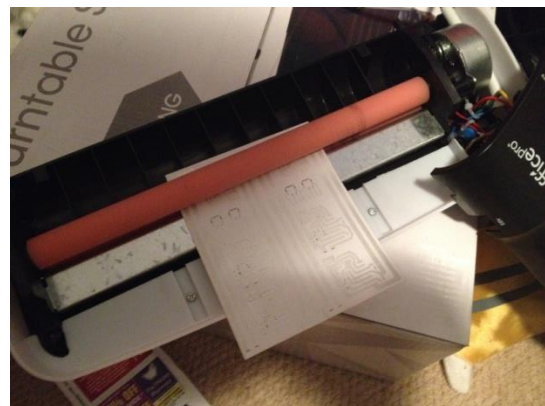


Figure 9-3 A4 Laminator Processing a Stenciled Array of Circuits



Figure 9-4 Laser-cut Solder Stencil

- The completed PCB can only have components soldered to it using hot air reflow methods – a soldering iron cannot be used. This will require a temperature profile controlled oven or a handheld reflow gun – it is helpful to have a reflow gun at least during early stages of testing so the movement of solder can be observed during the reflow process.



Figure 9-5 Handheld Reflow Soldering Station

NOTE: for specific information on the setup used by the author to generate the circuits demonstrated throughout this paper, please see Appendix F.

Procedure:

NOTE: this procedure is an outline of using the equipment and respective procedures employed specifically by the author, only brief insights into alternatives for mass production will be discussed. If different equipment is available (for instance for stencil manufacture) then procedures may have to be altered.

1. Preparing the artwork :

In order to pattern down the conductor in the shape of the PCB tracks, a stencil must first be generated from the CAD designed circuit. An important parameter in generating the machine tool path is to account for the width of the cutting tool (be it vinyl cutter blade, laser beam width etc.). In the case of a laser cutter, there is a fairly simple manner in which to gauge this value. First the power, speed and focal length parameters must be dialled in to optimal values for the given material being cut (in this case standard 80GSM printer paper was used) – this is to reduce the beam width as much as possible. Using these parameters a set of small rectangles are cut from the material with known dimensions (note that more rectangles provides better resolution). Very accurately lining these rectangles up and using a set of vernier callipers to measure their total width will allow for a reasonably accurate assumption on the discrepancy between the CAD design and the actual cut width, see Figure 9-6.



Figure 9-6 Measuring Laser Beam Width

In the author's case the beam width was measured as 0.1867mm. The artwork must then be inset by half of this beam width in order to create dimensionally accurate stencils – this action can be performed in any number of CAD packages after the artwork is exported from the PCB design

software as some form of vector or Gerber file. Some freeware suggestions are ViewMate for Gerber files and InkScape for vector files – either method is fine, the author used an educational release of the commercial package Vectorworks by Nemetschek. This step is vitally important at the scale of SMD electronics as can be demonstrated in Figure 9-7.

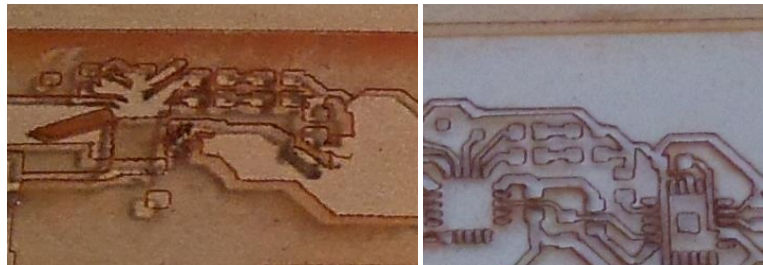


Figure 9-7 Before and After Beam Width Compensation

2. Generating the stencil (for stencil deposition methods):

The stencil can now be physically generated using a precision cutting device – ensure that the settings for cutting are set exactly as used to measure the cut width. In the case of using a laser cutter, care should be taken to ensure that the specimen is kept completely flat and will not shift during the cutting process, particularly due to pressure air blowing over the piece (which is necessary in most cases). This can be achieved by placing heavy objects at the corners of the specimen; however these must not be allowed to impact the collimator gantry. A more simple solution is to use adhesive tape for mounting but this is not always effective due to the low surface area presented for adhesion on a honeycomb cutting surface. If fine sections of the specimen are warping during cutting or there are free-floating surfaces, adding small cuts through these tracks in the artwork should be considered – they can then be bridged very easily in a later process for laying copper paste over solder pads. Despite this, very fine detail can still be achieved easily with the laser cutting method, such as that shown in Figure 9-8. Alternatively if a vinyl cutter is used, a low tack adhesive for transferring vinyl can be used to apply the stencil onto the substrate while keeping the artwork in registration with itself, including very thin members and floating surfaces.

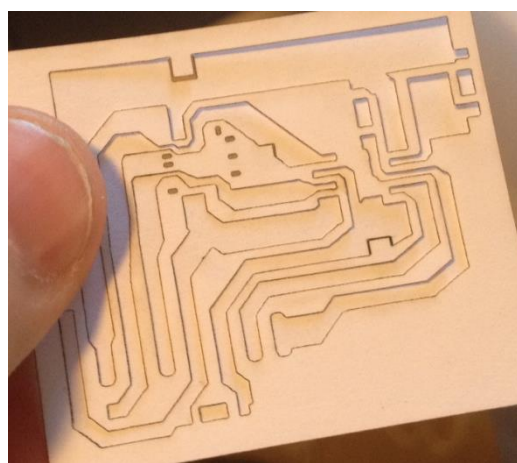


Figure 9-8 Laser-cut Sputter Deposition Stencil

3. Applying the stencil to the substrate:

The next step is to apply the stencil over the substrate to be used, in order to prevent deposited conductor from moving under the stencil and shorting tracks, the stencil must be adhered over its entire surface. The final solution used by the author was to apply a contact adhesive (in the form of an aerosol spray) to the rear of the stencil. It is important to provide a complete coating of the surface but applying too much may saturate the stencil and cause warping. If a vinyl cutter is used, this is easily taken care of by simply cutting the stencil from an adhesive vinyl. Care must be taken in both instances to ensure that the adhesion is not so strong as to tear or delaminate the substrate – even the smallest tear can destroy the circuit. This can be achieved by leaving the adhesive exposed to air (but adequately shielded from airborne contaminants) for an experimentally determined period (in the authors case ~2.5 minutes) to partially cure it before applying to the substrate. Lastly the stencil must be applied to the substrate entirely flat without any bubbles or ripples; this can be achieved relatively easily due to the adhesion not being so strong. It is helpful to hand press the substrate and stencil between two flat sheets to further ensure a complete and even adhesion.

In the case of mass production, this process can be achieved with an automated pressing device similar to what is used to automate solder stencilling. The top section of the press keeps the stencil flat and taught and will press the piece down onto the substrate during the spraying process and then remove it once complete. This requires a semi-rigid stencil material such as steel or aluminium sheet but also removes the issue of adhesives potentially damaging the substrate or having trace amounts remain which could cause environmental contamination.

4. Applying the Conductor:

The simplest method of applying the conductor without implementing any costly machinery is to use a standard hobby airbrush. After testing on a range of conductors, compositions and spray parameters, the following was determined to be most effective (at a small production level):

- Conductor – Alcohol and binder suspension with silver micro-particles in suspension. Often used/marketed as a circuit repair device.
- Spray pressure – 55 - 60 PSI
- Spray Nozzle Diameter – 0.2 -0.3mm
- Spray Technique – Dual action airbrush to control silver flow, spray distance of around 200mm, spray angle kept perpendicular to stencil at all times, increasing number of passes for increased conductance.

The author elected to use the product L100 produced by Kemo Electronic as it can be successfully atomized without any further viscosity modification at 58PSI without allowing much liquid to wick into the paper substrate. This product provides a very fine, flexible and highly conductive coating as shown in Figure 9-9.

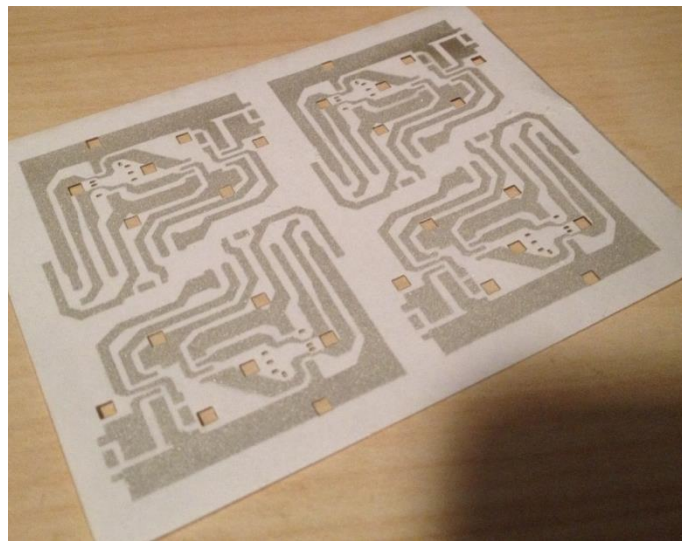


Figure 9-9 L100 Air-Sputter Deposited Circuit Boards

The main drawback of this product is that it is marketed in small quantities and is therefore very expensive at approximately \$5/mL. As an example, in experimentation by the author liberal spraying was applied to a patterned sheet of many instances of a design, the final track resistances being between 0.5 - 2 Ω (this is using more silver than what is necessary). This resulted in a final cost of a circuit as \$0.08/cm².

In the case of a micro-particle suspension conductor, it is also of vital importance to keep the particles evenly suspended through the suspension during application. This is easily achieved by vigorously agitating the suspension before pouring into the airbrush hopper and only applying small portions at a time at a time. It is also of course very important to keep the airbrush clean before and after each use to prevent silver building up and clogging the nozzle pin.

After spraying is finished, the stencil should be removed immediately to prevent bonding of the conductor between the substrate and stencil which can lead to de-lamination. This must be done very carefully to ensure the adhesive applied in the previous step does not tear the substrate. Finally, the circuits should be left for ~8 hours to fully cure before post-processing occurs.

5. Post-processing of Circuit:

In order to increase conductivity of the tracks after deposition as well to improve the surface finish, the circuits can be treated with from mild heat, intense light and/or pressure. Two very simple methods of post-processing are:

- Subject the circuit to a high intensity camera flash; this allows the silver micro-particles to partially sinter while leaving the paper unaffected.
- Pass the circuit sheet through a standard laminator by itself – the heat and mild pressure help to create stronger bonds between the silver micro-particles.

The last method requires some special (but relatively inexpensive) machinery to apply high strength pressure to the circuit. The author tested both a 6 tonne shot press as well as a modified pasta roller (adapted to have a much thinner rolling gap). The shot press was significantly more effective at reducing resistance and the pasta roller cannot provide effective enough pressure unless padded

with more paper (even after modification) – this often leads to ‘crinkling’ in the circuit which will often permanently destroy it.

Some notes on employing a shot press:

- Use flat, smooth plates of a tough, ductile material (such as aluminium or steel) as compression plates.
- Ensure the conductor is fully cured before pressing or some material can be impressed upon the compression plates, increasing the resistance of the circuit.
- Repeat pressing over several points on the circuit as pressure will not be applied evenly over the compression plates – points that have been sufficiently pressed can be identified easily as they will be noticeably shinier (this effect is very obvious with the naked eye as the silver surface will take on a flat mirror like quality as opposed to the pre-processed ‘glitter’).

6. Applying Copper Paste for Solder Flow:

Before components can be reflow soldered onto the circuit without destroying connections, a thick (relative to silver covering), solid and conductive layer must be applied onto the points that solder will flow. The method used by the author was to apply a viscous copper particle based paste through a solder stencil and allowing it to dry. A solder stencil can be generated using the same methods that were used to produce the conductor stencil (paper stencils are acceptable) but if this is not available, the paste is able to be applied by hand with a sharp instrument (such as a needle) with great care. It should also be noted that many ‘home-made’ solutions to stencil generation do not stringently require isolation between pins of small pads – this is not adequate for this step.

Again the stencil should be removed almost immediately after application to prevent premature curing leading to damage of the substrate. Due to the larger size of particles in a copper based paste, the edges will not be as clean as the silver tracks – this is often acceptable. Refer to Figure 9-10 for an example of the circuit completed up to this point.

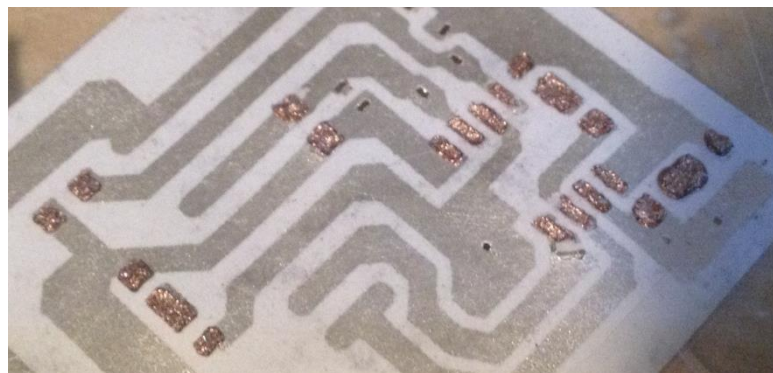


Figure 9-10 Copper Coated Solder Pads

7. Soldering Components:

Solder paste can now be applied to the copper coated pads of the circuit – this can be done by hand or through use of another solder stencil. If a stencil is used, it is recommended that a secondary layer be placed onto the substrate surface first with expanded apertures to account for the extra thickness lent by the copper. The author was unable to fully experiment with a wide range of solder paste compositions with this final design methodology. It is known that standard leaded solder

paste works very well but less toxic alternatives should be explored and have not yet been disproved to function correctly.

Finally the reflow process must be monitored very closely in order to prevent damage to the paper substrate. Ideally heating would occur very evenly and very slowly to prevent warping due to moisture in the substrate but this can be performed with a handheld reflow gun provided the section of paper is small enough. Standard 50% recycled printer paper is easily capable of withstanding temperatures of ~200°C without any loss of structural integrity or visual change.

A fully operational and flexibly robust prototype is shown in Figure 9-11.

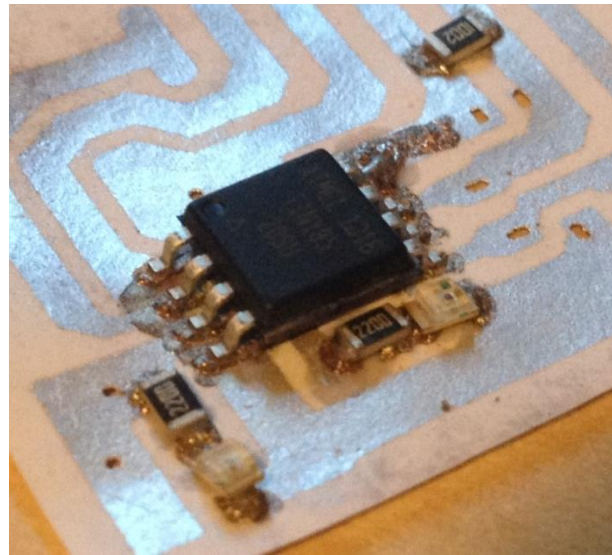


Figure 9-11 Components Reflow Soldered to Paper Substrate

APPENDIX B. REYNOLDS NUMBER CALCULATION

The Reynolds number is a dimensionless value that describes the relationship between inertia and viscosity of a fluid in some flow condition. It is given by EQN (9-1).

$$Re = \frac{\nu L}{\nu} \quad (9-1)$$

ν = kinematic viscosity = 15.68×10^{-6} (for air at sea level),

L = characteristic length (chord length), ν = Relative fluid velocity

In the case of MAVs, this value is extremely low due to the particularly short values for chord length in micro vehicles as well as the comparatively low relative wind speeds experienced. For instance with a stereotypical paper plane, having a mean aerodynamic chord length (see Appendix C) of ~110mm and assuming a relative wind speed of 2m/s yields EQN (9-2)

$$Re = \frac{2 \times 110 \times 10^{-3}}{15.68 \times 10^{-6}} \approx 14,030 \quad (9-2)$$

As a point of reference, almost all standard airfoils that are provided with experimental data do not contain any information on their flow conditions for values below 50,000 at which point they are considered highly inefficient.

APPENDIX C. MEAN AERODYNAMIC CHORD

The mean aerodynamic chord (MAC) is the line connecting the leading and trailing edges of a representation of an entire three-dimensional wing in a single two-dimensional cross section. It is used for the sake of simplification in terms of calculations that require particular geometries of a wing. In the case of a similar shape cross section, simply tapered delta wing (such as that of the paper planes being referenced in this paper) this is simply horizontally scaled depiction of either the root or tip chord. This allows the MAC to be calculated with simple formula (9-3).

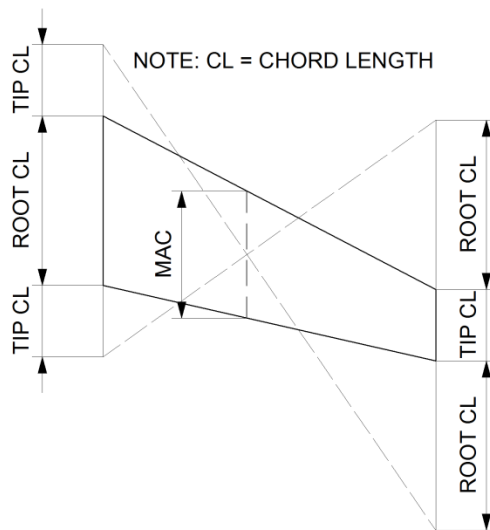


Figure 9-12 Visual Representation of Geometric Mean Chord (approx. MAC visualization)

$$MAC = A - \left(\frac{2(A-B)(0.5A+B)}{3(A+B)} \right) \quad (9-3)$$

$$MAC_{\text{dist from cent.}} = D * \left(\frac{1 + 2T}{3 + 3T} \right) \quad (9-4)$$

A = Tip Chord Length, *B* = Root Chord Length, *D* = Half Span

APPENDIX D. MISCELLANEOUS FAILED APPLICATION METHODS

A small set of other methods were attempted to apply the conductor onto the paper during early development of the project, these are briefly outlined here to prevent unwary readers from attempting to replicate them in the hopes they were a loophole the author didn't investigate.

Stencilled Epoxy ‘Squeegee’ Deposition – this method essentially consisted of attempting to apply a conductive epoxy in various viscosities through a stencil by use of a squeegee device. This was based upon the standard process of applying solder paste to circuit boards. As shown in Figure 9-13, if the epoxy was not viscous enough, the material was drawn through the fibrous matrix of the paper with capillary action and no electrical isolation between nets was achievable. Conversely if the mixture was viscous enough to not wick through the paper, as shown in Figure 9-14, it was found to be impossible to achieve thin tracks even with the thinnest possible stencils. This made the material significantly more brittle to flexure and wasted extreme amounts of epoxy. Ultimately both problems can be solved by atomizing a non-viscous suspension in thin layers using spray deposition.

NOTE: this method was later proved effective for coating solder pads with copper paste but generating entire conducting tracks still consumed too much materials and provided a circuit far less robust to flexure.



Figure 9-13 Silver Conductor Wicked into Matrix of Paper



Figure 9-14 High Resolution but Thick, Brittle and Wasteful Tracks

Aerosol Deposition – Some commercial products exist in aerosol sprays to ‘electro coat’ materials, particularly for RF shielding purposes. These products do not require any purchase of further equipment to allow for spray deposition. Unfortunately their purpose also lies far from that of generating small digital circuits. The only product able to be sourced was a Nickel Acrylic aerosol from RS Online for ~\$50. The majority of issues stemmed from the use of Nickel (which are expanded on in Section 6.2) but the point is that the product limits production to far less than ideal chemicals when a smaller amount of silver varnish AND an airbrush can be purchased for the same cost. Despite this, the material was able to produce rudimentary analogue circuits as shown in Figure 9-15.

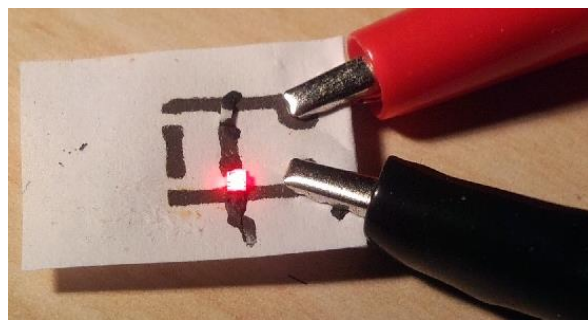


Figure 9-15 Nickel Based Circuits Produced with an Aerosol spray

APPENDIX E. MISCELLANEOUS FAILED CONDUCTOR MATERIALS

A small set of alternative conducting materials were investigated (most often because they were comparatively cheap), these are briefly outlined here to prevent unwary readers from attempting to replicate them in the hopes they were a loophole the author didn't investigate.

Carbon Nano-Particle Based Adhesive – Products have begun to gain some small popularity in terms of arts and crafts as well as niche hobby electronics for cold soldering with cheap conductive adhesives. Products such as WireGlue (pictured in Figure 9-17) can be bought for around \$20 AUD and air cures to a tough, mildly flexible conductor. Some circuits were attempted to be generated from WireGlue very early in the project. Measured resistances were well into the kΩ range even with tracks > 1mm thick – this rendered the material entirely unusable as a track conductor. The material was then attempted to be used as a conductive component mounting method (as shown in Figure 9-16) – resultant resistances over a short, thick connection were still orders of magnitude above what is required for digital communication.



Figure 9-16 Components Mounted with Carbon Based Conductive Adhesive



Figure 9-17 Bottle of WireGlue

Nickel Acrylic Mixture - Some commercial products exist in aerosol sprays to ‘electro coat’ materials, particularly for RF shielding purposes. One product in particular can be purchased from RS Online Australia for ~\$50 AUD simply named “Nickel Screening Compound”. Being that it is packaged in an aerosol spray, the system is ideal for low cost and technical knowledge spray deposition of a conductor. The Nickel was even able to achieve commendable resolution similar to that of the EX1 printer, as seen in Figure 9-18. However the structure of the Nickel that formed on the substrate was a very coarse flaky coat – this caused severe brittleness during flexure, greatly reduced

conductance from bulk and limited resolution. Additionally Nickel can be carcinogenic when inhaled and cause skin irritation on physical contact. Ultimately this mixture was simply not good enough in almost all significant parameters, although a small amount of functional analogue circuits were produced such as that shown in Figure 9-19.



Figure 9-18 Example of Resolution of Nickel Acrylic Spray on a set of SOIC component pads

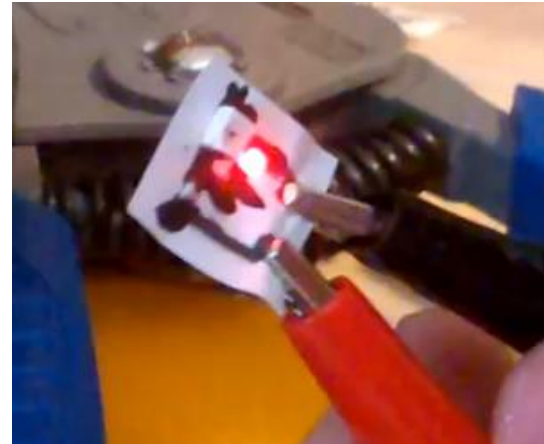


Figure 9-19 Example Analogue Circuit Produced with Stenciled Nickel Acrylic

APPENDIX F. AUTHORS EQUIPMENT SPECIFICATIONS

The following is an outline of specifications for various parts of machinery specifically used by the author in generation of the test control circuits discussed and displayed. Note that the exact same specifications are not required and many alternatives are often acceptable. For more information on alternatives and how the process is actually performed, refer to Appendix A.

Stencil Generation	50W CO2 laser-cutter distributed by CN-Coletech based in China
Stencil Material	80GSM 50% recycled Reflex printer paper
Substrate Material	80GSM 50% recycled Reflex printer paper
Primary Press Mech.	6,000kg H-frame SCA shot press
Secondary Press Mech.	600W, 2.6A OL289 OfficePro A4 laminator
Airbrush	0.2-0.3mm Nozzle Diameter, 7cc fluid cup capacity Aerograph hobby airbrush tool, NOTE: most effective pressure for this model was 58 PSI
Contact Adhesive	Selleys Kwik Grip Spray, 150g aerosol spray bottle
Conductive Silver Solution	L100 Kemo Electronic Conducting Silver, 2mL
Copper Paste/Paint	Caswell Copper Conductive Paint, 4oz
Solder Paste	AIM Leaded Solder Paste, Part NO: NS3046
Reflow Device	Handheld reflow gun – WEP smd rework station, model no: 852D+

10 BIBLIOGRAPHY

- [1] J. Meyer, F. d. Plessis and W. Clarke, "Design Considerations for Long Endurance," University Johannesburg, 2010.
- [2] D. Cohen, "Cambriddge Post," 15 September 2012. [Online]. Available: <http://www.postnewspapers.com.au/editions/20120915/pdf/paper.pdf>. [Accessed March 2013].
- [3] A. Andersoni, "Here come the drones!," WIRED, July 2013. [Online]. Available: <http://www.wired.co.uk/magazine/archive/2012/08/features/here-come-the-drones?page=all>. [Accessed March 2013].
- [4] R. Austin, Aspects of Airframe Design - Scale Effects, John Wiley & Sons Ltd, 2010.
- [5] S. Rainwater, "DARPA Plans Long Range Ship-launched UAVs," DARPA, 2013. [Online]. Available: <http://robots.net/article/3549.html>. [Accessed March 2013].
- [6] P. E. I. Pounds, "Paper Plane: Towards Disposable Low-Cost Folded Cellulose-Substrate," in *Proceedings of Australasian Conference on Robotics and Automation*, Victoria University of Wellington, 2012.
- [7] U. Researchers, "Amazon Expedition Discovers Dozens of New Animals," October 2010. [Online]. Available: <http://www.postnewspapers.com.au/editions/20120915/pdf/paper.pdf>. [Accessed March 2013].
- [8] D. Windestal, "FPV To Space and Back," RCExplorer, 2013. [Online]. Available: <http://rcexplorer.se/projects/2013/03/fpv-to-space-and-back/>. [Accessed March 2013].
- [9] M. Bruenig, P. Kambouris and T. Wark, "Deployment - Springbrook," CSIRO, 2012. [Online]. Available: <http://www.sensornets.csiro.au/deployments/63>. [Accessed March 2013].
- [10] W. J. Hyun, O. O. Park and B. D. Chin, "Foldable Graphene Electronic Circuits Based," *MaterialViews*.
- [11] W. Tee, "How PCB is manufactured," PCBInfo, 7 April 2005. [Online]. [Accessed Marcg 2013].
- [12] A. C. Siegel, S. T. Phillips and e. al, "Foldable Printed Circuit Boards on Paper Substrates," *Adv. Funct. Mater.*, 2010.
- [13] "Calculate and order Flexible Printed Circuits (FPC) ONLINE," Leiton, 2013. [Online]. Available: <http://www.leiton.de/flex-pcb.html>. [Accessed 29 October 2013].
- [14] Unknown, "Molded Circuitry," A Kit of No Parts, 2010. [Online]. Available: <http://web.media.mit.edu/~plusea/?p=1056>. [Accessed November 2013].

- [15] J. Li, F. Ye, S. Vaziri, M. Muhammed, M. C. Lemme and M. Östling, "Efficient Inkjet Printing of Graphene," *Material Views*, 2013.
- [16] S. B. Fuller, E. J. Wilhelm and J. M. Jacobson, "Ink-Jet Printed Nanoparticle Microelectromechanical," *JOURNAL OF MICROELECTROMECHANICAL SYSTEMS*, vol. 11, 2002.
- [17] N. A. Luechinger, E. K. Athanassiou and W. J. Stark, "Graphene-stabilized copper nanoparticles," *IOPScience*, 2008.
- [18] A. Briner, "Cartesian Co," Cartesian Co, 2013. [Online]. Available: <http://cartesianco.com/>. [Accessed November 2013].
- [19] J.-T. Wu, S. L.-C. Hsu, M.-H. Tsa, Y.-F. L. and W.-S. Hwang, "Direct ink-jet printing of silver nitrate–silver nanowire hybrid inks to fabricate," *Journal of Materials Chemistry*, 2012.
- [20] F. Weber, "How a High-Performance Sailplane is Manufactured," Fleugzeugbau, 2012. [Online]. Available: <http://www.dg-flugzeugbau.de/flugzeug-bauen-e.html>. [Accessed March 2013].
- [21] A. Liszewski, "Lego Mischief Machine Automatically Folds and Throws Paper Airplanes," Gizmodo, 2013. [Online]. [Accessed March 2013].
- [22] L. Fuyuno, "The Ultimate Paper Plane," Air & Space Magazine, 2008. [Online]. [Accessed March 2013].
- [23] J. Veitch, "Flight Log," Project Space Planes, 2012. [Online]. Available: <http://projectspaceplanes.com>. [Accessed March 2013].
- [24] M. Prigg, "The iPhone-controlled PAPER PLANE," DailyMail, October 2013. [Online]. Available: <http://www.dailymail.co.uk/sciencetech/article-2442339/The-iPhone-controlled-PAPER-PLANE-Traditional-toy-gets-makeover-using-smartphone-lets-fly-10-minutes.html>. [Accessed October 2013].
- [25] "Online Catalog," Plantraco, 2013. [Online]. Available: <http://www.microflight.com/Online-Catalog>. [Accessed October 2013].
- [26] A. M. Mitchell and J. Delery, "Research into vortex breakdown control," *Progress in Aerospace Sciences*, 2001.
- [27] M. Tama, Z. W. G. Rajagopalan and H. Hu, "Aerodynamic Performance of a Corrugated Dragonfly Airfoil," *Aerospace Sciences Meeting and Exhibit*, 2007.
- [28] S. B. Anderson, "A Look at Handling Qualities of Canard Configurations," *Atmospheric Flight Mechanics Conference*, vol. 10, 1986.
- [29] N. C. LAMBOURNE, D. W. BRYER and J. F. M. MAYBREY, "The Behaviour of the Leading-Edge Vortices over a," *AERONAUTICAL RESEARCH COUNCIL*, 1970.

- [30] A. B. KESEL, "AERODYNAMIC CHARACTERISTICS OF DRAGONFLY WING SECTIONS," *The Journal of Experimental Biology*, 2000.
- [31] A. Marchman, "Trailing edge flap," in *20th AIAA Aerospace Sciences Meeting*, Orlando, 1982.
- [32] M. I. JF and T. JE., "The impact of strakes on a vortex-flapped delta wing," in *AIAA Applied Aerodynamics Conference*, Danvers, 1983.
- [33] D. Rao and T. Buter, "Experimental andcomputations studies of a delta wing apex-flap," in *AIAA Applied Aerodynamics Conference*, Danvers, 1983.
- [34] K. SM, R. OK and T. DP, "Flow control over delta wings at high angles of attack," in *11th AIAA Applied Aerodynamics Conference*, 1993.
- [35] R. Wahls and R. Vess, "Experimental investigation of apex fence flaps on delta wings," *J Aircraft*, 1986.
- [36] S. K. Hebbar, M. R. Platzer and A. M. Alkhozam, "Experimental Study of Vortex Flow Control on Double-Delta," *JOURNAL OF AIRCRAFT*, vol. 33, 1996.
- [37] "Detached-eddy simulations and analyses on new vortical flows over a 76/40 double delta wing," Science Codex, June 2013. [Online]. Available: http://www.sciencecodex.com/detachededdy_simulations_and_analyses_on_new_vortical_flows_over_a_7640_double_delta_wing-114877. [Accessed October 2013].
- [38] L. Oolman, "Balloon Trajectory Forecasts," Polar Weather, 2012. [Online]. Available: http://weather.uwyo.edu/polar/balloon_traj.html. [Accessed March 2013].
- [39] "Opening GrADS to a world of extensions," OpenGrADS, 12 November 2009. [Online]. Available: <http://opengrads.org/>. [Accessed October 2013].
- [40] J. A. Cobano, D. Alejo and G. Heredia, "Multiple gliding UAV coordination for static," *International Conference on Robotics and Automation (ICRA)*, 2013.
- [41] W. H. Al-Sabban, L. F. Gonzalez and R. N. Smith, "Wind-Energy based Path Planning For Unmanned Aerial Vehicles," 2012.
- [42] R. Beard, D. Kingston, M. Quigley, D. Snyder, R. Christiansen, W. Johnson, T. McLain and M. A. Goodrich, "Autonomous Vehicle Technologies for SmallFixed-Wing UAVs," *JOURNAL OF AEROSPACE COMPUTING, INFORMATION, AND COMMUNICATION*, 2005.
- [43] "MPU-9150 Product Specification Revision 4.0," Invensense, 2012.
- [44] J. J. P. Valeton, K. Hermans, C. W. M. Bastiaansen, J. P. Dirk J. Broer, U. S. Schubert, G. P. Crawford and P. J. Smith, "Room temperature preparation of conductive silver features using spin-coating," *Journal of Materials Chemistry*, 2009.

- [45] N. B. Feng, K. Q. Mei, P. Y. Yin and J. U. Schlüter, "On the Aerodynamics of Paper Airplanes," in *27th AIAA Applied Aerodynamics Conference*, San Antonio, Texas, 2009.
- [46] E. C. Polhamus, A CONCEPT OF THE VORTEX LIFT OF SHARP-EDGE DELTA WINGS BASED ON A LEADING-EDGE-SUCTION ANALOGY, Washington DC: NATIONAL AERONAUTICS AND SPACE ADMINISTRATION, 1966.
- [47] "A Quick Derivation relating altitude to air," Portland State Aerospace Society, 2004.
- [48] R. Philpott and D. Bernard, Aircraft Flight, 3rd Ed, Pearson Educated Ltd, 1989.
- [49] F. Engineer, "Winglets and Sharklets," January 2013. [Online]. Available: <http://theflyingengineer.com/flightdeck/winglets-and-sharklets/>. [Accessed November 2013].
- [50] "Interactive Materials Charts," Cambridge University Materials Group, 2012. [Online]. Available: http://www-materials.eng.cam.ac.uk/mpsite/interactive_charts/. [Accessed November 2013].
- [51] H. Kurniawati, "Motion Planning Under Uncertainty," 2013. [Online]. Available: <http://robotics.itee.uq.edu.au/~ai/lib/exe/fetch.php?media=ai:planningunderunc2.pdf>. [Accessed October 2013].
- [52] B. Krasnow, "Ben Krasnow Blog," October 2013. [Online]. [Accessed November 2013].
- [53] "The Fate and Effects of," Kodak, 2003.
- [54] N. R. Lawrence, "Autonomous Soaring Flight for," University of Sydney, 2011.
- [55] R. Austin, UNMANNED AIRCRAFT SYSTEMS, Wiley, 2010.
- [56] S. Sanjeev, "Lift Distributions on Low Aspect Ratio Wings at," WORCESTER POLYTECHNIC INSTITUTE, 2004.
- [57] J. P. Schubert and U. S., "Inkjet Printing and Alternative Sintering of," *Radio Frequency Identification Fundamentals and Applications*, 2010.
- [58] S. Murphy, E. Lohse and C. J., "Applications of Colloidal Inorganic Nanoparticles: From," *Journal of the American Chemical Society*, 2012.
- [59] S. Shinohara, A. Obata, M. Seki, K. Ichihara and E. H. Ishida, "Study of Airfoils for the Unique Micro Wind Turbine Blade," *Design for Innovative Value Towards a Sustainable Society*, 2012.
- [60] Y. Zheng, Z. He, Y. Gao and J. Liu, "Direct Desktop Printed-Circuits-on-Paper," *Scientific Reports*, 2013.
- [61] M. Riley, V. Lowson and A. J., "Vortex Breakdown Control by Delta Wing Geometry," *Journal*

of Aircraft, 1995.

- [62] S. Lewis, B. Walker and J. A., "Reactive Silver Inks for Patterning High-Conductivity Features at," *Journal of the American Chemical Society*, 2012.